NACA

RESEARCH MEMORANDUM

for the

Air Materiel Command, U.S. Air Force

AN INVESTIGATION OF THE WING AND THE WING-FUSELAGE COMBINATION OF A FULL-SCALE MODEL OF THE REPUBLIC XP-91 AIRPLANE IN THE AMES 40- BY 80-FOOT WIND TUNNEL

By Lynn W. Hunton and Joseph K. Dew

Ames Aeronautical Laboratory
Moffett Field, Calif.

NATIONAL ADVISORY COMMITTEE
FOR AERONAUTICS

WASHINGTON
June 10, 1948

NACA RM No. SA8F09

NATIONAL ADVISORY COMMITTEE FOR AERONAUTICS

RESEARCH MEMORANDUM

for the

Air Materiel Command, U.S. Air Force

AN INVESTIGATION OF THE WING AND THE WING-FUSELAGE COMBINATION OF A FULL-SCALE MODEL OF THE REPUBLIC XP-91 AIRPLANE IN THE AMES 40- BY 80-FOOT WIND TUNNEL

By Lynn W. Hunton and Joseph K. Dew

SUMMARY

Wind-tunnel tests of a full-scale model of the Republic XP-91 airplane were conducted to determine the longitudinal and lateral characteristics of the wing alone and the wing-fuselage combination, the characteristics of the aileron, and the damping in roll of the wing alone. Various high-lift devices were investigated including trailing-edge split flaps and partial- and full-span leading-edge slats and Krueger-type nose flaps.

Results of this investigation showed that a very significant gain in maximum lift could be achieved through use of the proper leading-edge device. The maximum lift coefficient of the model with split flaps and the original partial-span straight slats was only 1.2; whereas a value of approximately 1.8 was obtained by drooping the slat and extending it full span. Improvement in maximum lift of approximately the same amount resulted when a full-span nose flap was substituted for the original partial-span slat.

INTRODUCTION

The Republic XP-91 airplane is a jet-and rocket-powered interceptor fighter with swept-back and inverse-tapered

wings. Owing to this unique wing plan form on which little data at present are available, the Air Materiel Command, U.S. Air Force, requested that tests of a full-scale model of the XP-91 be conducted in the Ames 40- by 80-foot wind tunnel to determine its general aerodynamic characteristics.

Presented herein are the longitudinal- and lateral-stability characteristics of the wing alone and the wing-fuselage combination, the characteristics of the aileron, and the damping-in-roll characteristics of the wing alone as measured on a rolling stand. To improve the maximum lift of the wing, several alternate leading-edge auxiliary lift devices were investigated and these results are also reported herein. With the exception of the maximum lift characteristics of the wing, no analysis or discussion of these data is presented in this report.

SYMBOLS

The results of the tests are presented as standard NACA coefficients of forces and moments referred to the stability axes shown in figure 1. The coefficients and symbols are defined as follows:

C_L lift coefficient $\left(\frac{\text{lift}}{qS}\right)$

C_D drag coefficient $\left(\frac{\text{drag}}{qS}\right)$

C_Y side-force coefficient $\left(\frac{\text{side force}}{qS}\right)$

C_m pitching-moment coefficient $\left(\frac{\text{pitching moment}}{qS\bar{c}}\right)$

C_n yawing-moment coefficient $\left(\frac{\text{yawing moment}}{qSb}\right)$

C_l rolling-moment coefficient $\left(\frac{\text{rolling moment}}{qSb}\right)$

C_{l_p} damping-in-roll parameter; rate of change of rolling-moment coefficient with wing-tip helix angle $\left[\frac{\partial C_l}{\partial(pb/2V)}\right]$

C_{h_a}	aileron hinge-moment coefficient $\left(\frac{\text{hinge moment}}{2qM_a}\right)$
pb/2V	wing-tip helix angle, radians
α	angle of attack of wing chord plane and/or fuselage reference axis, degrees
β	angle of sideslip, degrees
δ_a	aileron deflection, degrees
b	wing span measured perpendicular to plane of symmetry (31.33 ft)
$\bar{c}$	wing mean aerodynamic chord (10.59 ft) $\left(\frac{2}{S}\int_0^{b/2} c^2 dy\right)$
M_a	first moment of area aft of aileron hinge line about hinge line (22.11 ft^3)
p	angular velocity in roll, radians per second
q	free-stream dynamic pressure, pounds per square foot
R	Reynolds number
S	wing area (320 sq ft)
V	free-stream velocity, feet per second

Model and Equipment

The full-scale model of the XP-91 used for the tests was supplied through the Air Materiel Command by the Republic Aviation Corporation. A three-view drawing of the model giving pertinent dimensions is presented in figure 2.

The wing plan form is characterized by 37.5° of sweepback of the quarter chord[1] line and a tip-to-root chord ratio of

[1]Except where noted, all chords and spans used in this report are parallel and perpendicular to the plane of symmetry.

1.63 (inverse taper). The basic development of the wing is about the 50-percent chord line. The wing surface is determined by two airfoil sections laid out normal to this line and located 27 and 188 inches, respectively, from the plane of symmetry. Both sections are the same (maximum thickness of 10 percent at the 40-percent-chord point and a design lift coefficient of 0.17) except forward of the 0.15-chord point. Over this section, the ordinates and nose radius of the inboard section are reduced as shown in the table of ordinates given in figure 3. The wing surface at any spanwise station from 0 to 163 inches is generated by straight lines connecting the points of equal chordwise percentage on the two given sections. At station 163, the tip development begins and from this station to station 188 the airfoil section is altered to give the desired tip contour. The wing has zero dihedral and no twist.

Ailerons on the model were of an internal sealed balance type. The aileron chord aft of the hinge line was 27 percent of the wing chord and the balance chord was 30.9 percent of the aileron chord. (Balance area, after accounting for one-half seal area and for cutouts was 30.2 percent of the aileron area aft of the hinge line.) The left aileron only was tested and was rigged with an electric actuator, a selsyn motor indicator, and an electrical resistance-type bending strain gage for remote control and indication of the deflection angle and hinge moment, respectively. The maximum travel for the aileron was $\pm 18^{\circ}$.

The wing was equipped with two lift increasing devices: split flaps over the inboard section and leading-edge slats over the outboard section. The flaps were 40-percent span and 35.5-percent chord and could be deflected to 30°, 40°, 50°, and 60°.[2] The slat was originally only 49-percent span and could be extended forward only in the chord plane. However, in the course of the tests, modifications were made so that partial- and full-span slats could be tested either in the straight-out or drooped position. (See fig. 4.) Because the wing leading edge was fixed over the inboard section of the wing, the inboard slat had to be mounted ahead of the wing leading edge. Consequently, for the full-span-slat installation, the juncture of the inboard and outboard portion was discontinuous. Also investigated was a full-span Krueger-

[2]Flap deflection angles were measured in a plane perpendicular to the flap hinge line.

type nose flap. The dimensional details of this flap are shown in figure 4.

The model was so designed that the wing could be tested alone to determine its static force characteristics and its damping-in-roll characteristics. For the wing-alone force tests the wing was mounted on a faired sting support boom at a 5° incidence, and the boom in turn was attached to the three-strut support system. A photograph of this installation is shown in figure 5. The force tests of the wing and fuselage combination were made with the model mounted on the three-strut support system in the standard manner as shown in the photograph of figure 6. The incidence of the wing with reference to the fuselage reference line was 0°.

The investigation of the damping-in-roll characteristics of the wing was conducted in the tunnel test section with the wing mounted on the rolling apparatus shown in the photograph of figure 7. The rolling apparatus consisted of a support stand on which was mounted a variable-speed electric drive motor, a geared reducer, and a torque tube set in two roller bearings with the axis of rotation coincident with the center line of the tunnel. The angle of incidence of the wing with respect to the rolling axis could be varied from -1° to 29°. A resistance-type torsion strain gage equipped with slip rings and brushes (installed between the geared reducer and torque tube) and a recording oscillograph were used to measure the rolling resistance torque of the wing in a steady roll.

TESTS

Force tests were made to determine the static longitudinal and lateral characteristics through an angle-of-attack range for both wing alone and the wing plus fuselage, each with the wing clean, with partial-span split flaps, and with various combinations of leading-edge devices. The wing-alone investigation also included tests of the left aileron to determine effectiveness and hinge moments at several angles of sideslip with the wing clean, with split flaps down, with the outboard leading-edge straight slats extended, and with flaps and slats extended.

Tests were made of the wing in steady roll to determine the damping-in-roll (C_{l_p}) characteristics of the wing clean,

with split flaps deflected, and with flaps and the outboard straight slats extended. For each configuration, the angle of incidence of the wing with respect to the axis of roll was varied from approximately -1° to 29° in 5° increments. For all tests, the dynamic pressure was held constant at 25 pounds per square foot and the value of $\frac{pb}{2V}$ varied from about 0.02 to 0.11 by varying the speed of rotation of the wing. The C_{l_p} data presented herein are average values for the wing in one complete rolling cycle as determined from the integrations of the recorded damping-torque time histories.

All tests were run at a dynamic pressure of 25 pounds per square foot which corresponds to an airspeed of about 100 miles per hour at standard sea-level conditions and to a test Reynolds number of 9.3×10^6 based on the mean aerodynamic chord of 10.59 feet.

CORRECTIONS

No support-strut tares have been applied to either the wing alone or wing-fuselage-combination data. The tares for the support struts (configuration used in the tests of the wing-fuselage combination) are known to be relatively small with the exception of the drag tare (ΔC_D is of the order of 0.0030 at zero lift).

To evaluate the sting-support boom tares for the wing-alone tests, static pressure measurements over the boom were made. All forces and moments except for drag have been corrected for these tares. The drag tare of the boom, although probably quite large, could not be measured readily owing to the difficulty of supporting the wing in the presence of the boom but not attached to it. Since the drag tares of the boom and support struts are known to be appreciable ($\Delta C_D \cong 0.0180$), the absolute values of the drag data, as presented herein for the wing alone, have little significance other than to show the effect of various configuration changes.

Corrections for air-stream inclination and tunnel-wall effects have been applied to all the static force data. Brief investigations of tunnel-wall corrections for swept wings have indicated that corrections for boundary effects are determined primarily by the spans and areas of models and are not greatly

affected by sweep. Hence, the following standard corrections for unswept wings have been applied to the angle of attack and drag coefficient data:

$$\Delta\alpha = 0.706\ C_L$$

$$\Delta C_D = 0.012\ C_L^2$$

For the dynamic rolling tests of the wing, a correction was investigated involving the influence of the tunnel walls on the measured damping in roll. As an approximation, interference effects were determined for two positions of the wing (horizontal and vertical), it being assumed in both cases that the test section was rectangular and that the static induction effects of the wing at rest closely approximated those of a wing in steady roll. The computations showed that the measured damping moments were 1 percent low for the wing in the horizontal position and 7 percent high for the wing in the vertical position. Since in these tests average rolling-moment data were obtained for a complete cycle in roll, the over-all effect of this wall interference was of the order of 3 percent which has been neglected in the data reported herein.

RESULTS AND DISCUSSION

The results of this investigation of the wing alone and the wing-fuselage combination are presented in figures 8 through 37 as outlined in table I. In figures 8 to 14 are shown the general longitudinal characteristics of the model, and in figures 15 to 20 are given the aerodynamic characteristics of the model in sideslip. Data showing the effectiveness of the aileron are presented in figures 21 to 36, and in figure 37 are shown the results of tests of the damping in roll of the wing at several values of lift coefficient. All forces and moments are referred to the stability axes originating at a center-of-gravity position located on the wing-chord plane and at the 25-percent mean aerodynamic chord for the wing-alone tests and at the 18-percent M.A.C. for the wing plus fuselage tests. All angle-of-attack measurements refer to the wing-chord plane and/or to the fuselage reference axis since the incidence of the wing to fuselage was 0°.

Early in the investigation of the wing, it was found that the straight slat (outboard only) was relatively ineffective in increasing $C_{L_{max}}$. (See fig. 11.) In an effort to improve $C_{L_{max}}$, a slat was added to the inboard section of the wing and provisions made to test either or both the inboard and outboard slats in the straight or a drooped position. As a possible alternate for the slat, a full-span Krueger-type nose flap was also provided. Details of these leading-edge devices are given in figure 4, and the characteristics of the model equipped with split flaps and various leading-edge configurations are presented in figures 10 through 13. To facilitate comparison, the lift curves near stall for these configurations are reproduced in figure 38 and the approximate values of the usable $C_{L_{max}}$ (flaps 40°) are summarized in the following table:

Leading edge		$C_{L_{max}}$ (approx.)
Outboard	Inboard	
Plain	Plain	1.1
Straight slat	Plain	1.2
Plain	Straight slat	1.2
Straight slat	Straight slat	1.2
Droop slat	Plain	1.2
Plain	Droop slat	1.2
Droop slat	Droop slat	1.8
Droop slat (sealed)	Droop slat	1.7
Nose flap	Nose flap	1.7

For the optimum[3] straight slat position (0.05 M.A.C.),

[3]The optimum straight slat position was based on the most favorable drag characteristics since further extension of the slat showed negligible increases in lift.

either partial or full span, an increment in maximum lift coefficient of only about 0.1 was obtainable. However, by rotating these same slats down to a drooped position it was found that, although no significant improvement in $C_{L_{max}}$ resulted from the individual installation of either the outboard or inboard partial-span slat in the drooped position, an increase in $C_{L_{max}}$ of 0.7 was obtainable with the full-span drooped slat. Likewise, the full-span Krueger-type nose flap caused a similar improvement in $C_{L_{max}}$ of about 0.6. This impressive improvement in the maximum lift characteristics of the wing leads to the following generalizations: First, the upwash induced at the wing tips by sweepback is apparently reduced to such an extent by the inverse taper (as would be predicted by the theoretical results of reference 1) that a uniform spanwise distribution of section lift coefficient results which causes separation to occur simultaneously over the entire span. Thus, to effectively delay this separation, any corrective measure must be applied to the full span; and second, the relatively sharp leading-edge radius (about 0.6-percent chord) of the wing promotes laminar separation at the leading edge which can be controlled to a large extent by an increase in camber of the leading edge such as was effected by either the drooped slat or the nose flap. The ineffectiveness of the full-span straight slat was apparently due to separation at the nose of the slat. When in the drooped position, the slat was acting primarily as a camber-changing device relieving laminar separation and not as a true slat energizing the boundary-layer air to relieve turbulent separation. Evidence substantiating this is given in the results of the tests of the wing with the full-span drooped slats where closing of the slot behind the outboard slat caused little effect on the value of $C_{L_{max}}$.

Ames Aeronautical Laboratory,
National Advisory Committee for Aeronautics,
Moffett Field, Calif.

REFERENCE

1. DeYoung, John: Theoretical Additional Span Loading Characteristics of Wings With Arbitrary Sweep, Aspect Ratio, and Taper Ratio. NACA TN No. 1491, 1947.

TABLE I.- INDEX TO THE BASIC DATA FIGURES

General configuration	Variable	Fig. No.
Longitudinal characteristics		
Plain wing	Fuselage	8
Wing alone	Flap angle	9
Wing + flaps	Fuselage	10
Wing alone + flaps	Straight slats	11
Wing-fuselage + flaps	Drooped slats	12
Wing-fuselage + flaps	Full-span L.E. devices	13
Wing-fuselage + F.S. drooped slats	Flap angle	14
Lateral-stability characteristics		
Wing alone, plain	β	15
Wing alone + flaps	β	16
Wing alone + straight slats	β	17
Wing alone + straight slats + flaps	β	18
Wing-fuselage, plain	β	19
Wing-fuselage + F.S. drooped slats + flaps	β	20
Aileron characteristics		
Wing alone, plain	δ_a	21
Wing alone + flaps	δ_a	22

TABLE I.- CONTINUED

General configuration	Variable	Fig. No.
Aileron Characteristics (Cont.)		
Wing alone + straight slats	δ_a	23
Wing alone + straight slats + flaps	δ_a	24
Wing alone, plain - $\beta = 0.1^\circ$	α	25
Do. $\beta = 5.2^\circ$	α	26
Do. $\beta = 8.6^\circ$	α	27
Do. $\beta = -4.3^\circ$	α	28
Do. $\beta = -7.9^\circ$	α	29
Wing alone+ flaps - $\beta = 0^\circ$	α	30
Wing alone + straight slats - $\beta = 0.1^\circ$	α	31
Wing alone + straight slats - $\beta = 5.2^\circ$	α	32
Wing alone + straight slats - $\beta = 8.6^\circ$	α	33
Wing alone + straight slats - $\beta = -4.3^\circ$	α	34
Wing alone + straight slats - $\beta = -7.9^\circ$	α	35
Wing alone + straight slats + flaps - $\beta = 0^\circ$	α	36
Damping-in-roll characteristics		
Wing alone	Flaps and straight slats	37

FIGURE LEGENDS

Figure 1.- Sign convention for the standard NACA coefficients. All forces, moments, angles, and control surface deflections are shown as positive.

Figure 2.- Three-view drawing of the Republic XP-91 full-scale model with tail removed.

Figure 3.- Details of the Republic XP-91 inverse taper wing.

Figure 4.- The forms of the leading-edge auxiliary lift devices investigated.

Figure 5.- The plain wing mounted on the support boom in the Ames 40- by 80-foot wind tunnel.

Figure 6.- The wing-fuselage installation in the Ames 40- by 80-foot wind tunnel; partial-span drooped slats and split flaps extended.

Figure 7.- View of the installation of the plain wing mounted on the rolling wing stand in the Ames 40- by 80-foot wind tunnel.

Figure 8.- Aerodynamic characteristics of the wing and wing-fuselage combination. Plain wing.

Figure 9.- Effect of deflection of split flaps on the aerodynamic characteristics of the wing alone.

Figure 10.- Aerodynamic characteristics of the wing and wing-fuselage combination. Flaps, 40°.

Figure 11.- Effect of various outboard straight leading-edge slat positions on the aerodynamic characteristics of the wing alone. Flaps, 40°.

Figure 12.- Effect of various drooped leading-edge slats on the aerodynamic characteristics of the wing-fuselage model. Flaps, 40°.

Figure 13.- Comparison of the aerodynamic characteristics of the wing-fuselage model with inboard and full-span straight slats extented 0.05 M.A.C., and full-span nose flaps. Split flaps, 40°.

Figure 14.- Effect on the aerodynamic characteristics of the wing-fuselage combination of deflecting trailing-edge split flaps. Full-span drooped slats.

Figure 15.- Effect of sideslip on the aerodynamic characteristics of the wing alone. Plain wing. (a) C_D, α, C_m vs C_L.

Figure 15.- Concluded. (b) C_Y, C_n, C_l vs C_L.

Figure 16.- Effect of sideslip on the aerodynamic characteristics of the wing alone. Flaps, 40°. (a) C_D, α, C_m vs C_L.

Figure 16.- Concluded. (b) C_Y, C_n, C_l vs C_L.

Figure 17.- Effect of sideslip on the aerodynamic characteristics of the wing alone. Outboard straight slats extended. 0.05 M.A.C. (a) C_D, α, C_m vs C_L.

Figure 17.- Concluded. (b) C_Y, C_n, C_l vs C_L.

Figure 18.- Effect of sideslip on the aerodynamic characteristics of the wing alone. Flaps, 40°, outboard straight slats extended 0.05 M.A.C. (a) C_D, α, C_m vs C_L.

Figure 18.- Concluded. (b) C_Y, C_n, C_l vs C_L.

Figure 19.- Aerodynamic characteristics of the wing-fuselage combination in sideslip. Plain wing. (a) C_D, α, C_m vs C_L.

Figure 19.- Concluded. (b) C_Y, C_n, C_l vs C_L.

Figure 20.- Aerodynamic characteristics of the wing-fuselage combination in sideslip. Split flaps, 40°, full-span leading-edge drooped slats extended. (a) C_D, α, C_m vs C_L.

Figure 20.- Concluded. (b) C_Y, C_n, C_l vs C_L.

Figure 21.- Effect of aileron deflection on the aerodynamic characteristics in pitch of the Republic XP-91 wing alone. Plain wing. (a) α, C_m, C_n vs C_L.

Figure 21.- Concluded. (b) C_l, C_{h_a} vs C_L.

Figure 22.- Effect of aileron deflection on the aerodynamic characteristics in pitch of the Republic XP-91 wing alone. Flaps, 40°. (a) α, C_m, C_n vs C_L.

Figure 22.- Concluded. (b) C_l, C_{h_a} vs C_L.

Figure 23.- Effect of aileron deflection on the aerodynamic characteristics in pitch of the Republic XP-91 wing alone. Outboard straight slats extended 0.05 M.A.C. (a) α, C_m, C_n vs C_L.

Figure 23.- Concluded. (b) C_l, C_{h_a} vs C_L.

Figure 24.- Effect of aileron deflection on the aerodynamic characteristics in pitch of the Republic XP-91 wing alone. Flaps, 40°, outboard straight slats extended 0.05 M.A.C. (a) α, C_m, C_n vs C_L.

Figure 24.- Concluded. (b) C_l, C_{h_a} vs C_L.

Figure 25.- Aileron characteristics on the Republic XP-91 wing. Plain wing; β, 0.1°. (a) C_l and C_{h_a} vs δ_a.

Figure 25.- Concluded. (b) C_n and C_m vs δ_a.

Figure 26.- Effect of aileron deflection on the aerodynamic characteristics of the Republic XP-91 wing. Plain wing; β, 5.2°. (a) C_l, C_{h_a} vs δ_a.

Figure 26.- Concluded. (b) C_n, C_m vs δ_a.

Figure 27.- Effect of aileron deflection on the aerodynamic characteristics of the Repbulic XP-91 wing. Plain wing, β, 8.6°. (a) C_l, C_{h_a} vs δ_a.

Figure 27.- Concluded. (b) C_n, C_m vs δ_a.

Figure 28.- Effect of aileron deflection on the aerodynamic characteristics of the Republic XP-91 wing. Plain wing; β, -4.3°. (a) C_l, C_{h_a} vs δ_a.

Figure 28.- Concluded. (b) C_n, C_m vs δ_a.

Figure 29.- Effect of aileron deflection on the aerodynamic characteristics of Republic XP-91 wing. Plain wing; β, -7.9°. (a) C_l, C_{h_a} vs δ_a.

Figure 29.- Concluded. (b) C_n, C_m vs δ_a.

Figure 30.- Effect of aileron deflection on the aerodynamic characteristics of the Republic XP-91 wing. Flaps, 40°; β, 0°. (a) C_l, C_{h_a} vs δ_a.

Figure 30.- Concluded. (b) C_n, C_m vs δ_a.

Figure 31.- Effect of aileron deflection on the aerodynamic characteristics of the Republic XP-91 wing. Outboard straight slats extended 0.05 M.A.C.; β, 0.1°.
(a) C_l and C_{h_a} vs δ_a.

Figure 31.- Concluded. (b) C_n and C_m vs δ_a.

Figure 32.- Effect of aileron deflection on the aerodynamic characteristics of the Republic XP-91 wing. Outboard straight slats extended 0.05 M.A.C.; β, 5.2°.
(a) C_l, C_{h_a} vs δ_a.

Figure 32.- Concluded. (b) C_n, C_m vs δ_a.

Figure 33.- Effect of aileron deflection on the aerodynamic characteristics of the Republic XP-91 wing. Outboard straight slats extended 0.05 M.A.C.; β, 8.6°.
(a) C_l, C_{h_a} vs δ_a.

Figure 33.- Concluded. (b) C_n, C_m vs δ_a.

Figure 34.- Effect of aileron deflection on the aerodynamic characteristics of the Republic XP-91 wing. Outboard straight slats extended 0.05 M.A.C.; β, -4.3°.
(a) C_l, C_{h_a} vs δ_a.

Figure 34.- Concluded. (b) C_n, C_m vs δ_a.

Figure 35.- Effect of aileron deflection on the aerodynamic characteristics of the Republic XP-91 wing. Outboard straight slats extended 0.05 M.A.C.; β, -7.9°.
(a) C_l, C_{h_a} vs δ_a.

Figure 35.- Concluded. (b) C_n, C_m vs δ_a.

Figure 36.- Effect of aileron deflection on the aerodynamic characteristics of the Republic XP-91 wing. Flaps 40°; outboard straight slats extended 0.05 M.A.C.; β, 0°.
(a) C_l, C_{h_a} vs δ_a.

Figure 36.- Concluded. (b) C_n, C_m vs δ_a.

Figure 37.- Damping-in-roll parameter variation with lift coefficient for the wing plain, with flaps, and with flaps and outboard straight slats extended 0.05 M.A.C.

Figure 38.- Comparison of the maximum trimmed-lift coefficients for the model with and without various leading-edge high-lift devices. Flaps, 40°.

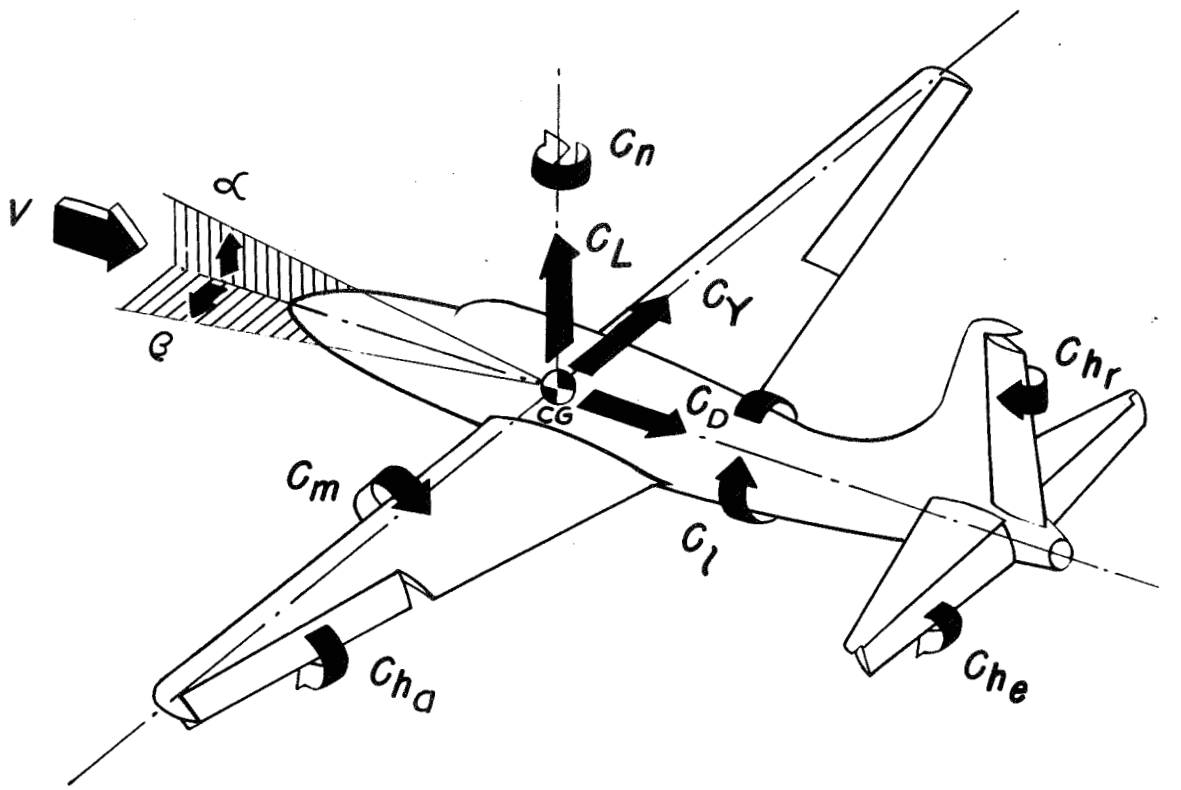

Figure 1.- Sign convention for the standard NACA coefficients. All forces, moments, angles, and control surface deflections are shown as positive.

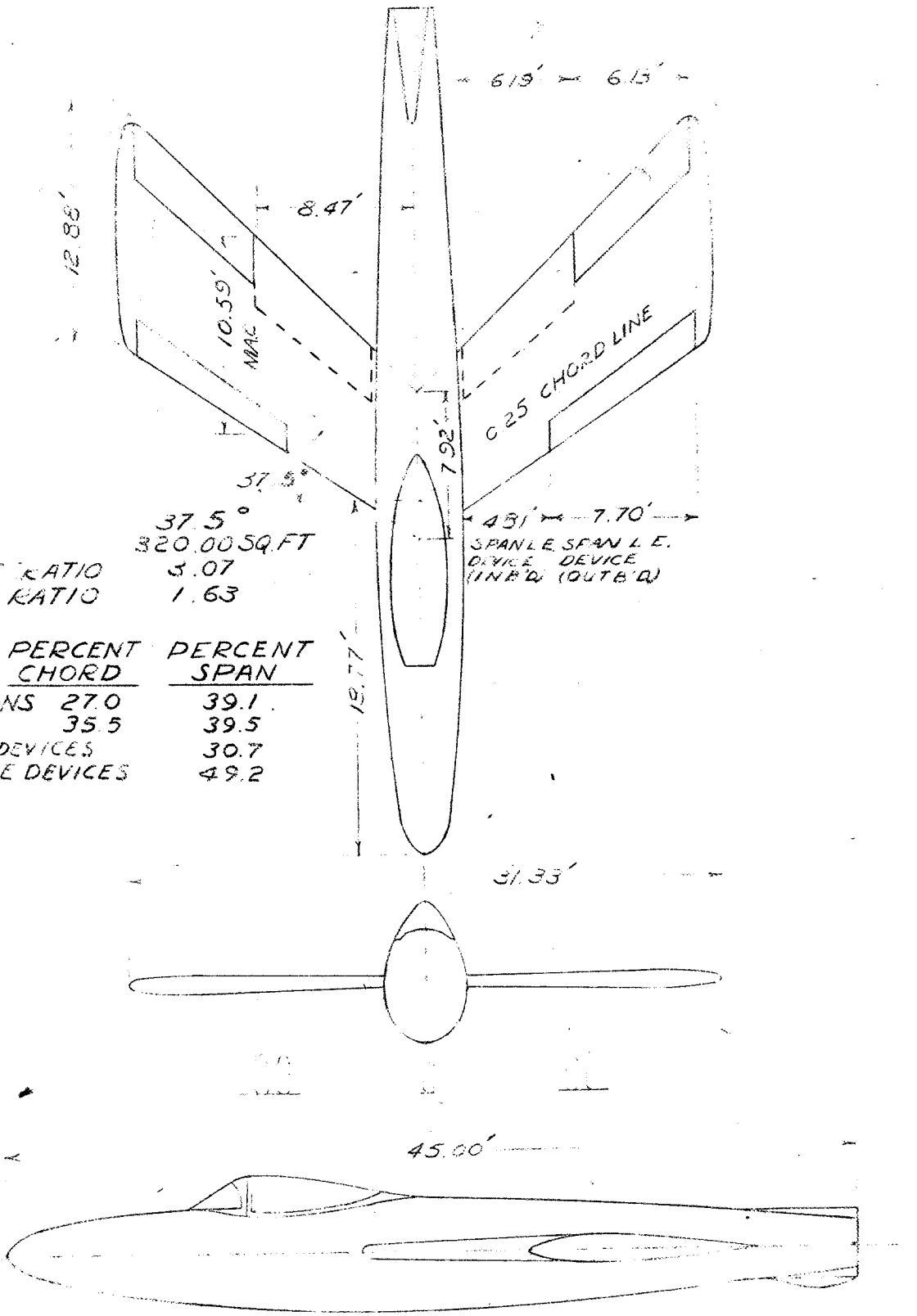

SWEEP	37.5°
AREA	320.00 SQ.FT
ASPECT RATIO	3.07
TAPER RATIO	1.63

	PERCENT CHORD	PERCENT SPAN
AILERONS	27.0	39.1
FLAPS	35.5	39.5
INBD. L.E. DEVICES		30.7
OUTBD. L.E. DEVICES		49.2

FIGURE 2.- THREE-VIEW DRAWING OF THE REPUBLIC XP-91 FULL-SCALE MODEL WITH TAIL REMOVED

AD9

WING-AIRFOIL ORDINATES
CHORDS ⊥ TO 0.50-CHORD LINE

x %c	y (UPPER) % CHORD		y (LOWER) % CHORD	
	STA. 27	STA. 188	STA. 27	STA. 188
.5	.839	.876	.683	.715
.75	1.024	1.061	.844	.881
1.25	1.331	1.378	1.090	1.132
2.5	1.896	1.943	1.520	1.562
5	2.680	2.721	2.104	2.141
7.5	3.270	3.294	2.520	2.545
10	3.747	3.756	2.844	2.863
15	4.485		3.325	
20	5.015		3.650	
25	5.405		3.875	
30	5.670		4.010	
35	5.835		4.090	
40	5.910		4.090	
45	5.895		4.035	
50	5.775		3.905	
55	5.570		3.705	
60	5.255		3.440	
65	4.855		3.105	
70	4.365		2.710	
75	3.795		2.265	
80	3.145		1.785	
85	2.435		1.290	
90	1.680		.790	
95	.880		.335	
100	----		----	

L.E.R. (STA 27) = 0.569 %C
L.E.R. (STA 188) = 0.615 %C
L.E.R. HEIGHT = 0.042 %C
T.E.R. = 0.032"

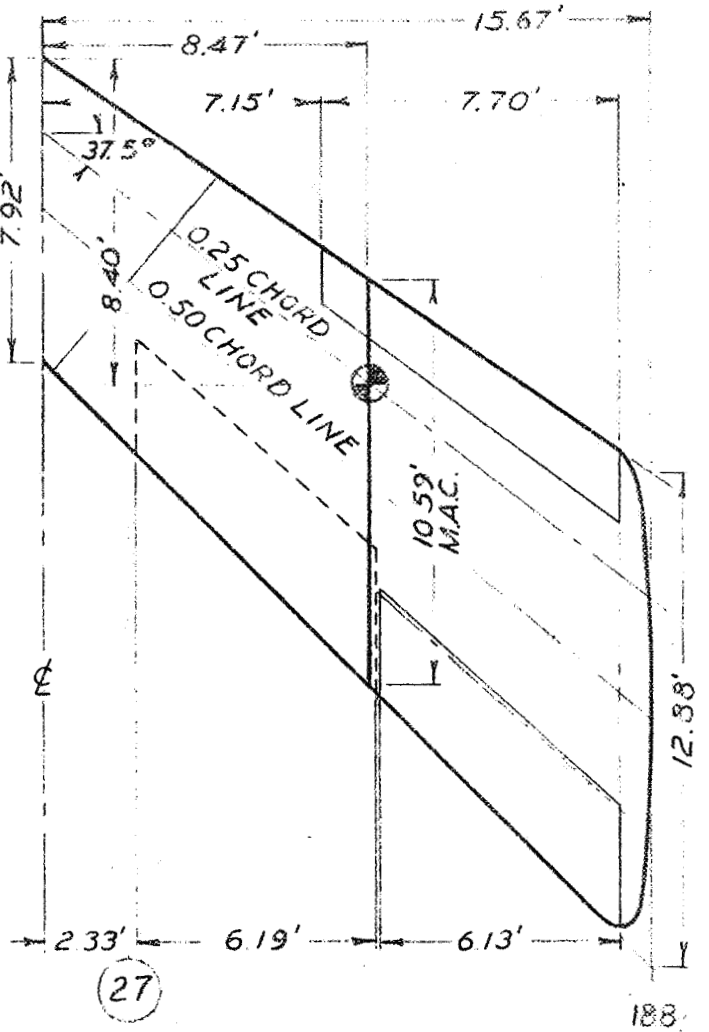

AILERON CROSS SECTION

FIGURE 3.- DETAILS OF THE REPUBLIC XP-91 INVERSE TAPER WING.

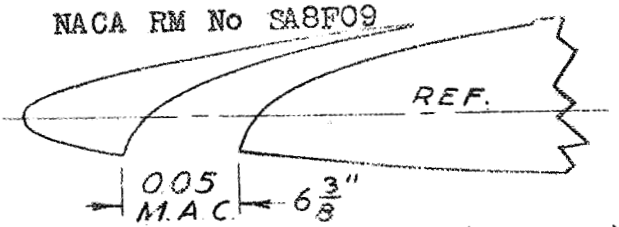

STRAIGHT SLAT (OUTBD.)

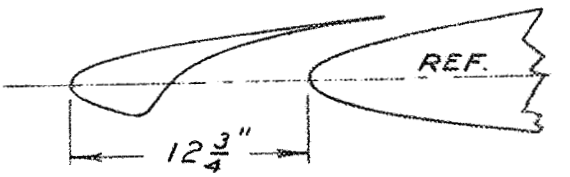

STRAIGHT SLAT (INBD.)

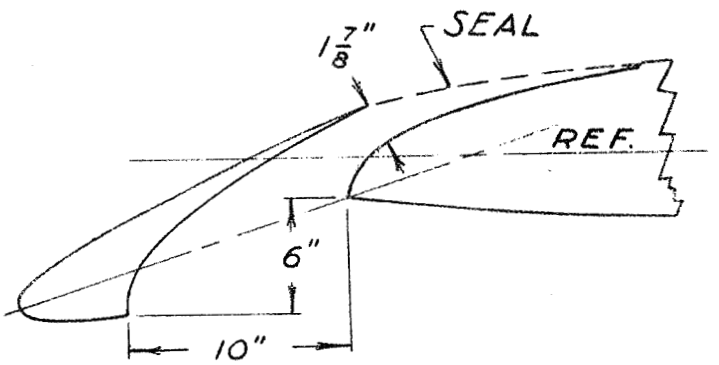

DROOPED SLAT (OUTBD.)

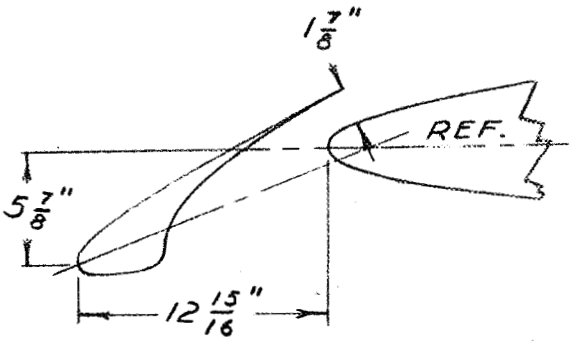

DROOPED SLAT (INBD.)

NOTE: ALL SLAT DIMENSIONS ARE CONSTANT ALONG SPAN.

NOSE FLAP ORDINATES PARALLEL TO AIRPLANE ℄	
x INCHES	ORDINATE INCHES
.61	.80
.92	.97
1.53	1.26
3.05	1.79
6.11	2.54
9.17	3.09
12.22	3.53

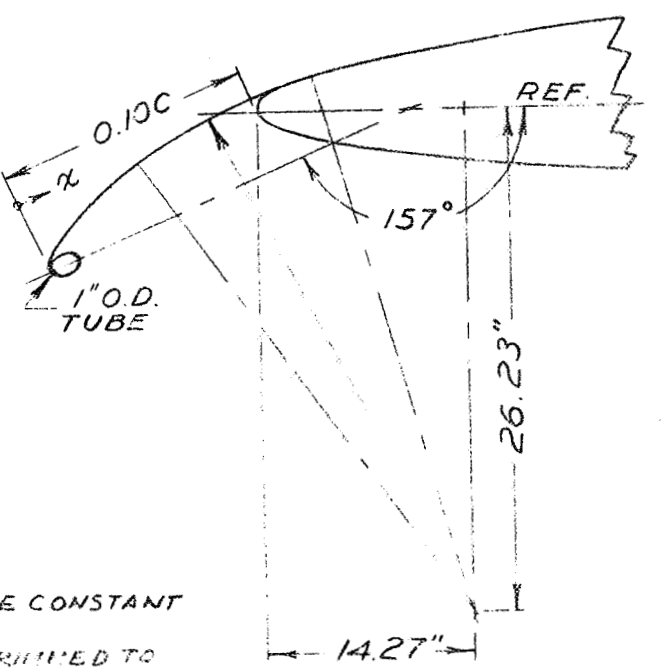

NOTE: ALL NOSE-FLAP DIMENSIONS ARE CONSTANT ALONG SPAN.
NOSE-FLAP TRAILING EDGE TRIMMED TO OBTAIN A CONSTANT PERCENT CHORD FLAP.

NOSE FLAP

FIGURE 4.- THE FORMS OF THE LEADING-EDGE AUXILIARY LIFT DEVICES INVESTIGATED.

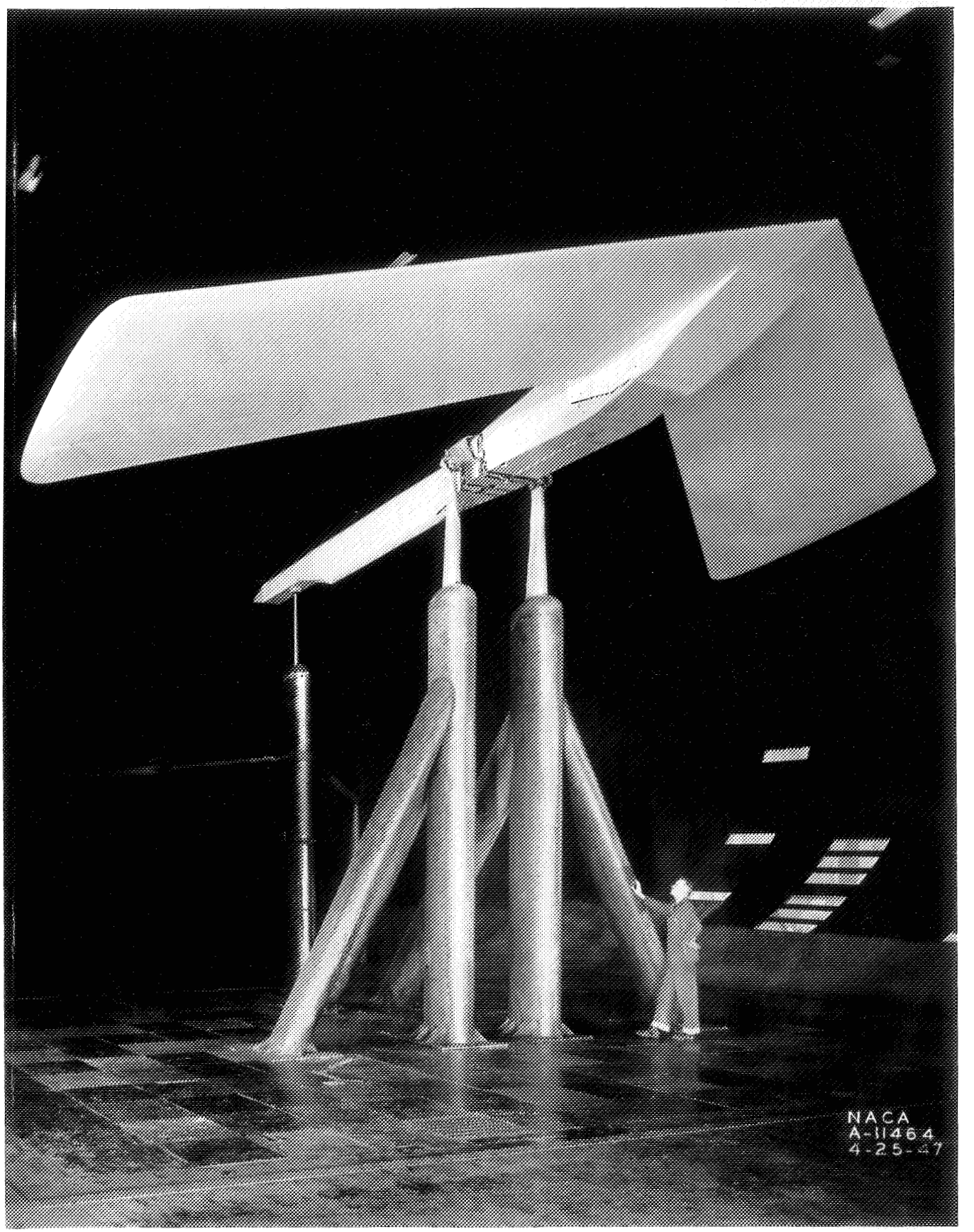

Figure 5.- The plain wing mounted on the support boom in the Ames 40- by 80-foot wind tunnel.

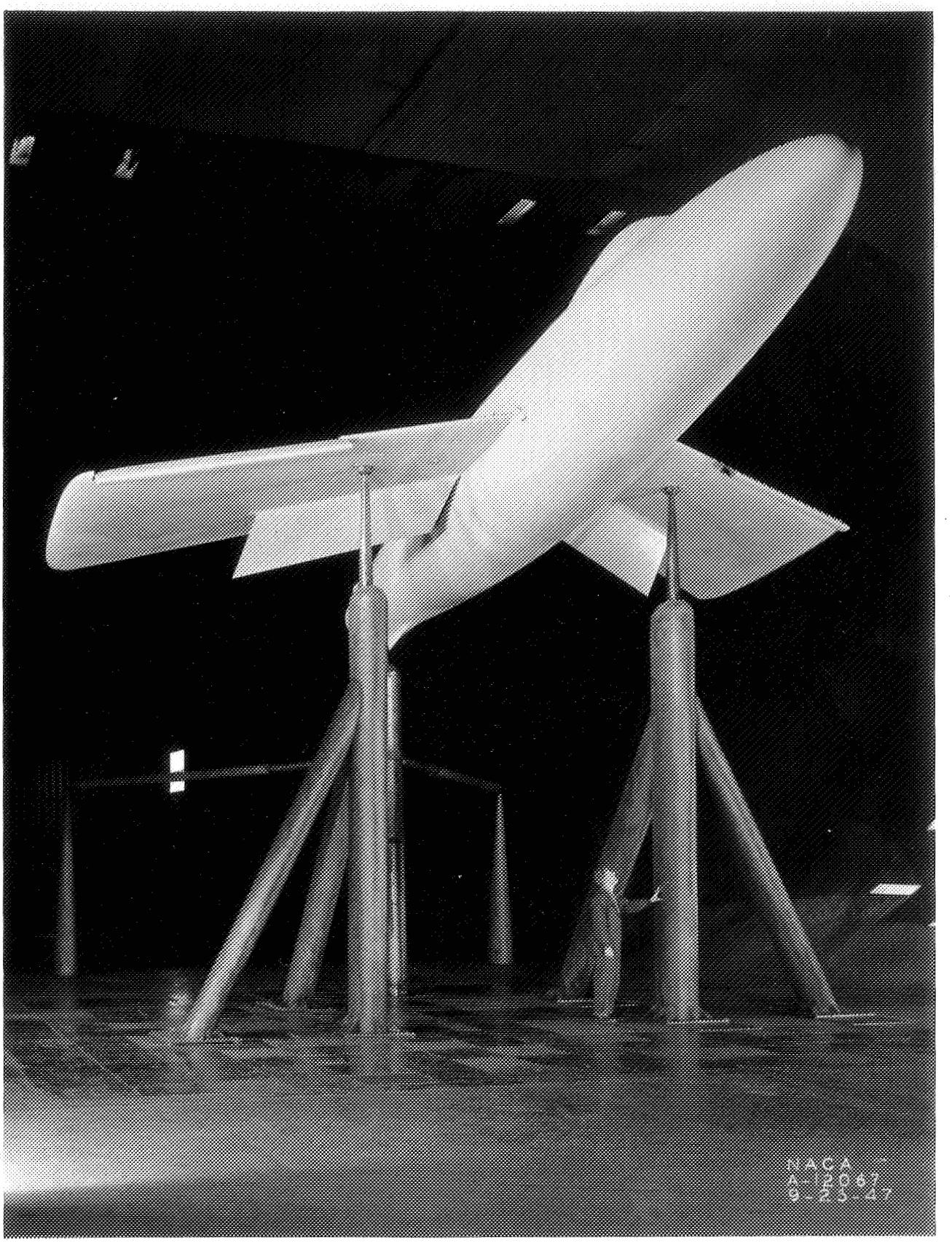

Figure 6.— The wing-fuselage installation in the Ames 40- by 80-foot wind tunnel; partial-span drooped slats and split flaps extended.

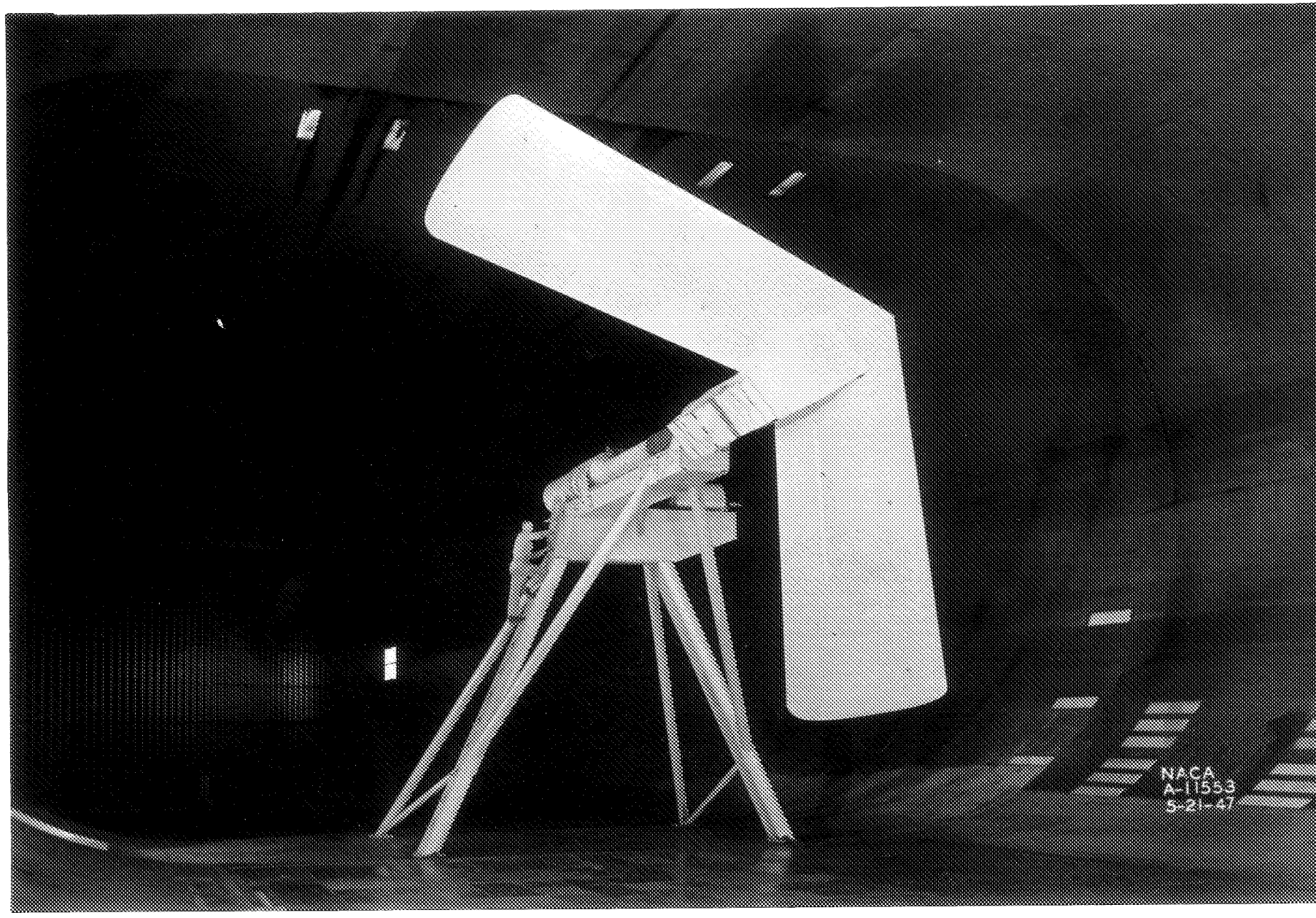

Figure 7.- View of the installation of the plain wing mounted on the rolling wing stand in the Ames 40- by 80-foot wind tunnel.

SYMBOL	CONFIGURATION	
○	WING	C.G. AT 0.25M.A.C.
□	WING-FUSELAGE	C.G. AT 0.18M.A.C.

LIFT COEFFICIENT, C_L

1.2
1.0
.8
.6
.4
.2
0
-.2

DRAG COEFFICIENT, C_D

0 .1 .2 .3 .4 .5 .6

PITCHING-MOMENT COEFFICIENT, C_m

.08 .04 0 -.04 -.08

ANGLE OF ATTACK, α, DEGREES

-4 0 4 8 12 16 20 24 28

FIGURE 8.- AERODYNAMIC CHARACTERISTICS OF THE WING AND WING-FUSELAGE COMBINATION. PLAIN WING.

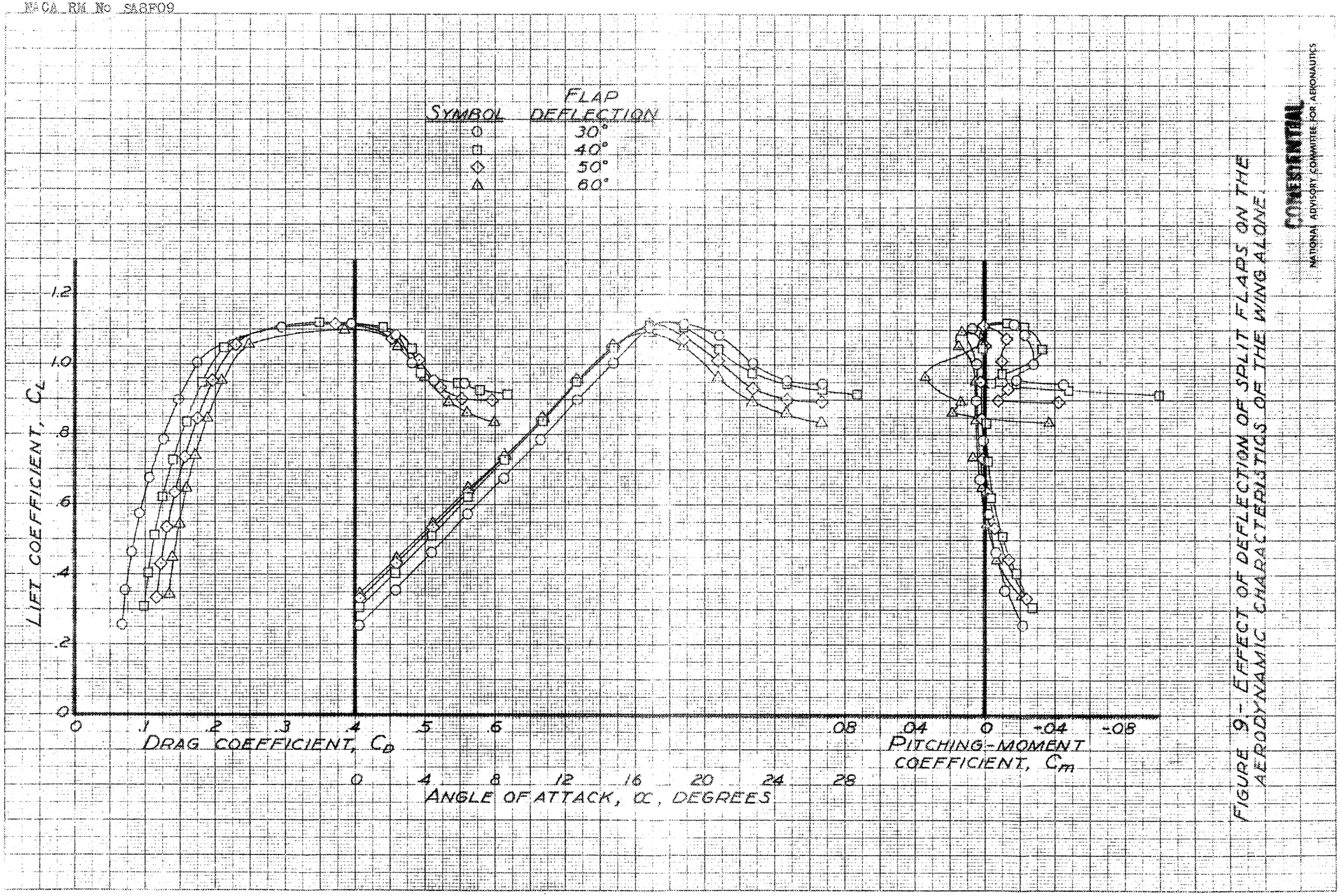

FIGURE 9.- EFFECT OF DEFLECTION OF SPLIT FLAPS ON THE AERODYNAMIC CHARACTERISTICS OF THE WING ALONE.

SYMBOL CONFIGURATION
○ WING C.G. AT 0.25 M.A.C.
□ WING-FUSELAGE C.G. AT 0.18 M.A.C.

LIFT COEFFICIENT, C_L

1.2
1.0
.8
.6
.4
.2
0

DRAG COEFFICIENT, C_D

0 .1 .2 .3 .4 .5 .6

PITCHING-MOMENT COEFFICIENT, C_m

.08 .04 0 -.04 -.08

ANGLE OF ATTACK, α, DEGREES

0 4 8 12 16 20 24 28

FIGURE 10.- AERODYNAMIC CHARACTERISTICS OF THE WING AND WING-FUSELAGE COMBINATION. F_{LAPS}, 40°.

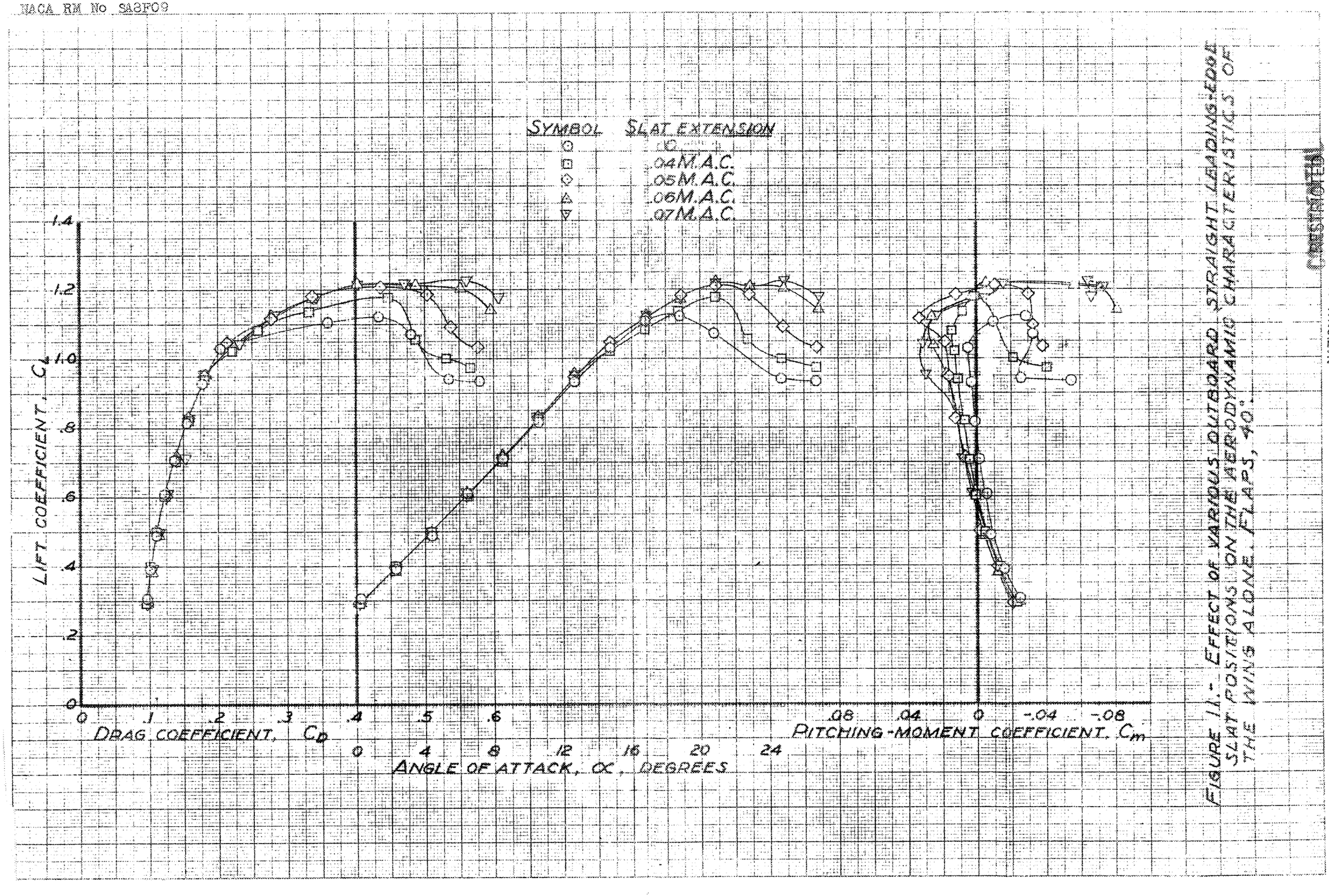

FIGURE 11.- EFFECT OF VARIOUS OUTBOARD STRAIGHT LEADING-EDGE SLAT POSITIONS ON THE AERODYNAMIC CHARACTERISTICS OF THE WING ALONE. FLAPS, 40°.

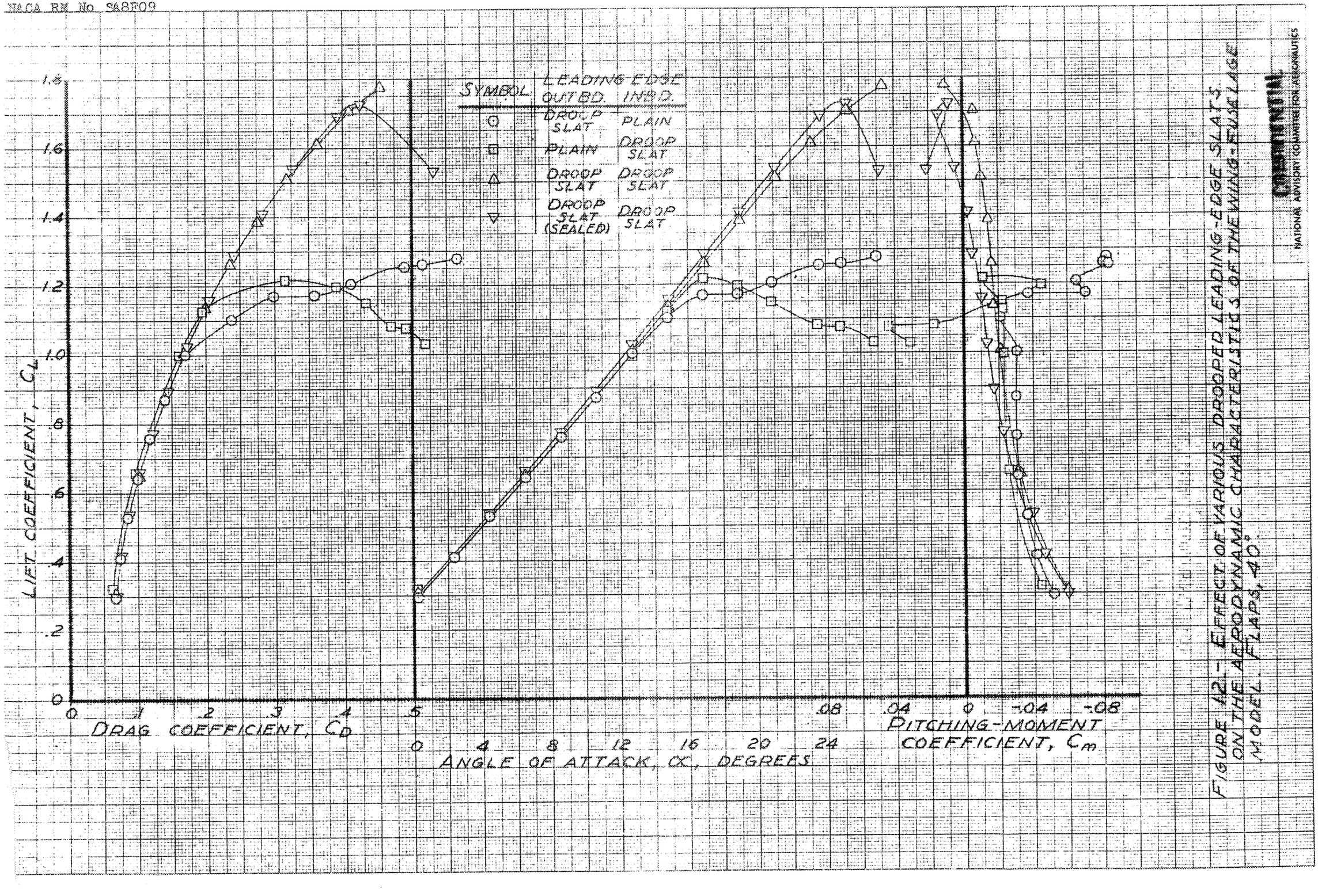

FIGURE 12.- EFFECT OF VARIOUS DROOPED LEADING-EDGE SLATS ON THE AERODYNAMIC CHARACTERISTICS OF THE WING-FUSELAGE MODEL. FLAPS, 40°.

CONFIDENTIAL

NATIONAL ADVISORY COMMITTEE FOR AERONAUTICS

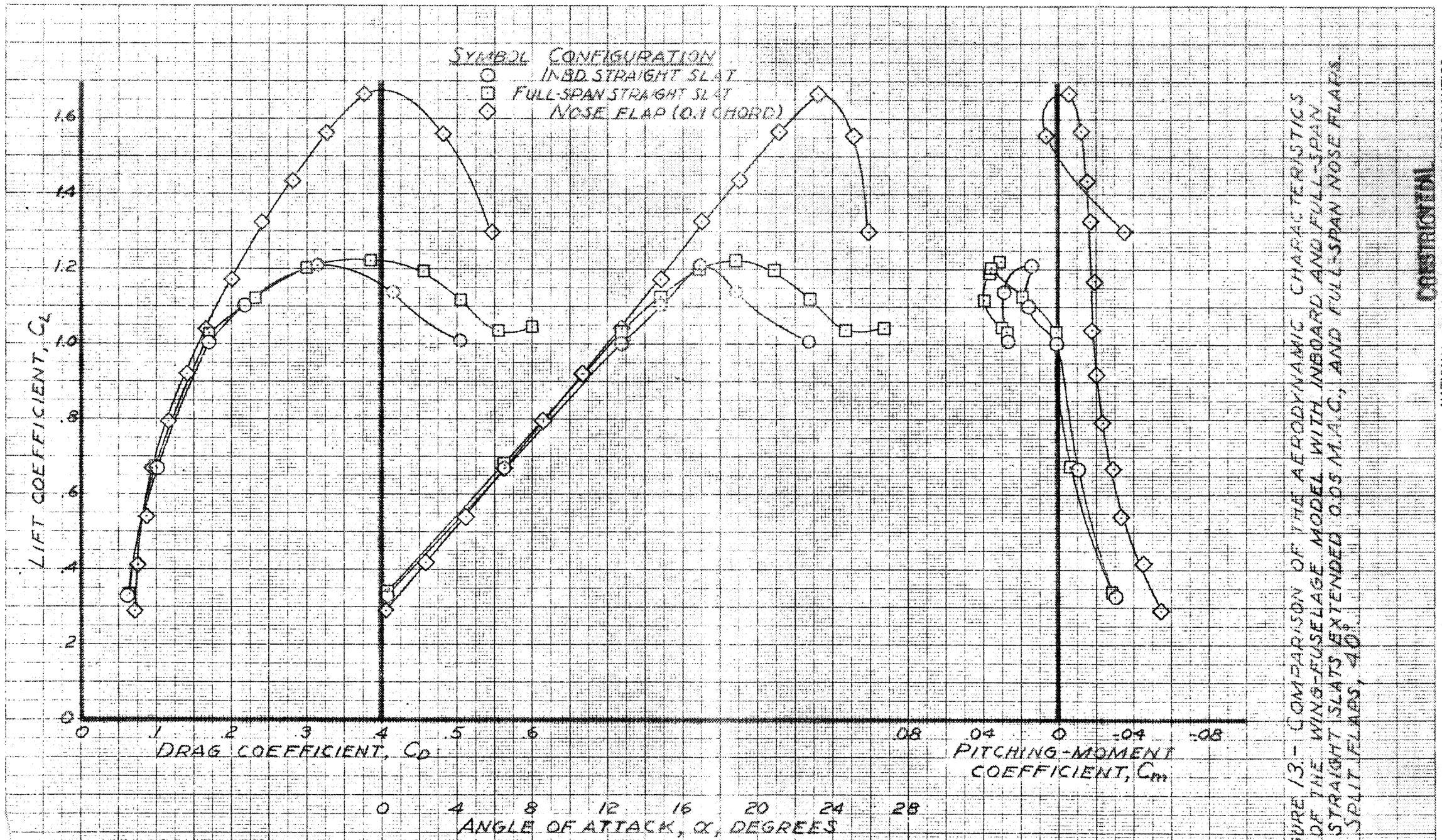

FIGURE 13.- COMPARISON OF THE AERODYNAMIC CHARACTERISTICS OF THE WING-FUSELAGE MODEL WITH INBOARD AND FULL-SPAN STRAIGHT SLATS EXTENDED 0.05 M.A.C., AND FULL-SPAN NOSE FLAPS. SPLIT FLAPS, 40°.

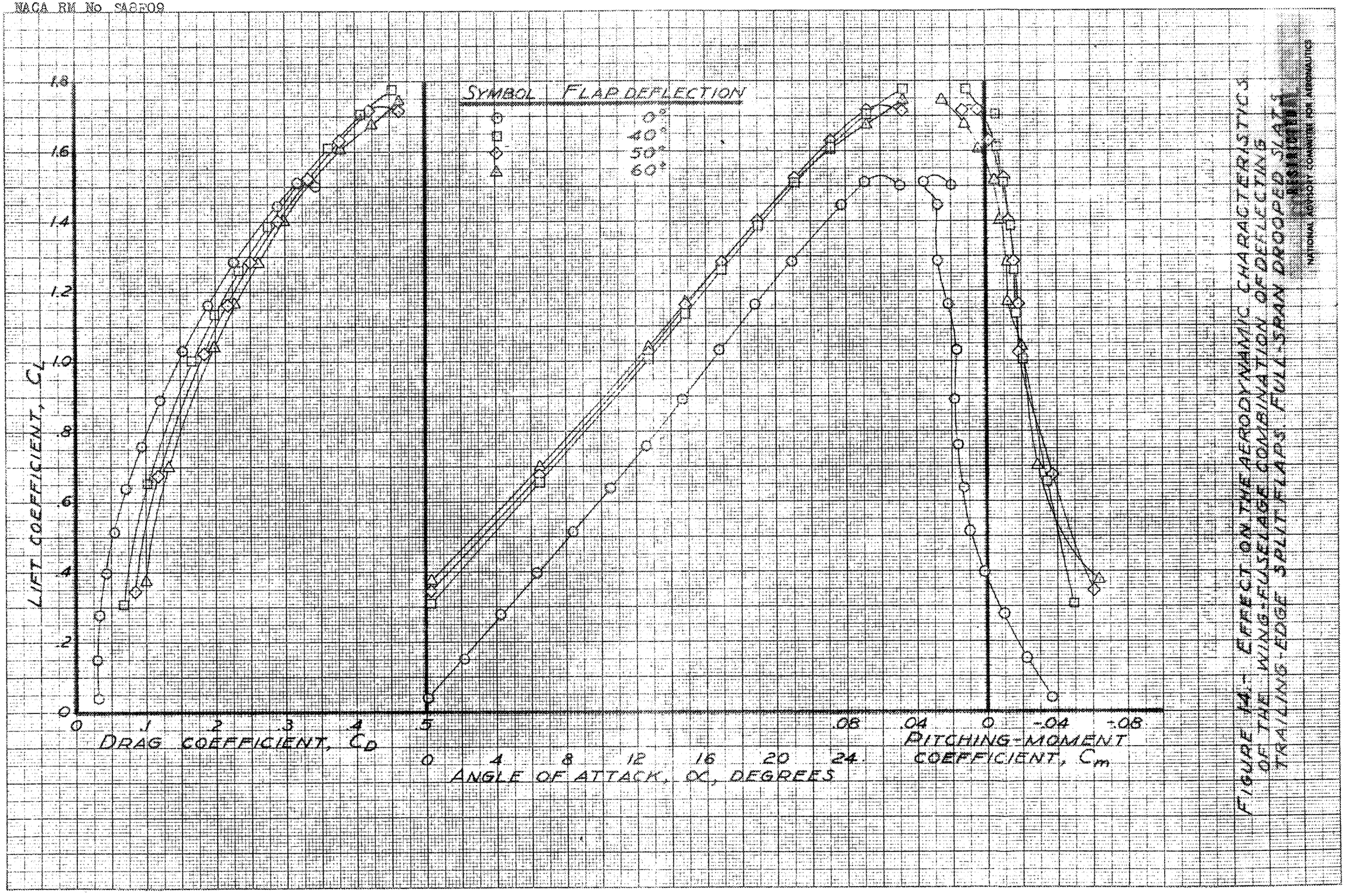

FIGURE 14.- EFFECT ON THE AERODYNAMIC CHARACTERISTICS OF THE WING-FUSELAGE COMBINATION OF DEFLECTING TRAILING-EDGE SPLIT FLAPS. FULL-SPAN DROOPED FLAP.

NATIONAL ADVISORY COMMITTEE FOR AERONAUTICS

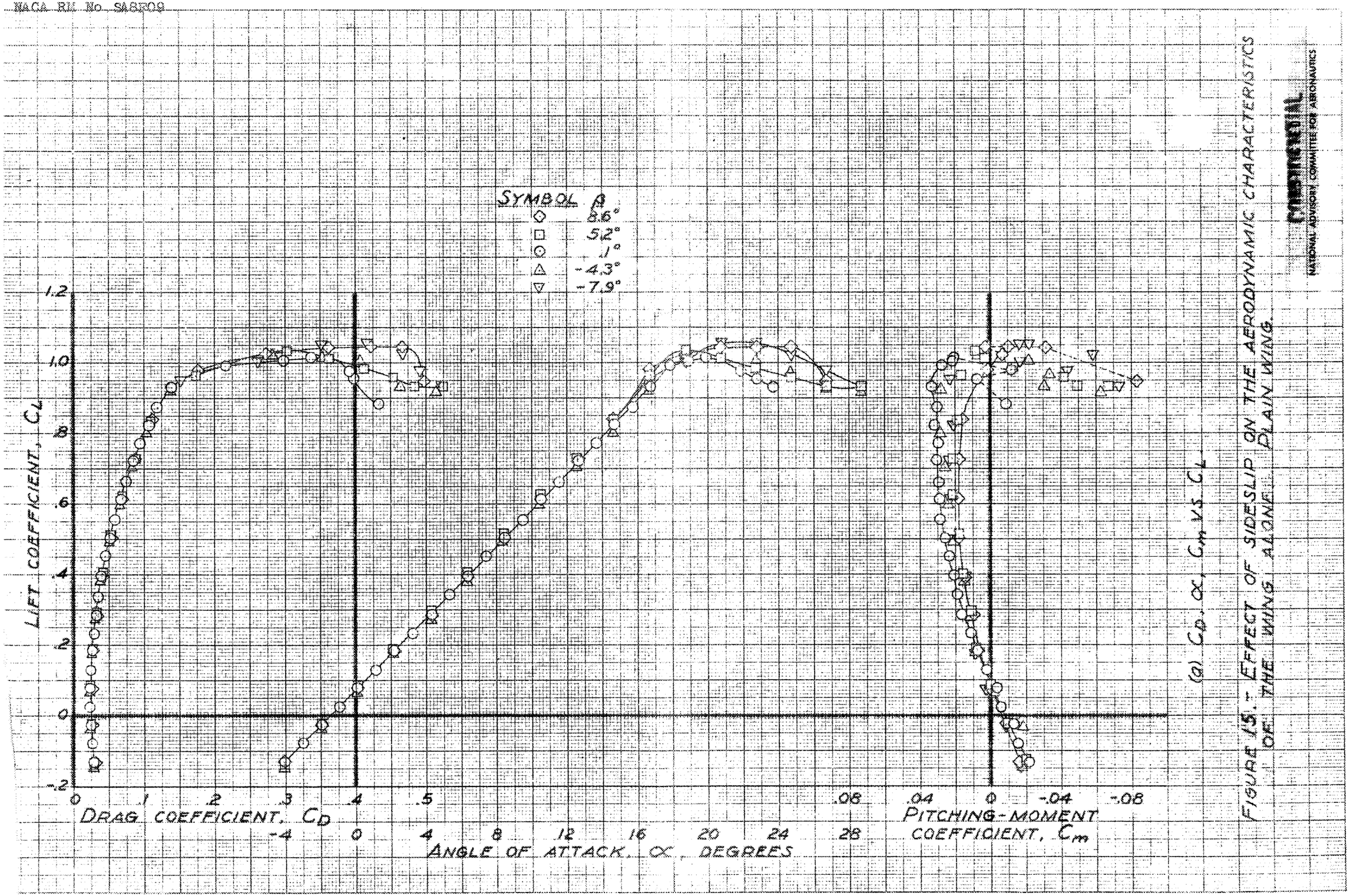

FIGURE 15.- EFFECT OF SIDESLIP ON THE AERODYNAMIC CHARACTERISTICS OF THE WING ALONE. PLAIN WING.

NATIONAL ADVISORY COMMITTEE FOR AERONAUTICS

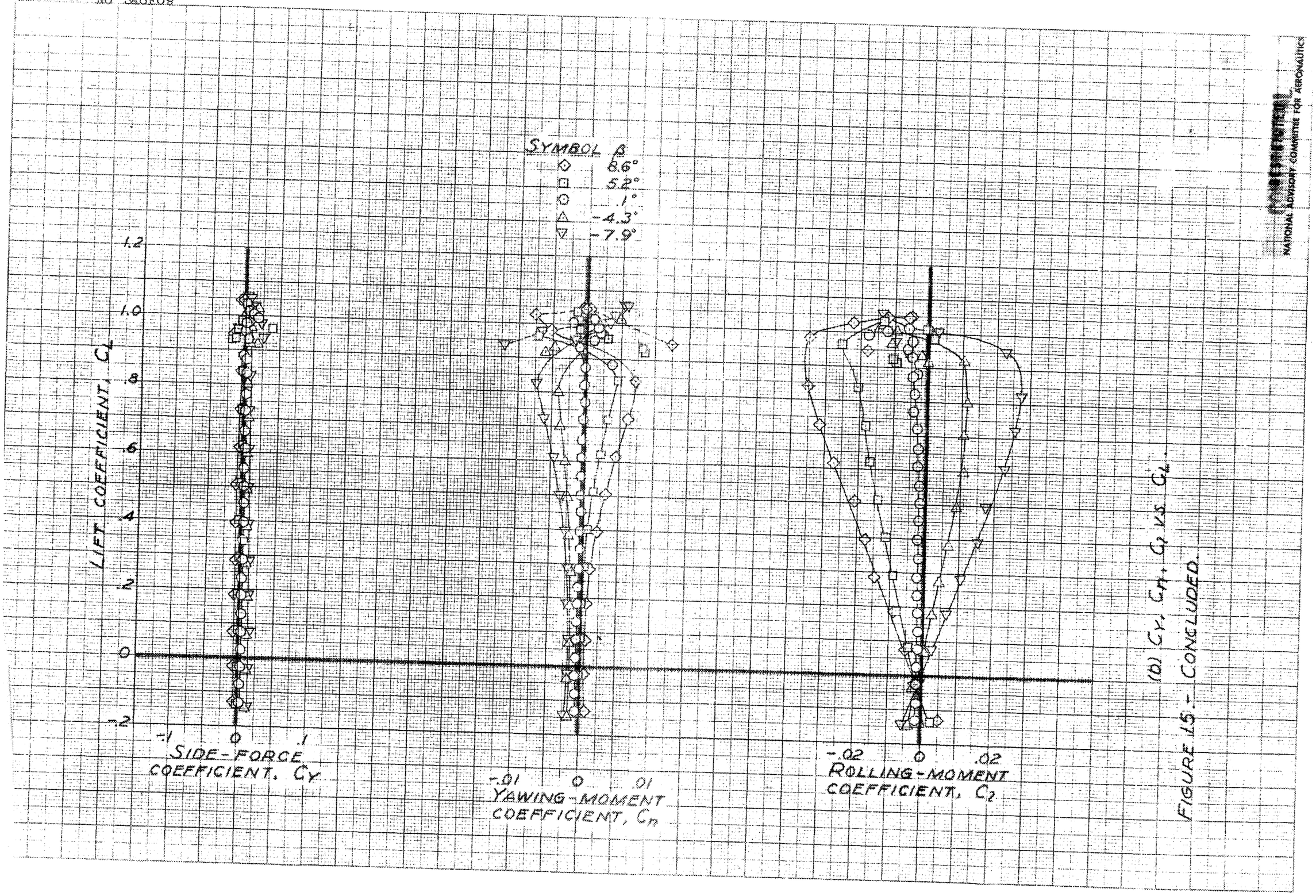

FIGURE 15.- CONCLUDED.

(b) C_Y, C_n, C_l vs. C_L.

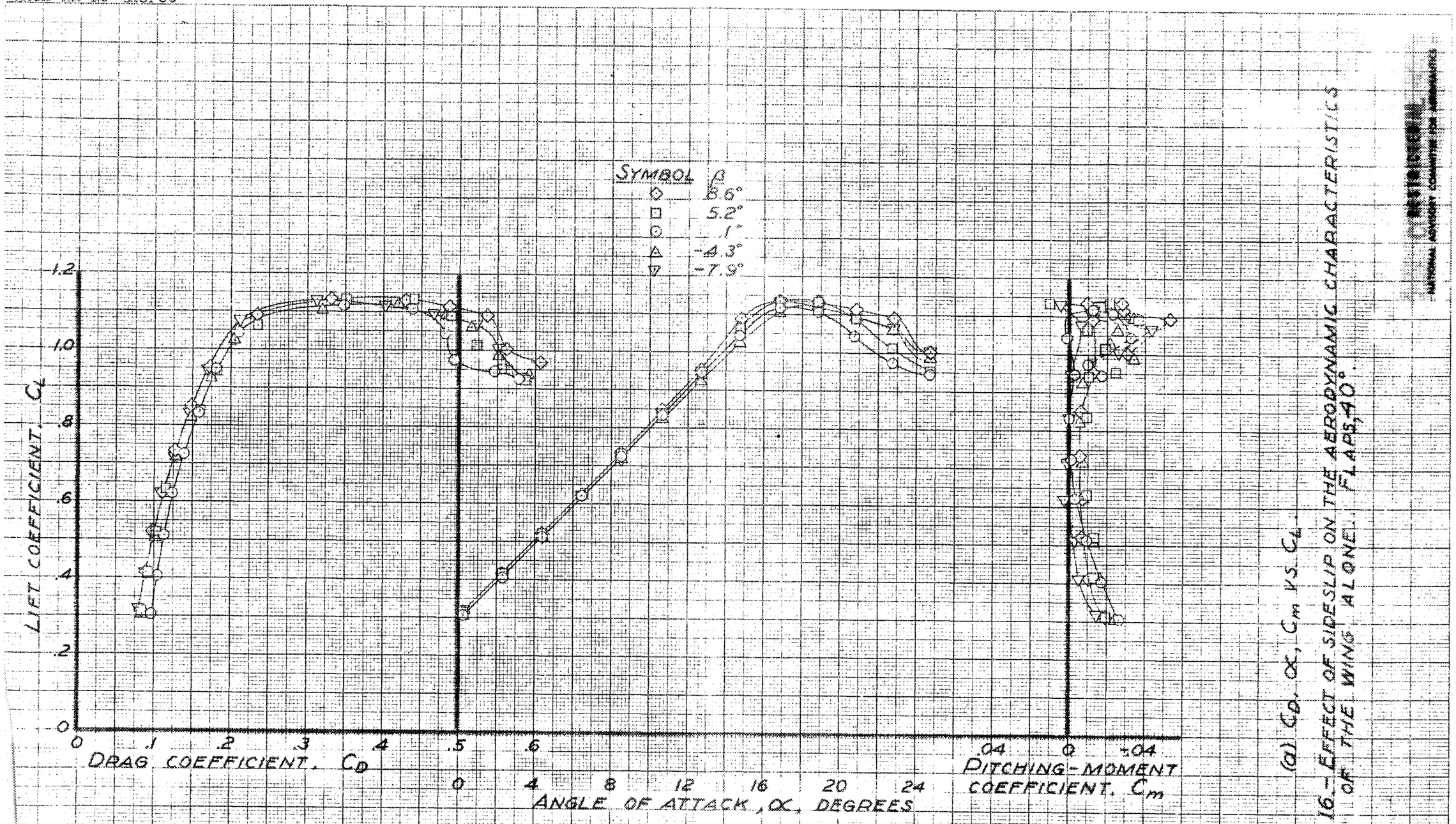

(a) C_D, α, C_m vs. C_L.

FIGURE 16.- EFFECT OF SIDESLIP ON THE AERODYNAMIC CHARACTERISTICS OF THE WING ALONE. FLAPS 40°.

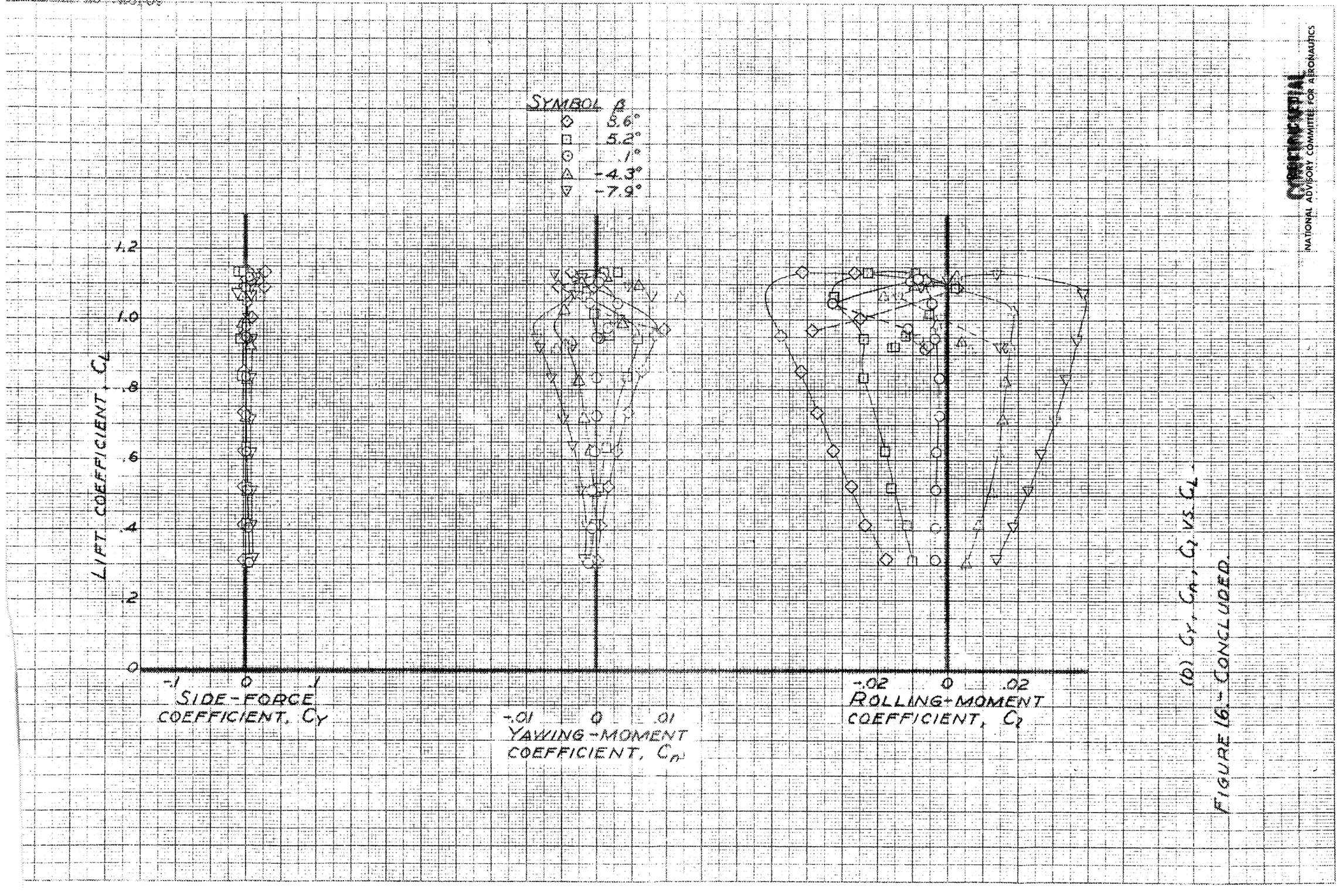

(b) C_Y, C_n, C_l vs. C_L.

FIGURE 16.- CONCLUDED.

FIGURE 17.- EFFECT OF SIDESLIP ON THE AERODYNAMIC CHARACTERISTICS OF THE WING ALONE - OUTBOARD STRAIGHT FLAPS EXTENDED.

(a) C_D, α, C_m vs. C_L.

ϕ, 0.05 M.A.C.

SYMBOL	β
◇	5.6°
□	5.2°
○	.1°
△	-4.3°
▽	-7.9°

LIFT COEFFICIENT, C_L

0 .2 .4 .6 .8 1.0 1.2

DRAG COEFFICIENT, C_D

0 .1 .2 .3 .4 .5

ANGLE OF ATTACK, α, DEGREES

0 4 8 12 16 20 24 28

PITCHING-MOMENT COEFFICIENT, C_m

.04 0 -.04 -.08

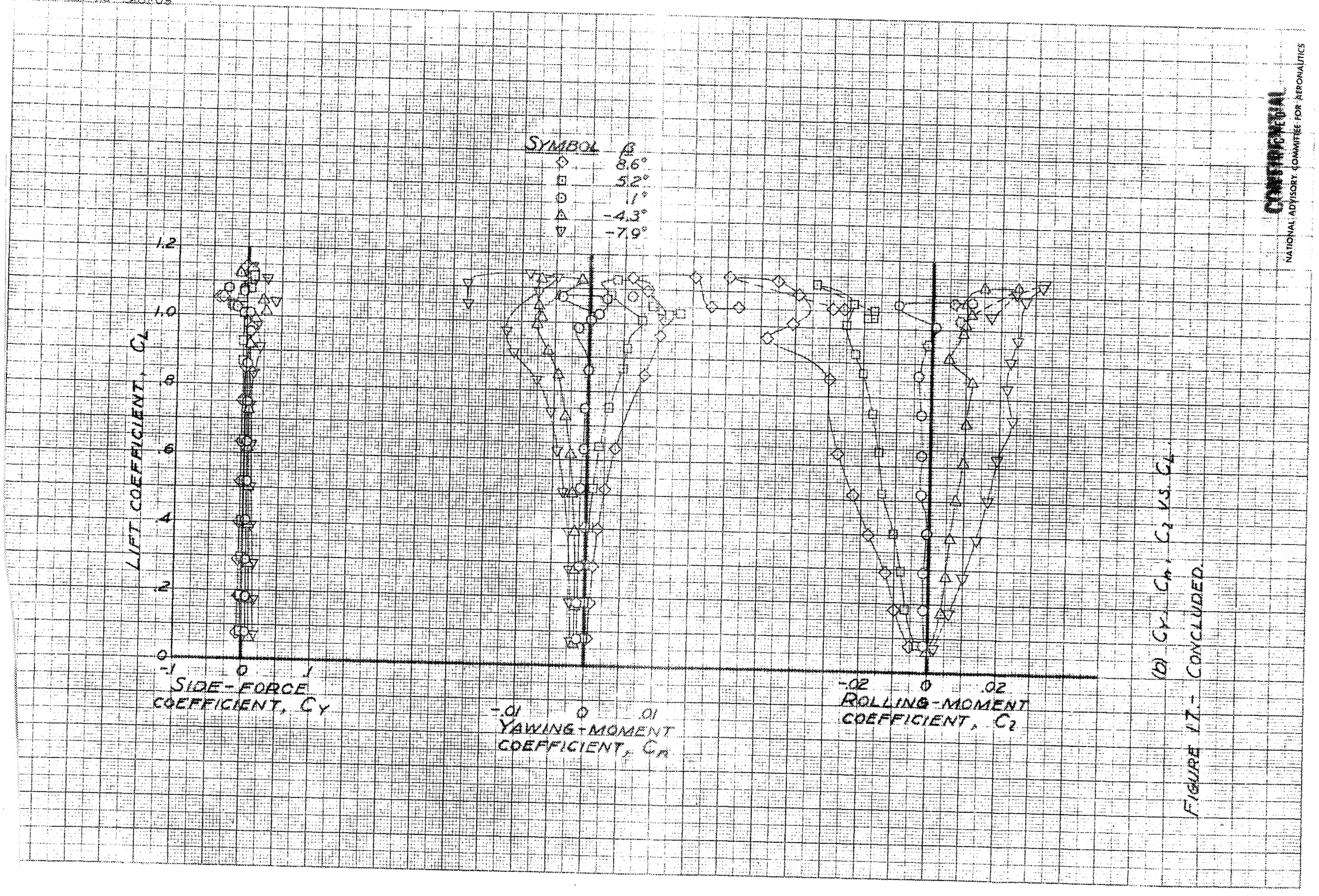

(b) C_Y, C_n, C_l vs C_L.

FIGURE 17.- CONCLUDED.

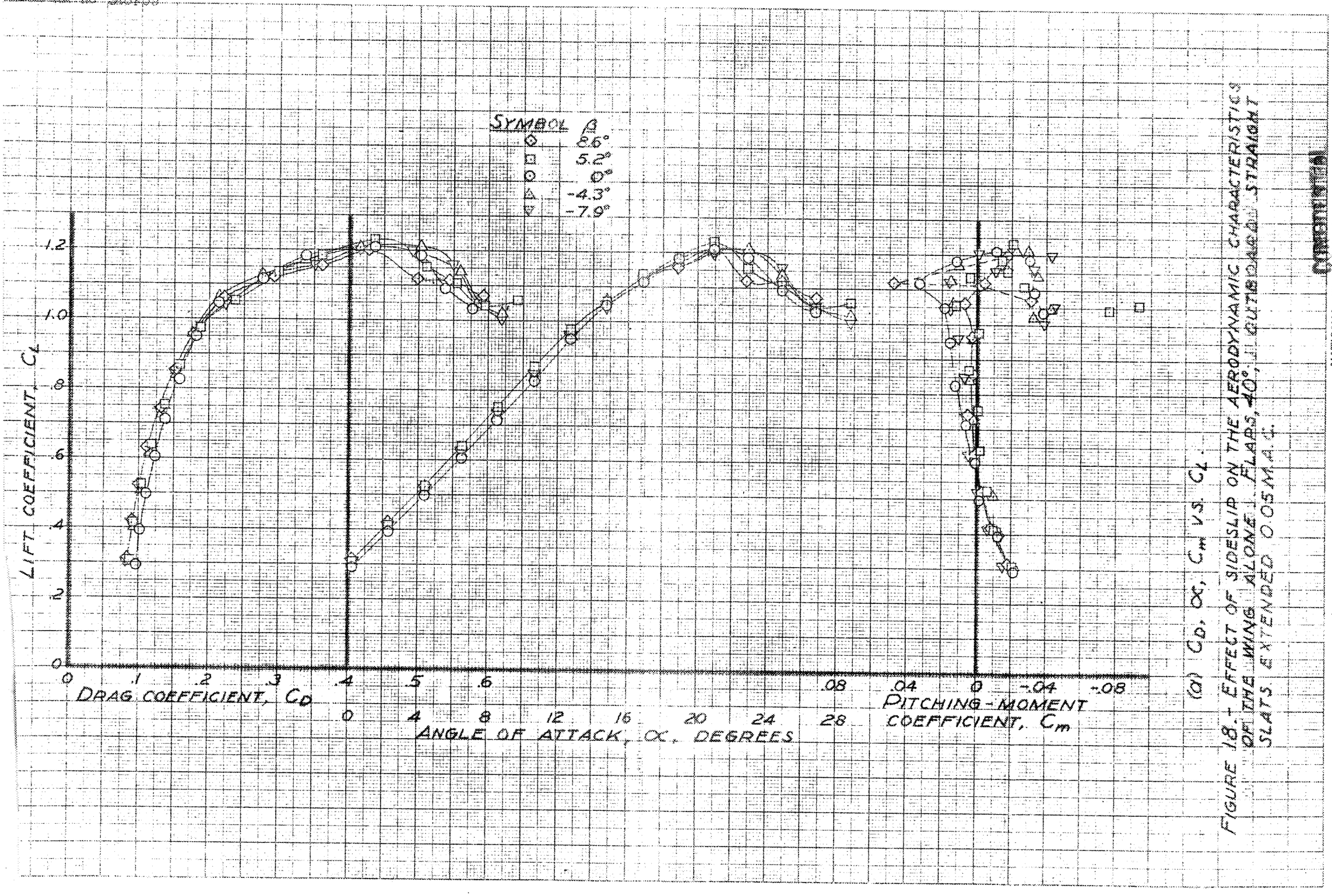

FIGURE 18.- EFFECT OF SIDESLIP ON THE AERODYNAMIC CHARACTERISTICS OF THE WING ALONE - FLAPS, 40°; LANDING GEAR RETRACTED; STRAIGHT SLATS EXTENDED. 0.05 M.A.C.

(a) C_D, α, C_m vs. C_L.

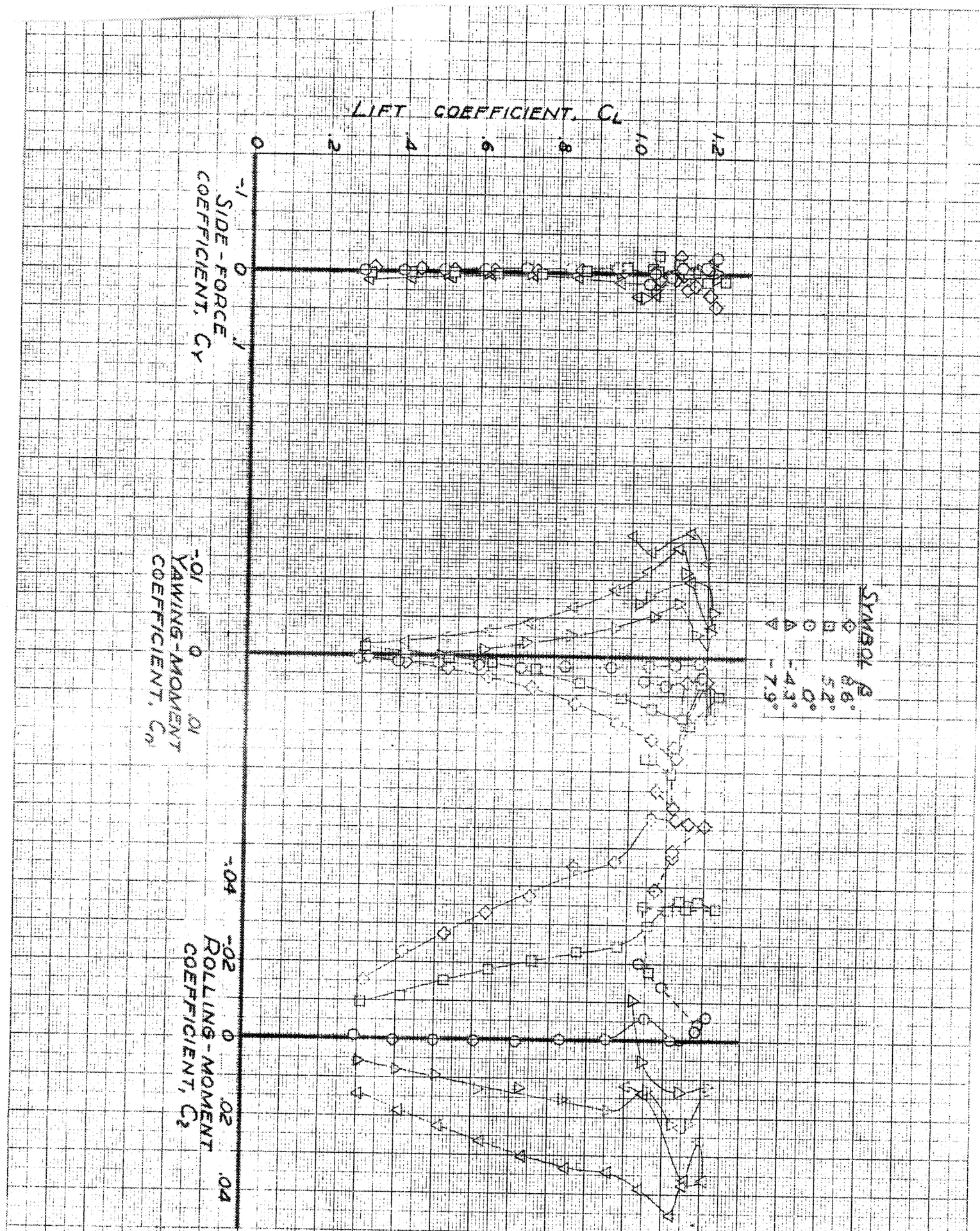

(b) C_Y, C_n, C_l vs. C_L.

FIGURE 18 - CONCLUDED.

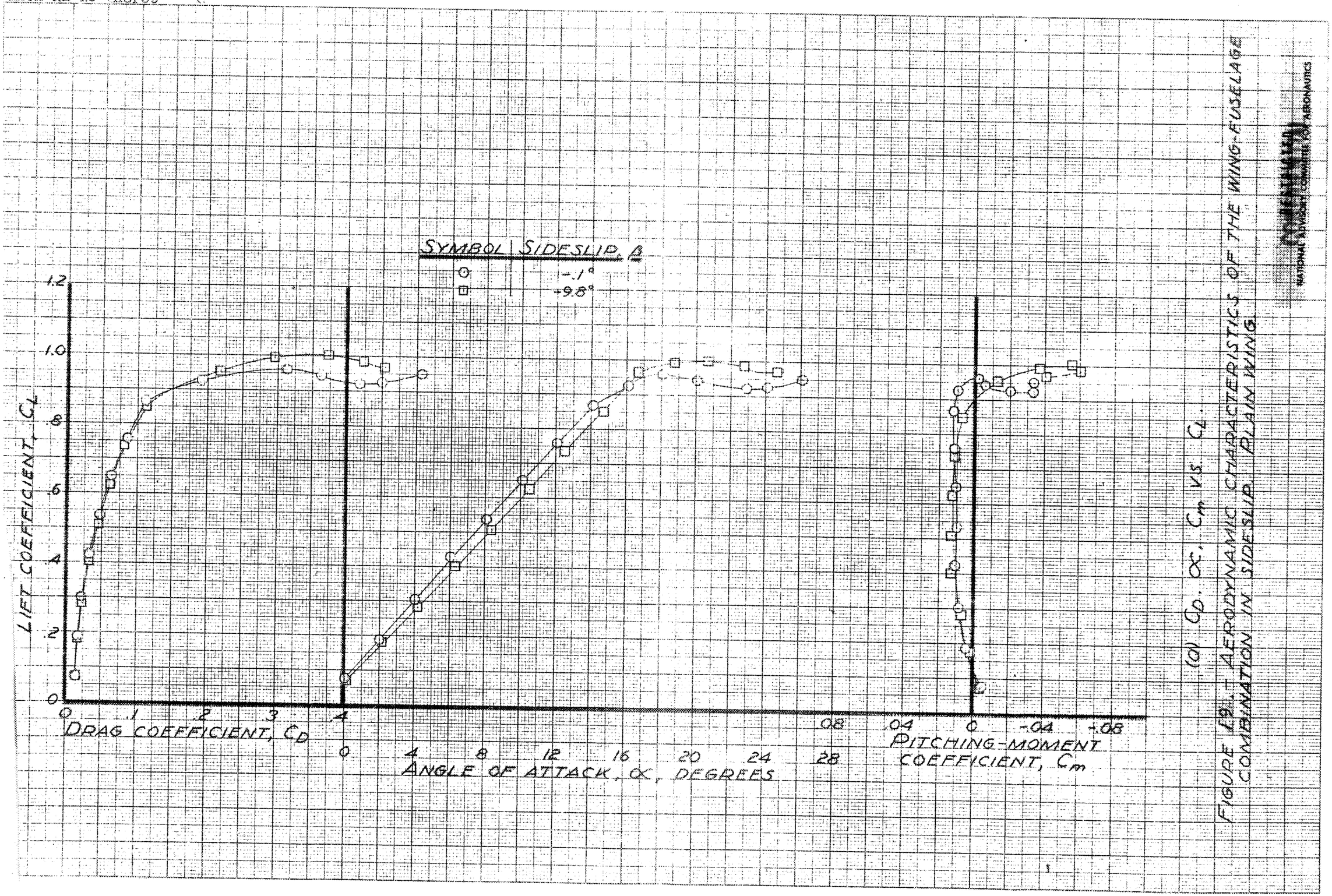

FIGURE 19.- AERODYNAMIC CHARACTERISTICS OF THE WING-FUSELAGE COMBINATION IN SIDESLIP. PLAIN WING

(a) C_D, α; C_m vs. C_L.

NATIONAL ADVISORY COMMITTEE FOR AERONAUTICS

SYMBOL	SIDESLIP, β
○	-1°
□	-9.6°

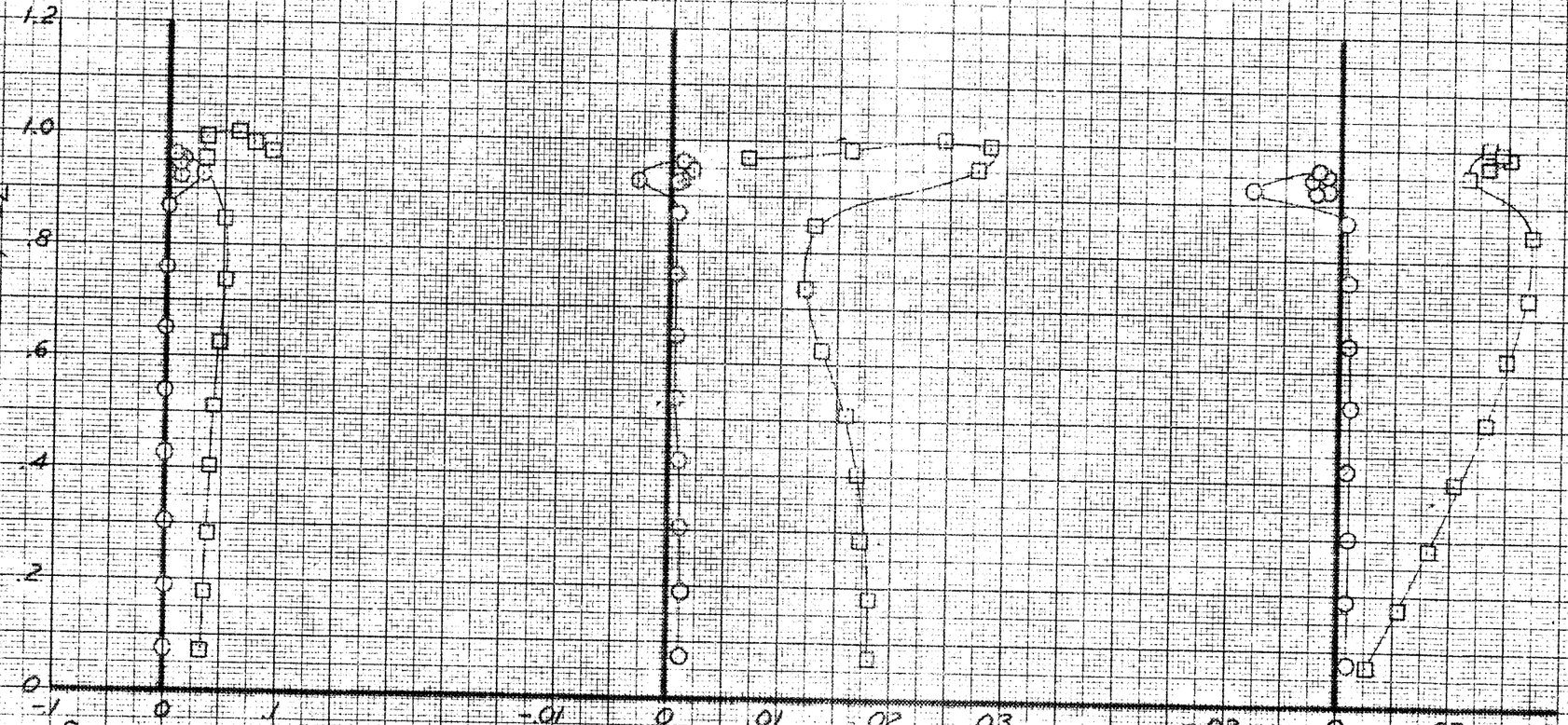

FIGURE 19.- CONCLUDED

(b) C_Y, C_n, C_l vs. C_L.

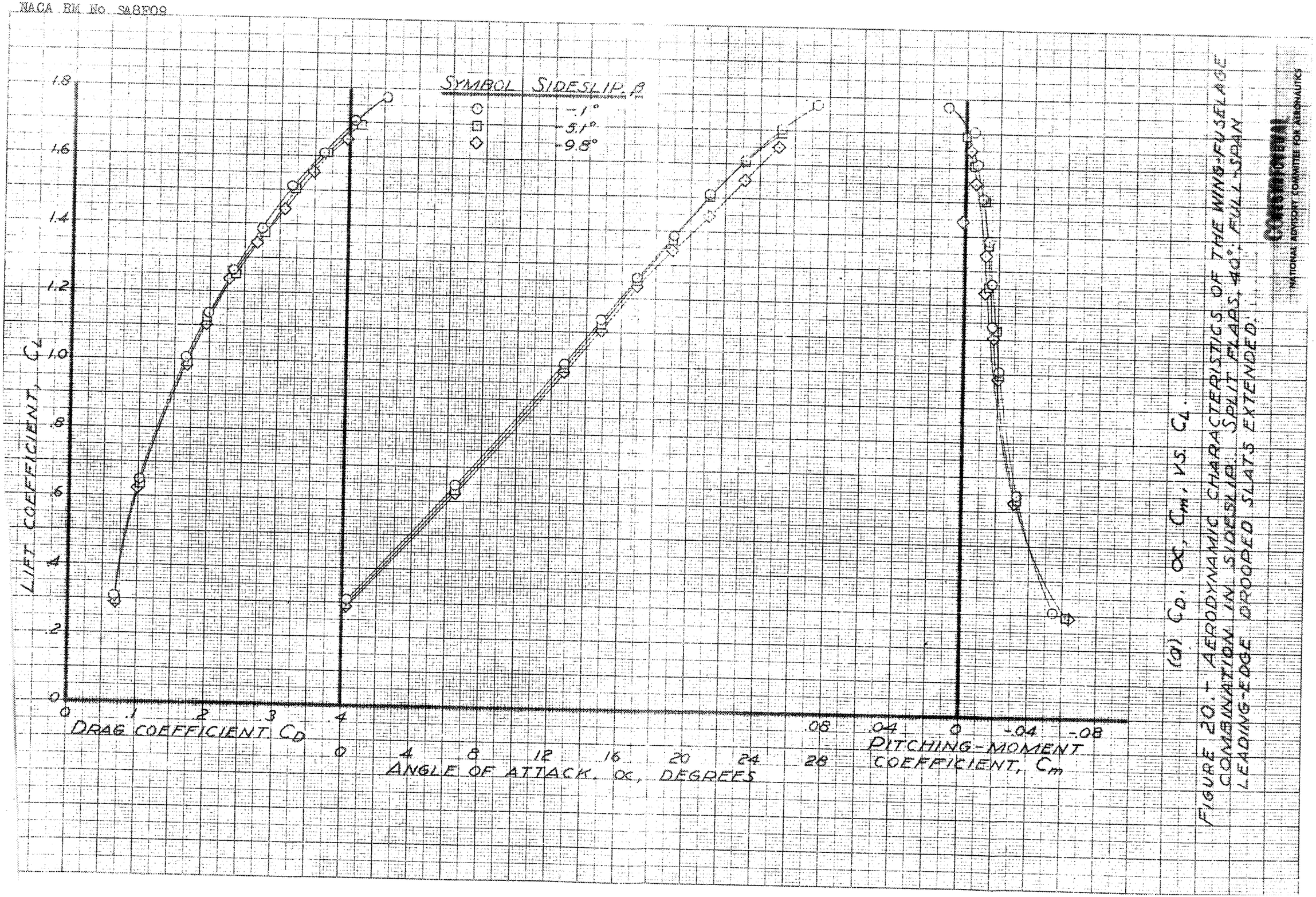

FIGURE 20.- AERODYNAMIC CHARACTERISTICS OF THE WING-FUSELAGE COMBINATION IN SIDESLIP. C_L, C_D, α, C_m, VS. (a) SPLIT FLAPS, 40°; FULL SPAN LEADING-EDGE DROOPED SLATS EXTENDED.

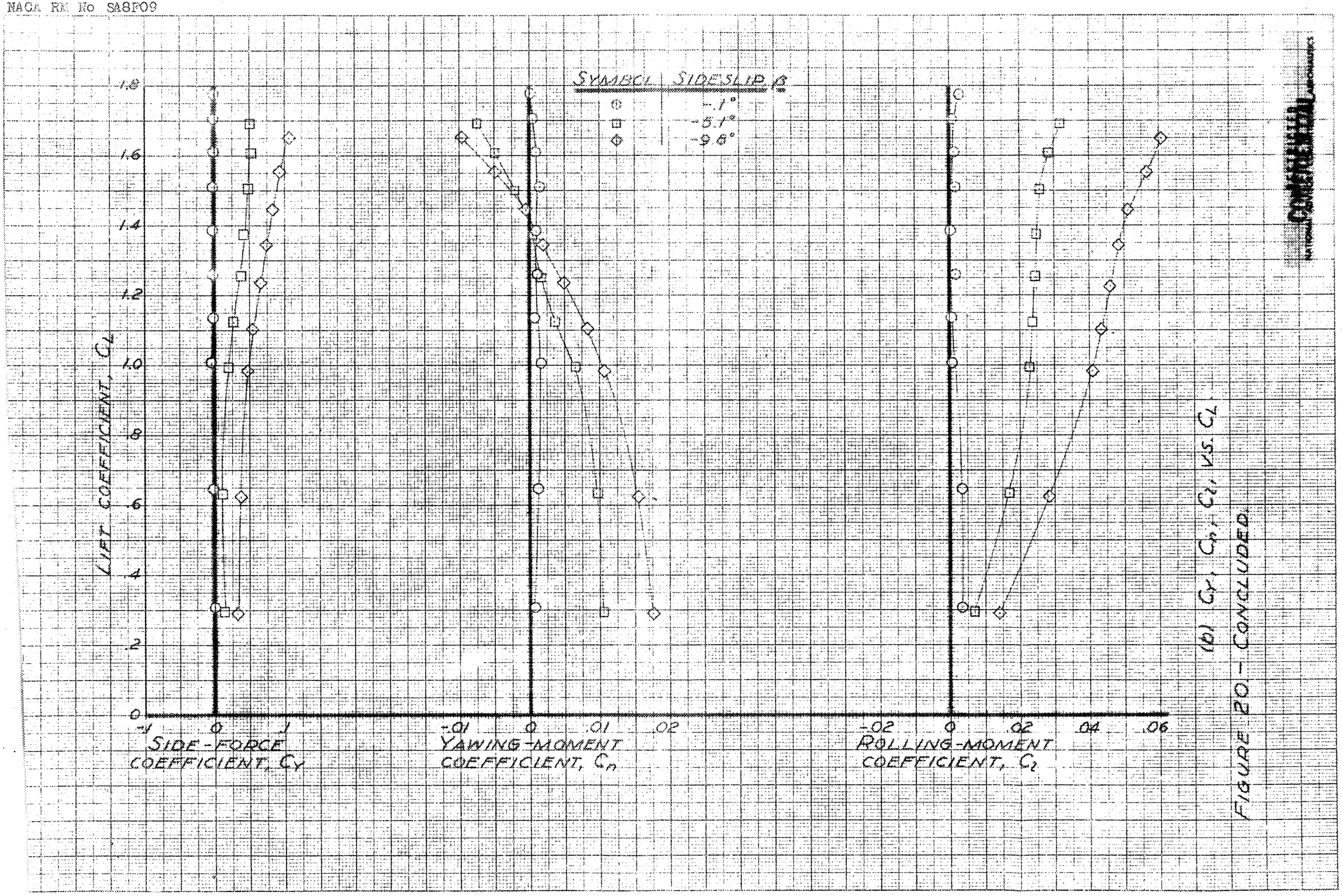

FIGURE 20 - CONCLUDED.

(b) C_Y, C_n, C_l, VS. C_L

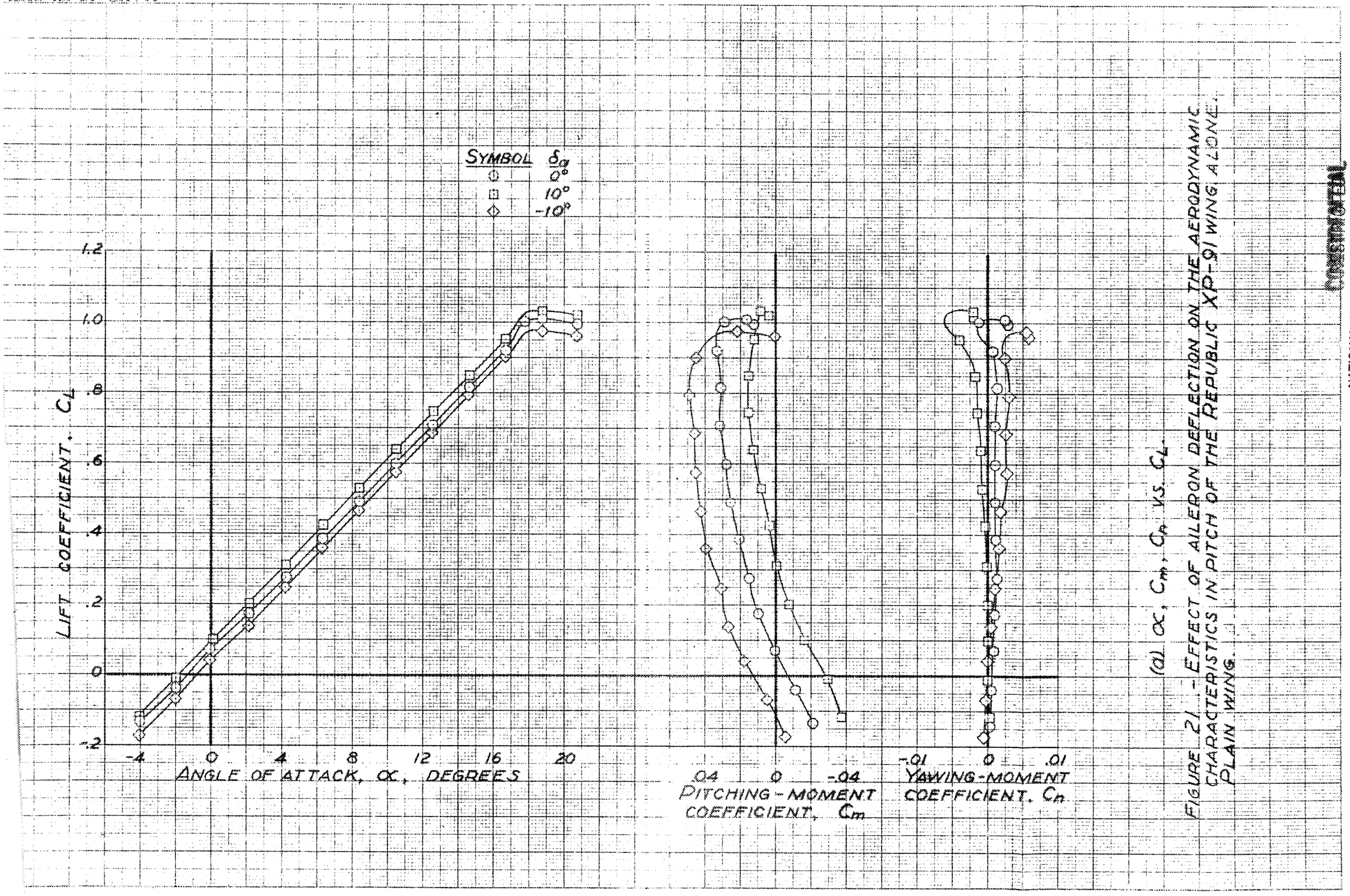

FIGURE 21.- EFFECT OF AILERON DEFLECTION ON THE AERODYNAMIC CHARACTERISTICS IN PITCH OF THE REPUBLIC XP-91 WING ALONE.
PLAIN WING.

(a) α, C_m, C_n vs. C_L.

CONFIDENTIAL

NATIONAL ADVISORY COMMITTEE FOR AERONAUTICS

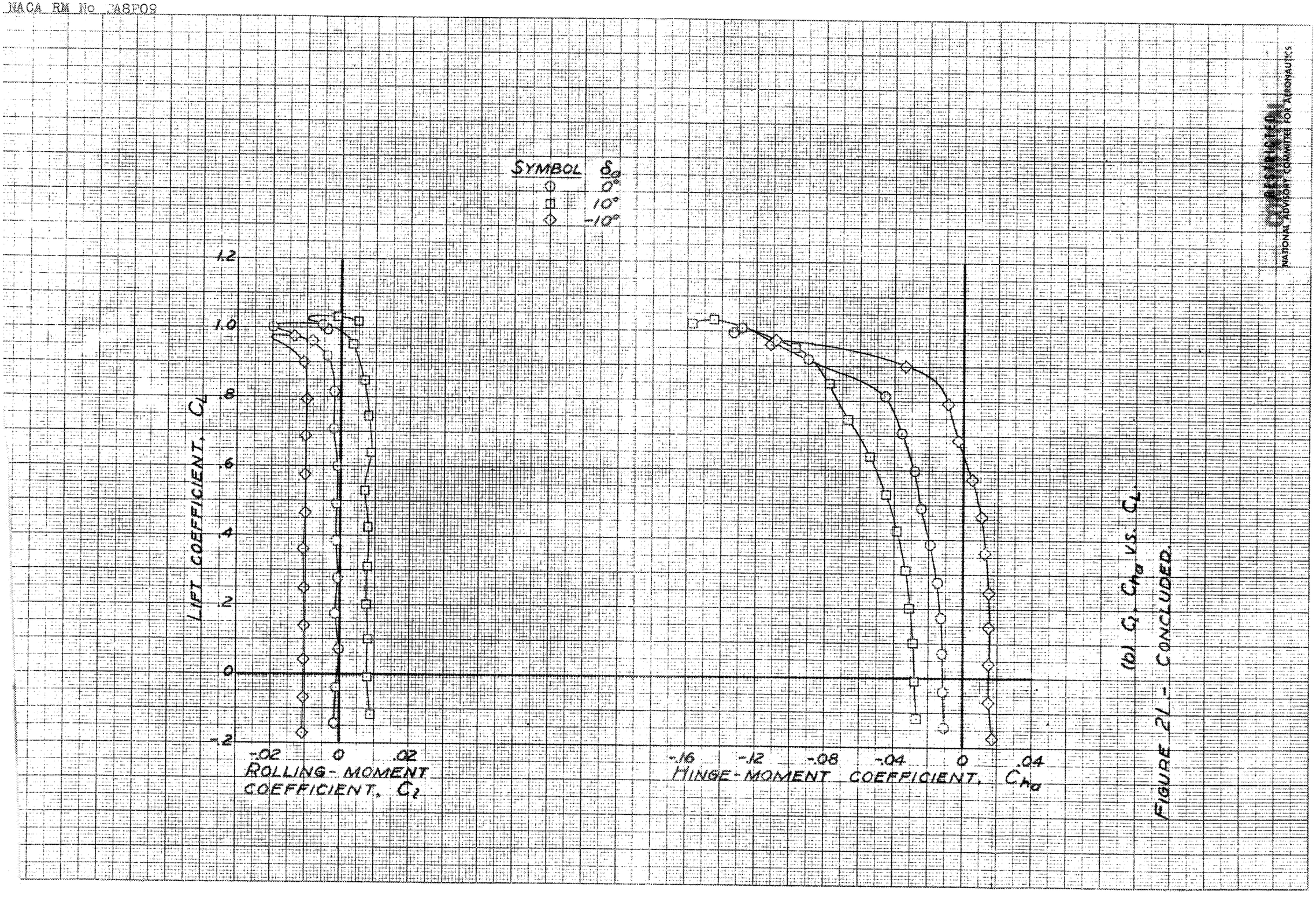

(b) C_l, C_{h_e} vs. C_L.

FIGURE 21.- CONCLUDED.

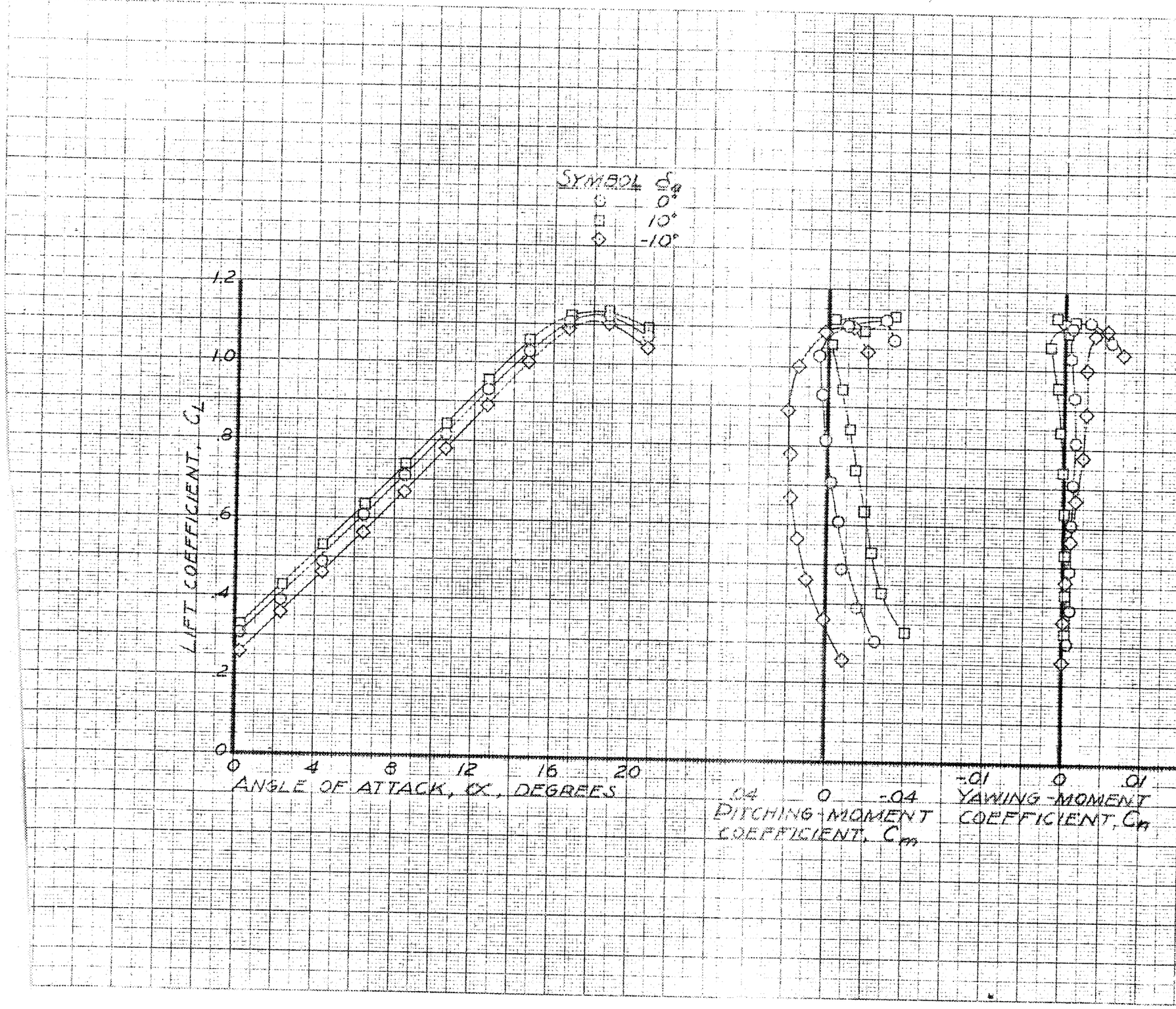

FIGURE 22. - EFFECT OF AILERON DEFLECTION ON THE AERODYNAMIC CHARACTERISTICS IN PITCH OF THE REPUBLIC XP-91 WING ALONE FLAPS, 40°.

(a) α, Cm, Cn VS. CL.

CONFIDENTIAL

NATIONAL ADVISORY COMMITTEE FOR AERONAUTICS

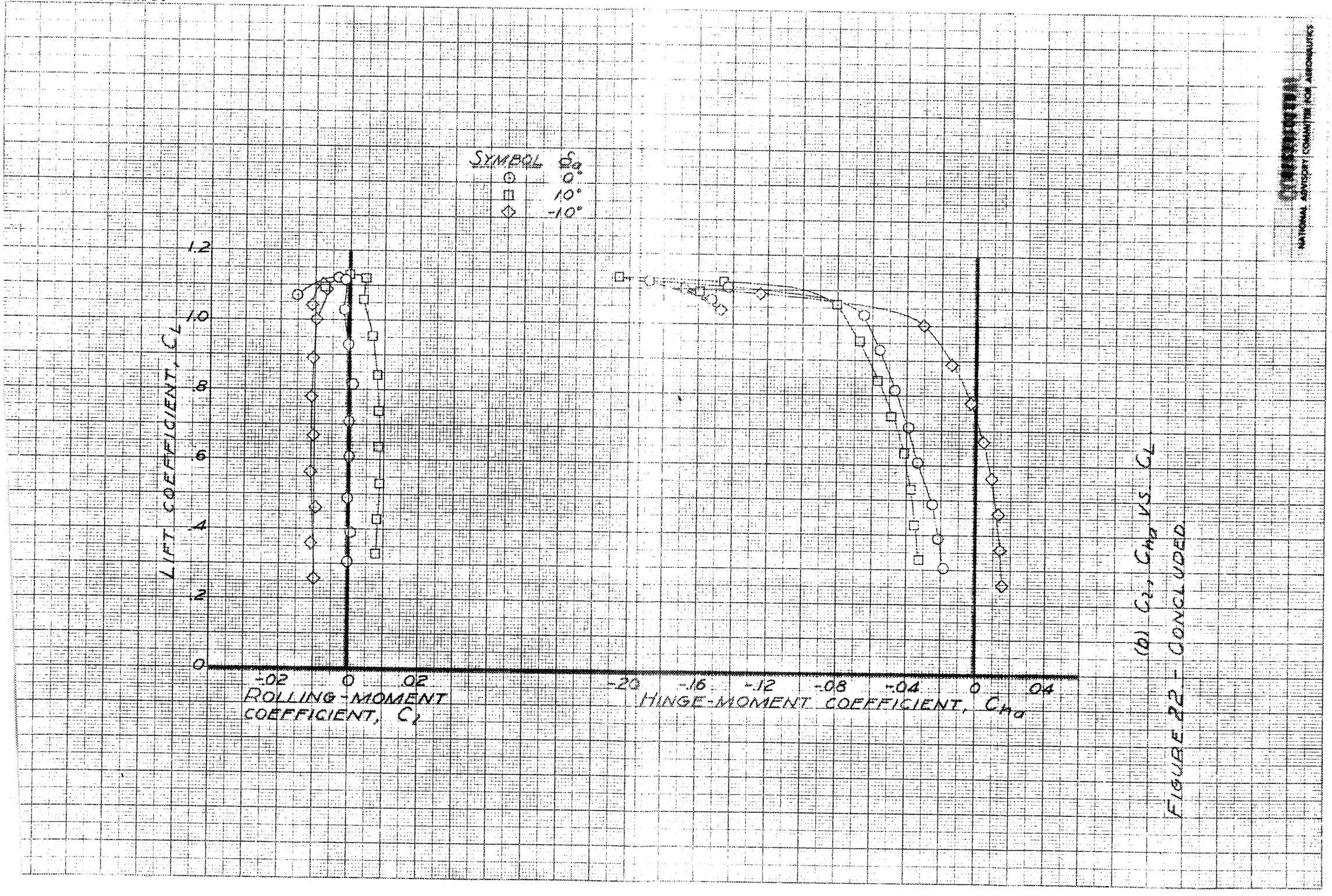

(b) C_l, C_{h_a} vs C_L

FIGURE 22 - CONCLUDED

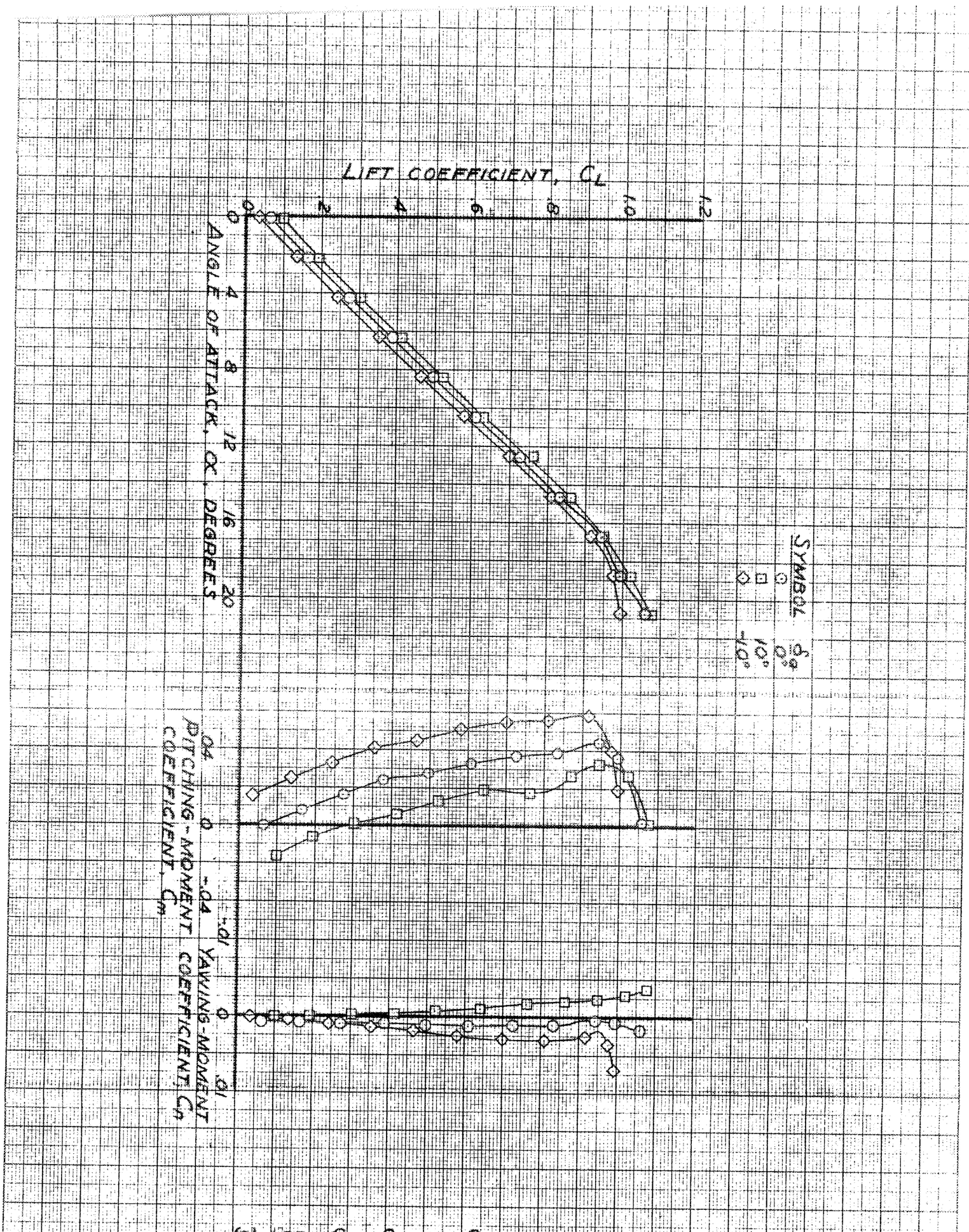

(a) α, C_m, C_n vs. C_L.

FIGURE 23.- EFFECT OF AILERON DEFLECTION ON THE AERODYNAMIC CHARACTERISTICS IN PITCH OF THE REPUBLIC XP-91 WING ALONE. OUTBOARD STRAIGHT FLAPS EXTENDED 0.05 M.A.C.

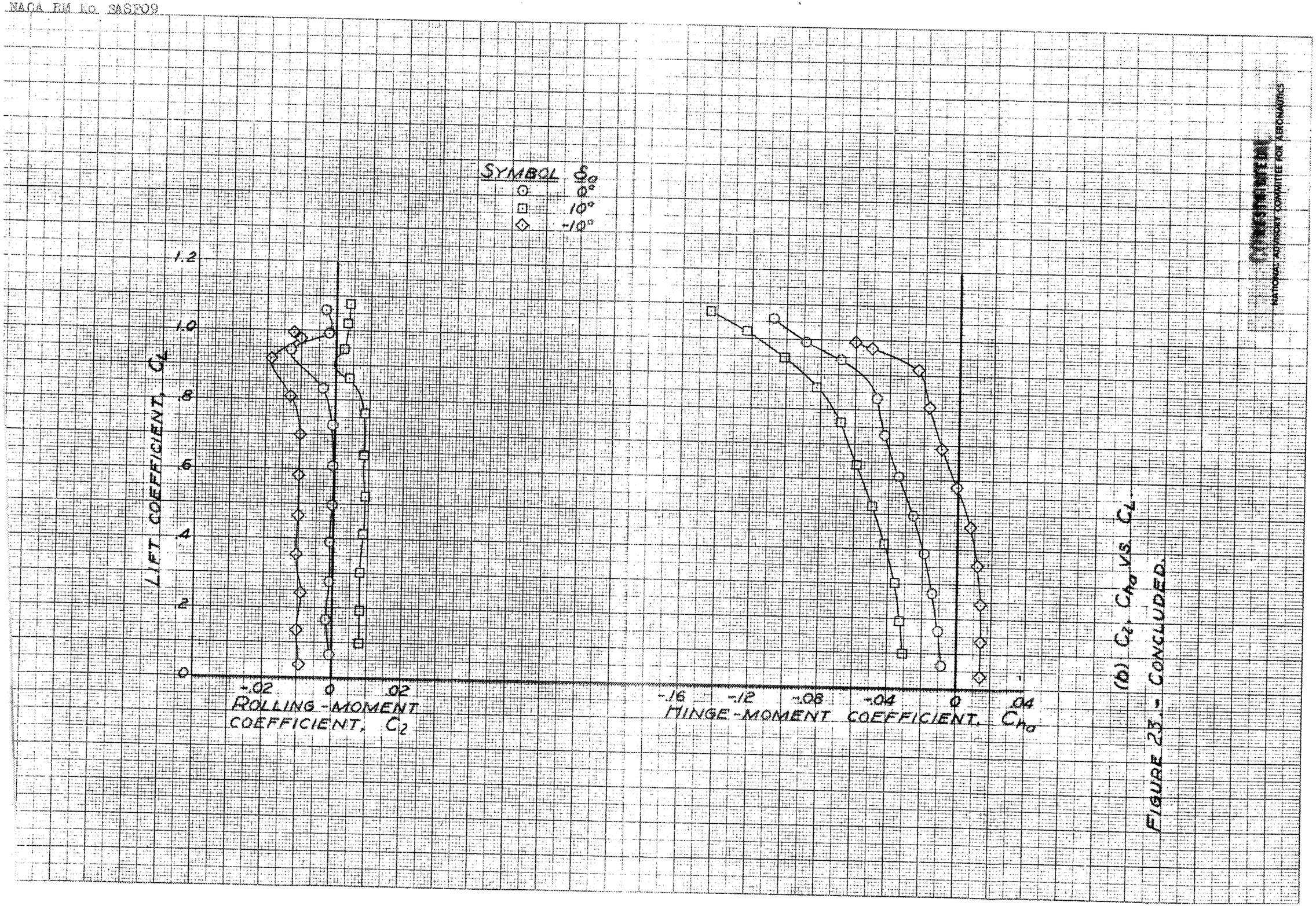

(b) C_l, C_{h_0} vs. C_L.

FIGURE 23.- CONCLUDED.

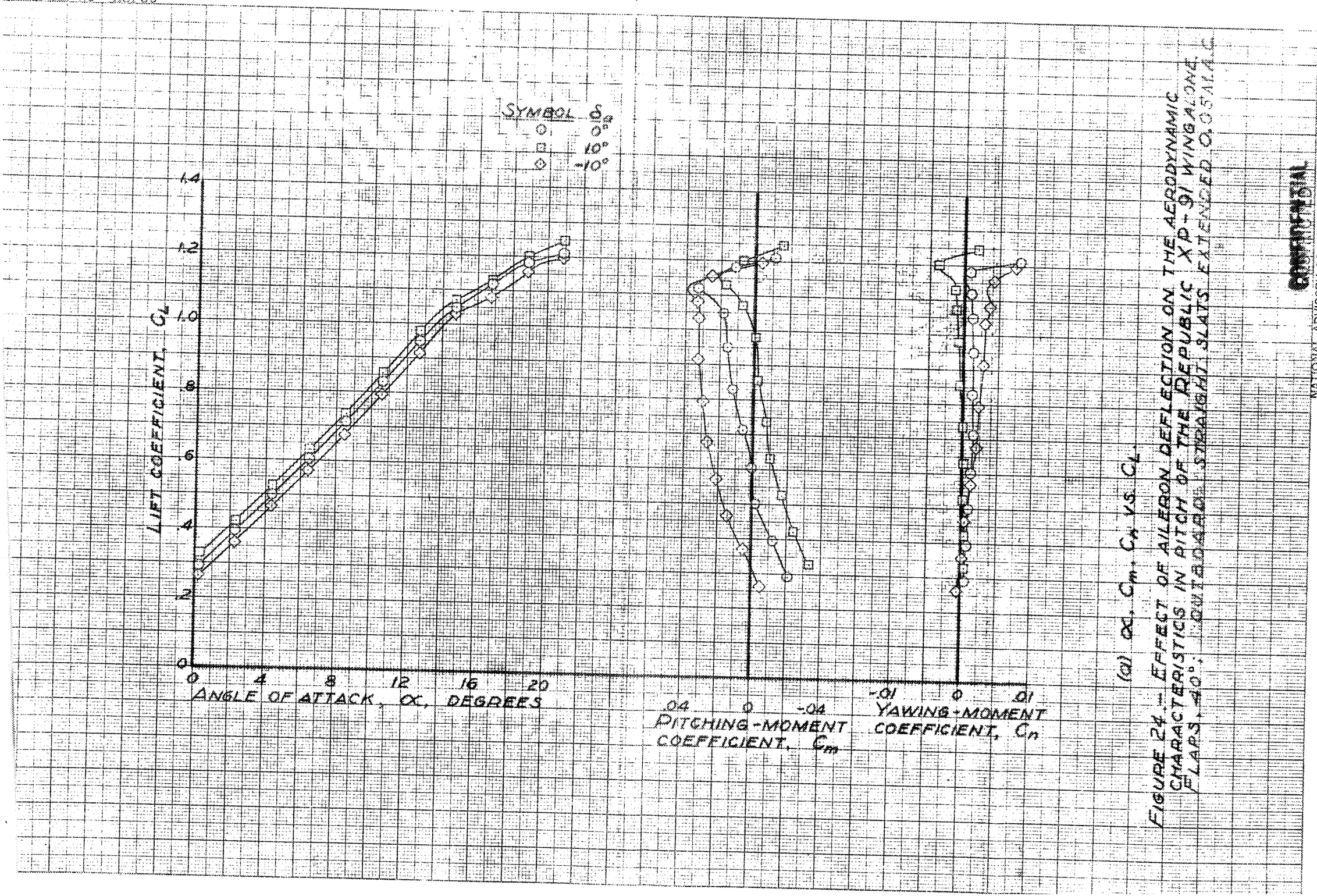

FIGURE 24.- EFFECT OF AILERON DEFLECTION ON THE AERODYNAMIC CHARACTERISTICS IN PITCH OF THE REPUBLIC XP-91 WING ALONE. FLAPS, 40°; OUTBOARD SLATS EXTENDED 0.05 MAC.

(a) α, C_m, C_n vs. C_L.

CONFIDENTIAL

NATIONAL ADVISORY COMMITTEE FOR AERONAUTICS

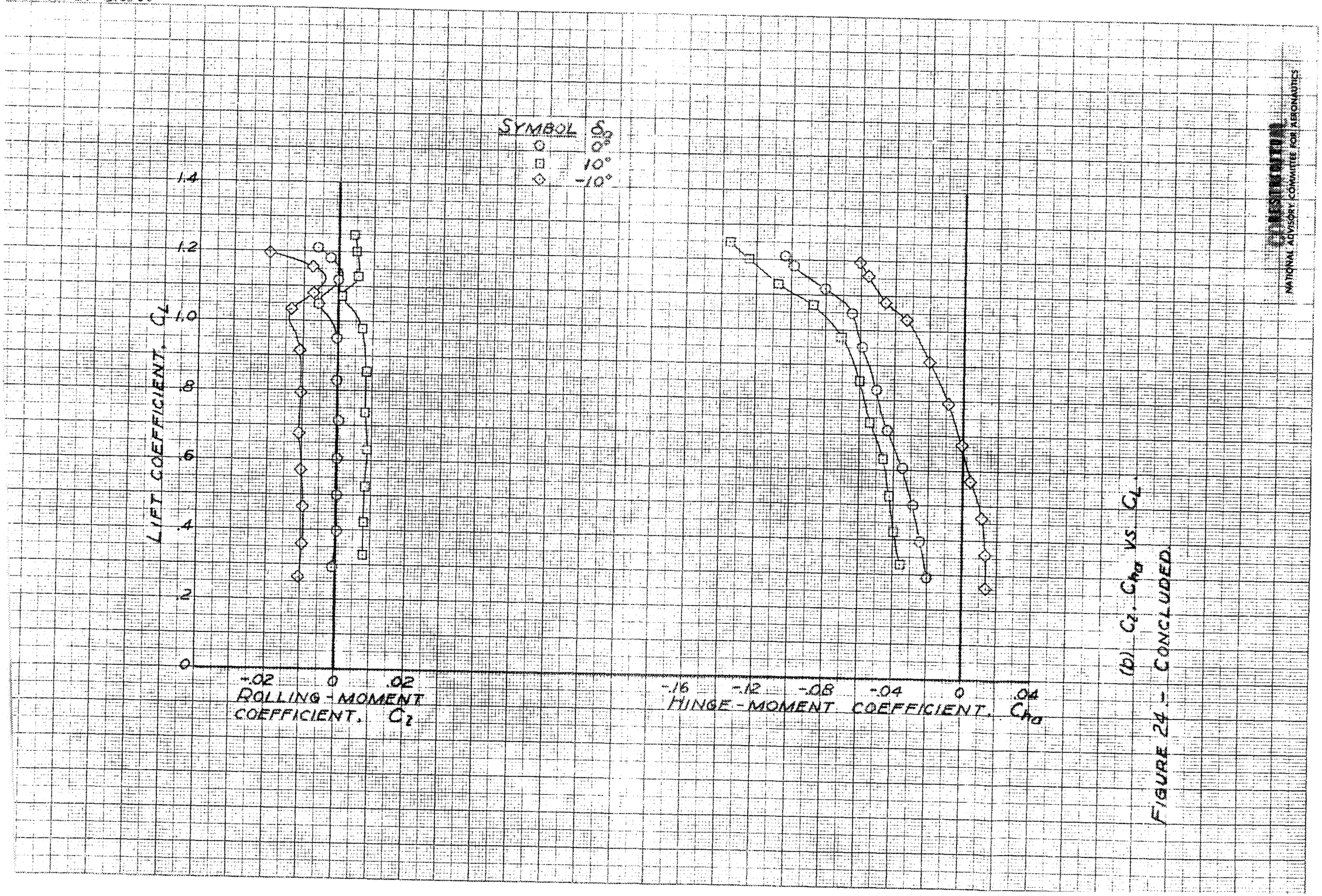

(b) C_l, C_{h_α} vs. C_L.

FIGURE 24.- CONCLUDED.

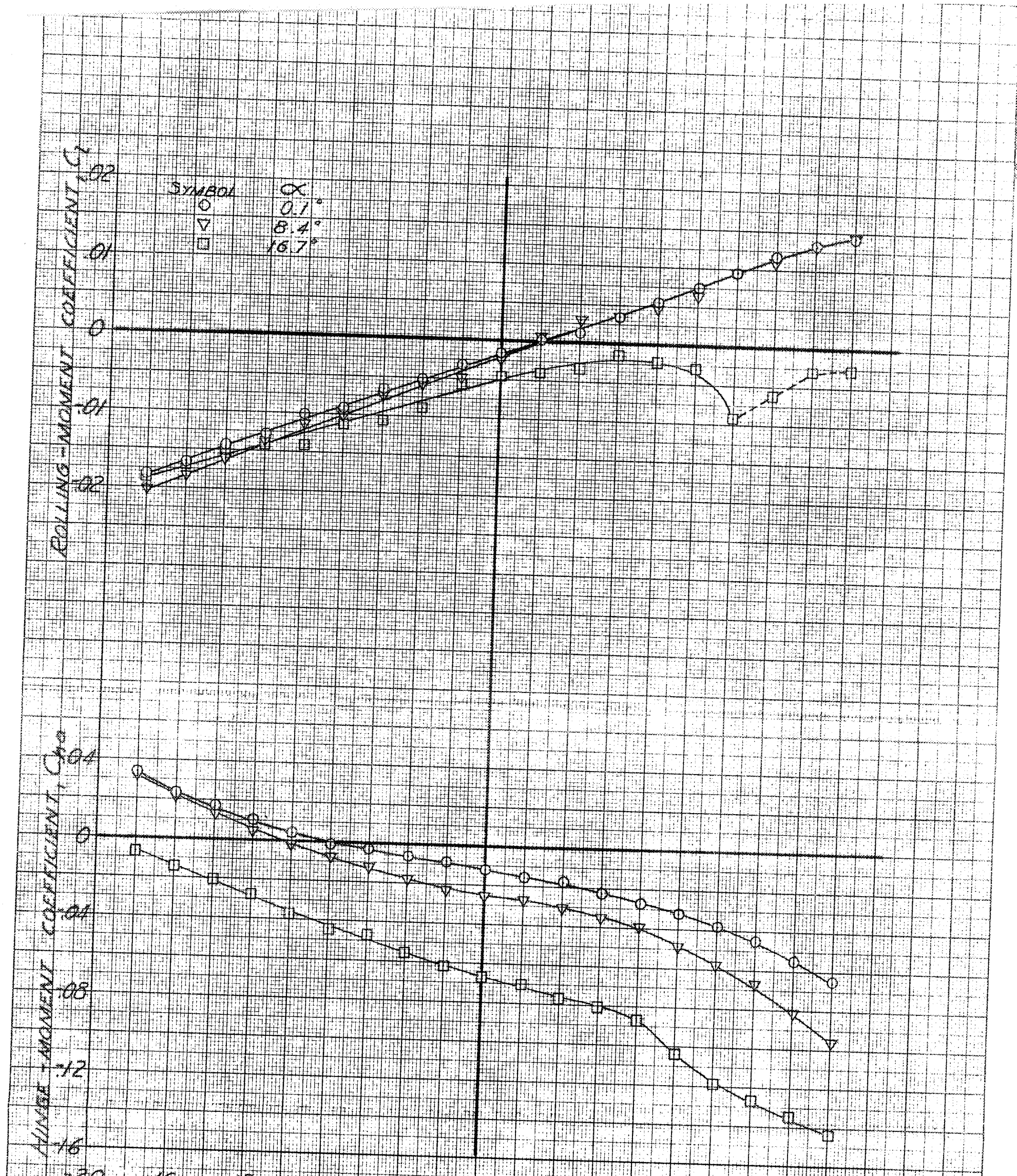

(a) C_l AND C_{n_a} VS. δ_a

FIGURE 25.- AILERON CHARACTERISTICS ON THE REPUBLIC XP-91 WING. PLAIN WING; β, 0.1°.

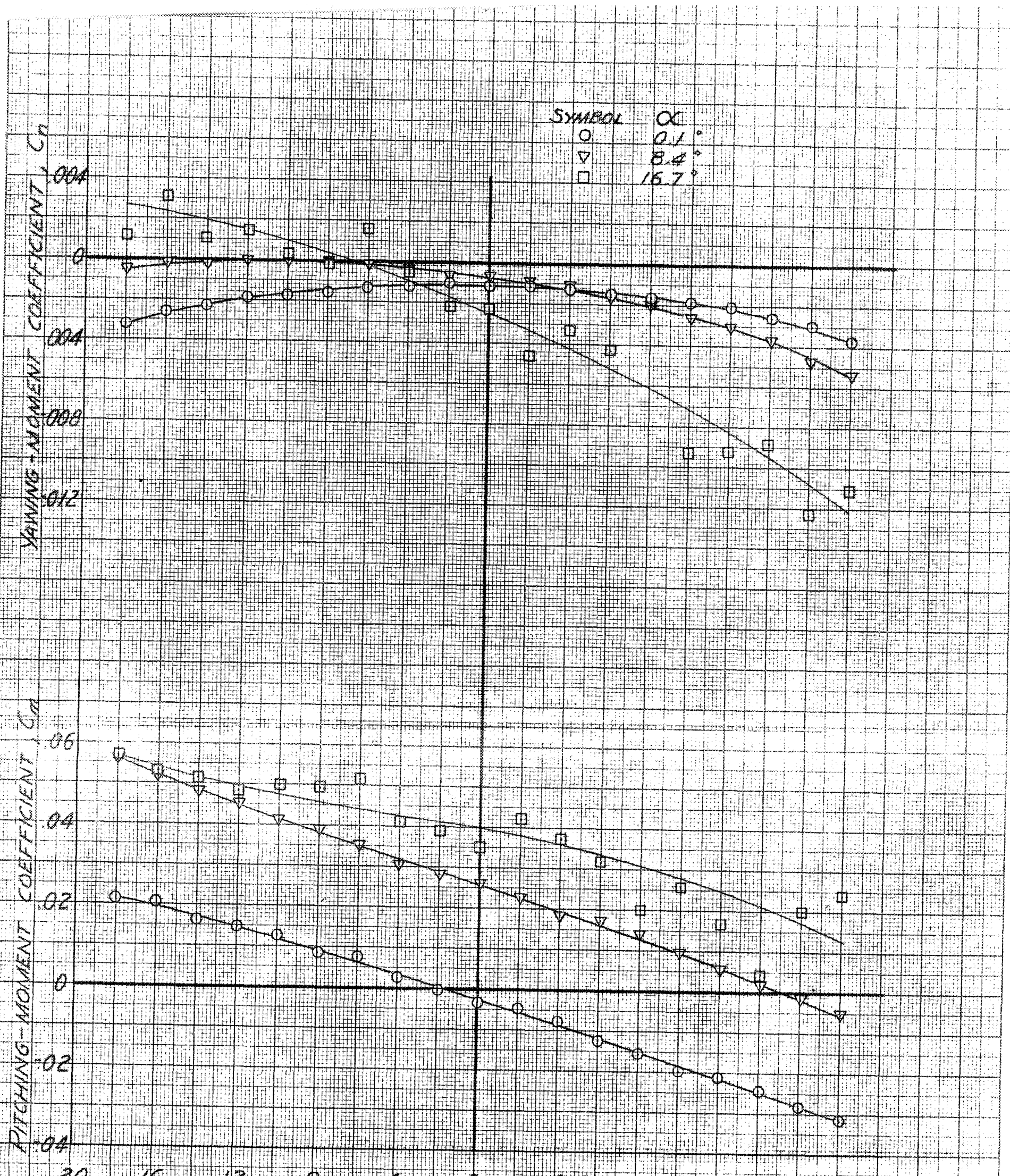

(b) C_n AND C_m VS. δ_a

FIGURE 25.- CONCLUDED.

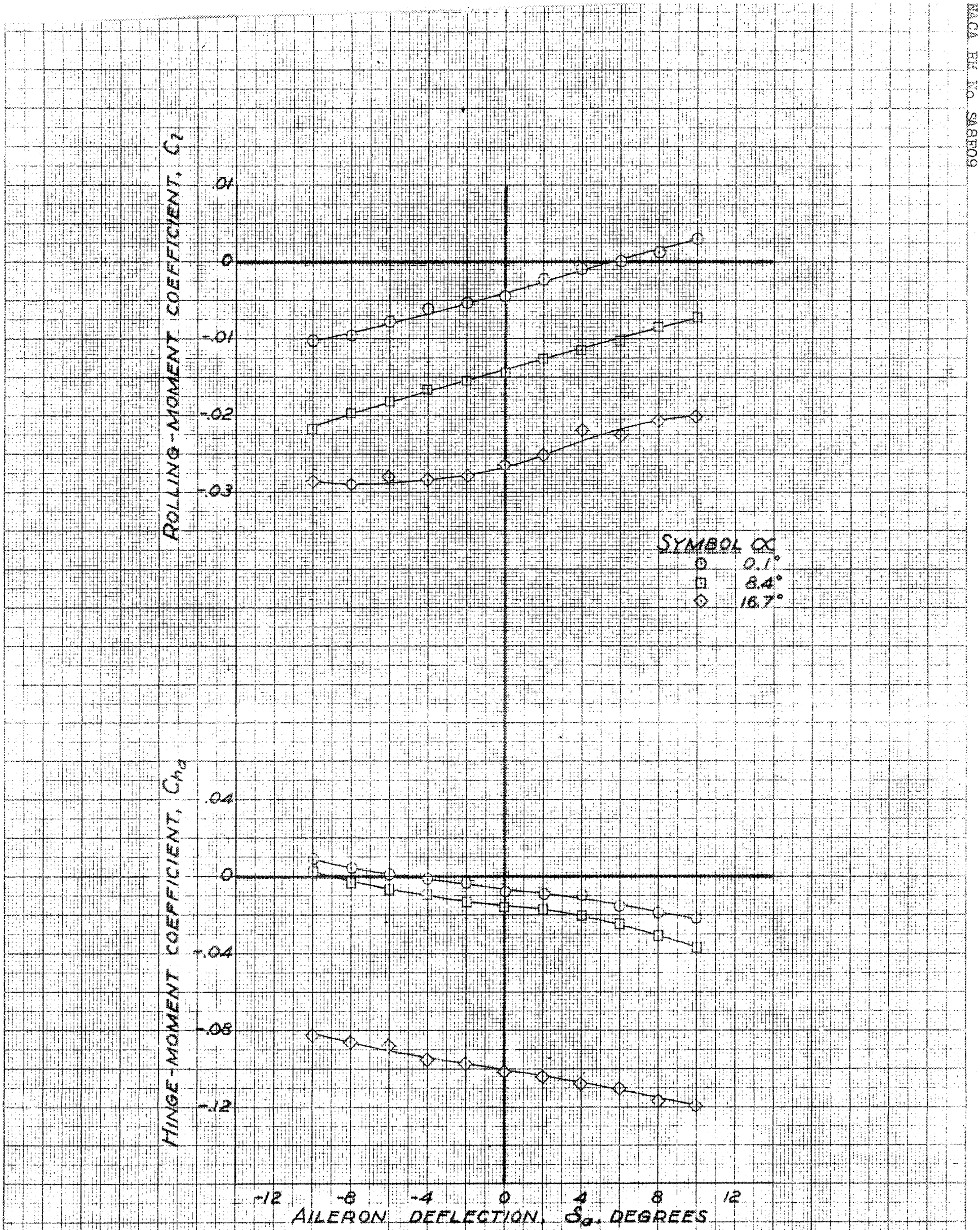

(a) C_l, C_{h_a} vs δ_a

FIGURE 26.- EFFECT OF AILERON DEFLECTION ON THE AERODYNAMIC CHARACTERISTICS OF THE REPUBLIC XP-91 WING. PLAIN WING; β, 5.2°.

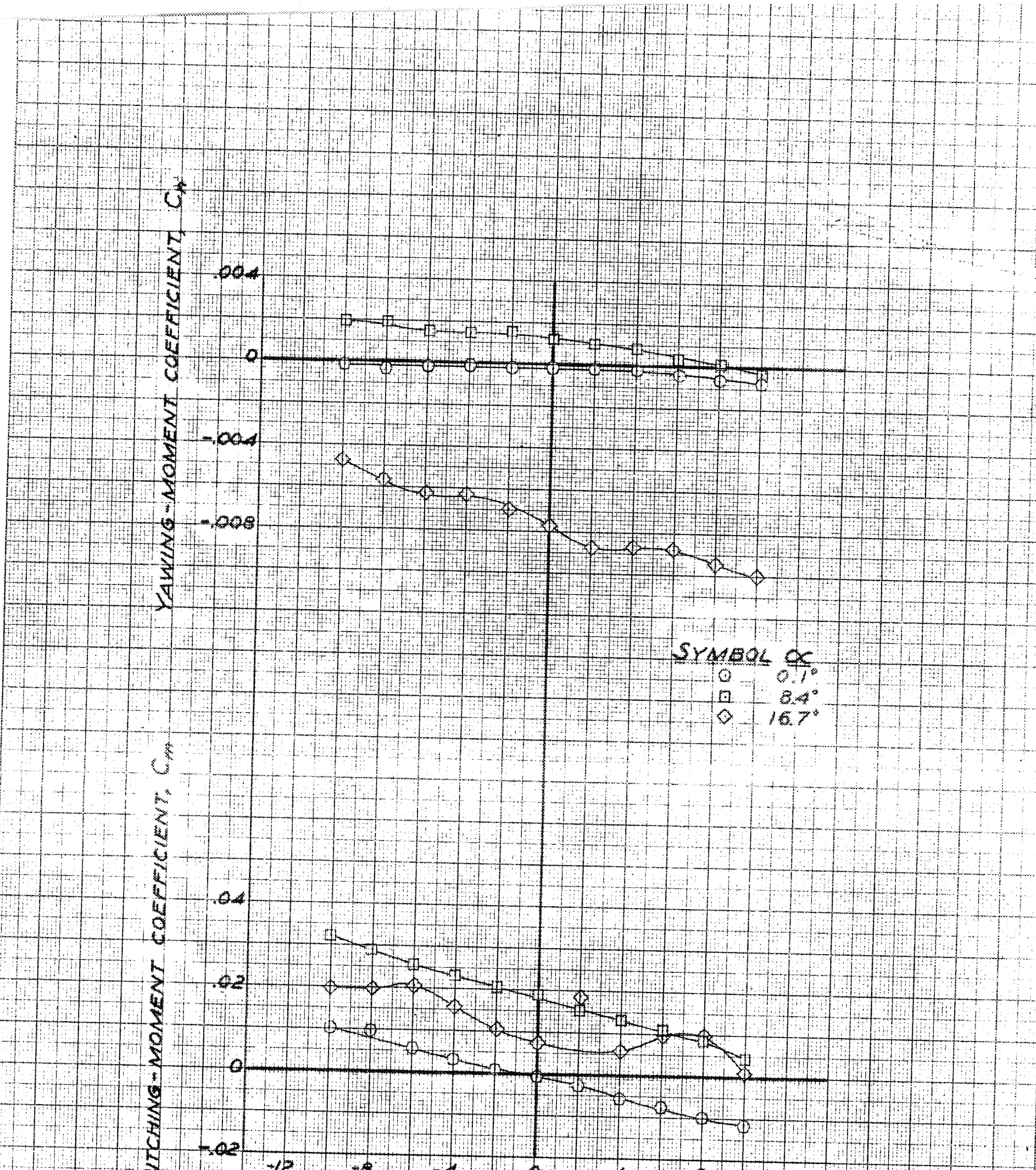

(b) C_n, C_m vs. δ_a.

FIGURE 26 - CONCLUDED.

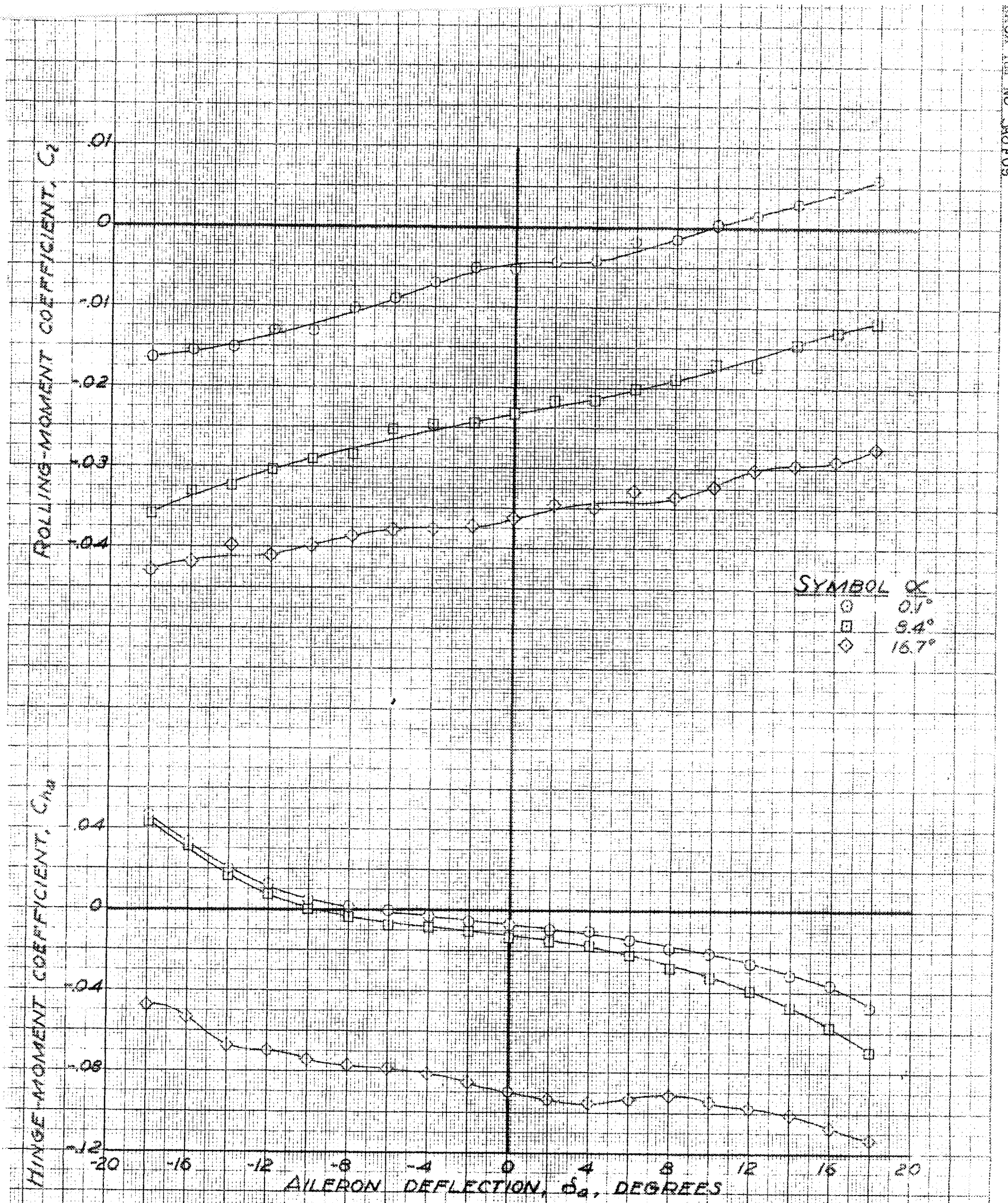

(a) C_l, C_{h_a} vs. δ_a.

FIGURE 27.- EFFECT OF AILERON DEFLECTION ON THE AERODYNAMIC CHARACTERISTICS OF THE REPUBLIC XP-91 WING. PLAIN WING, δ_f 8.6°.

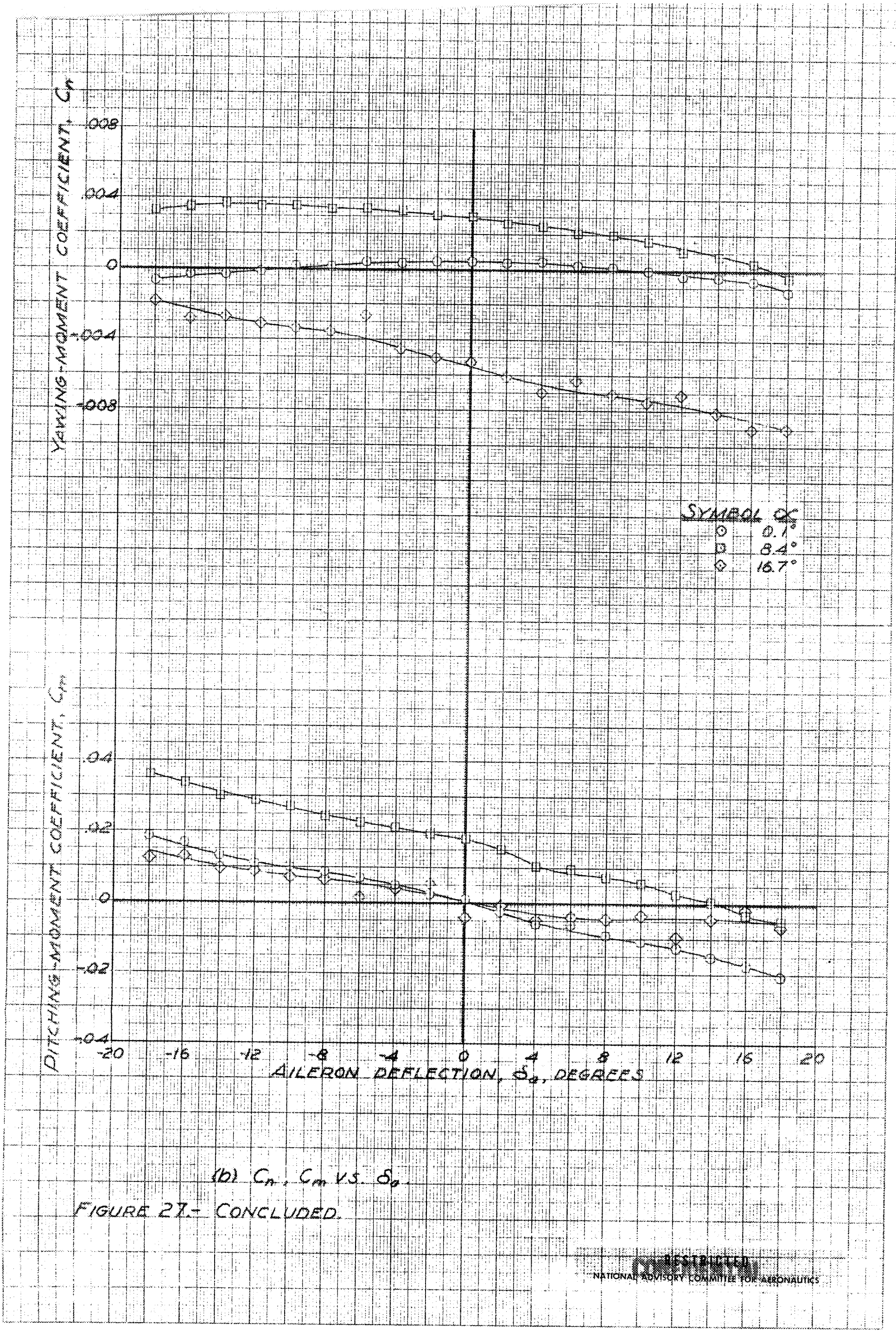

(b) C_n, C_m vs. δ_a.

FIGURE 27.- CONCLUDED.

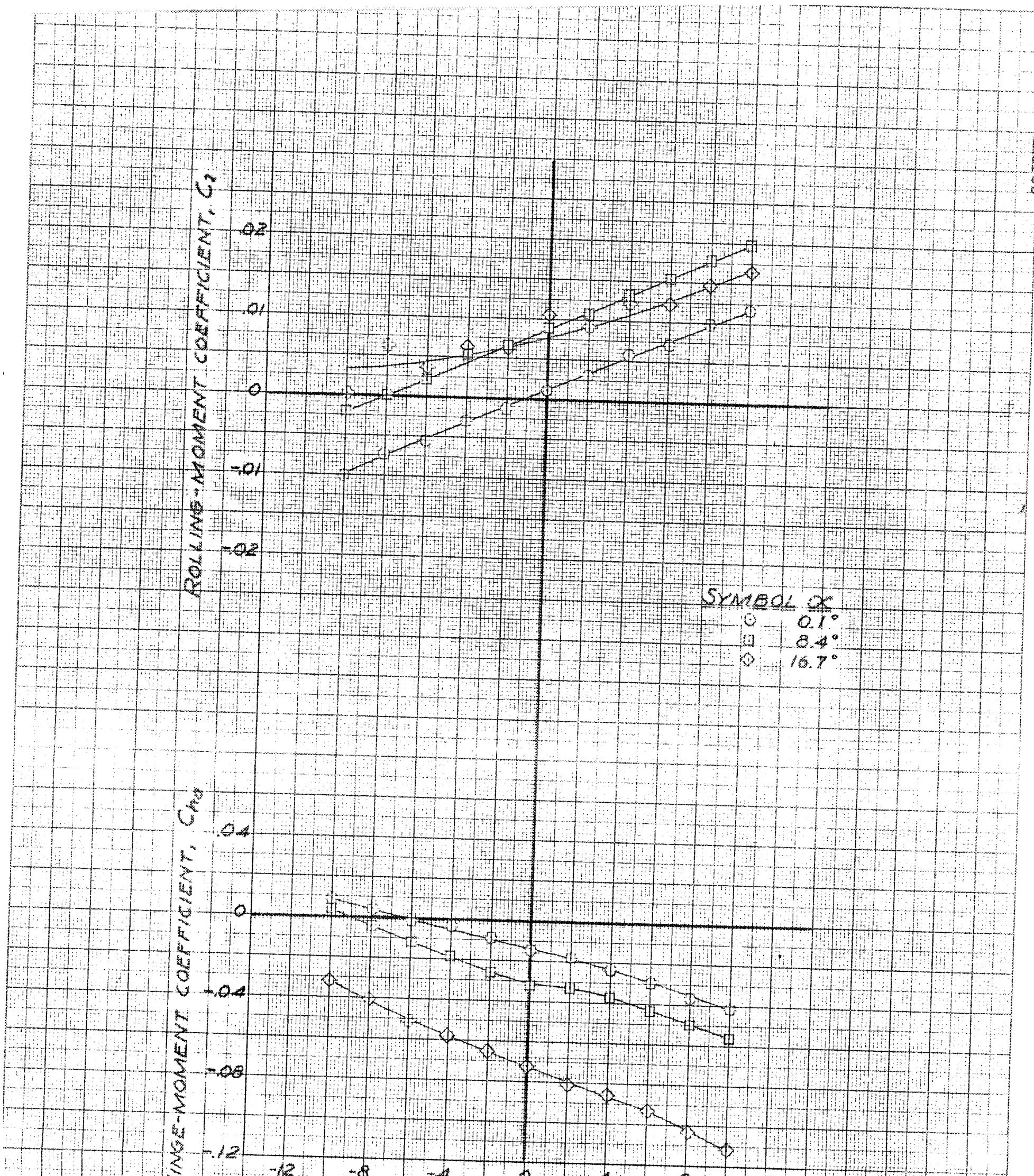

(a) C_l, C_{h_a} vs. δ_a.

FIGURE 28.- EFFECT OF AILERON DEFLECTION ON THE AERODYNAMIC CHARACTERISTICS OF THE REPUBLIC XP-91 WING. PLAIN WING; β, -4.3°.

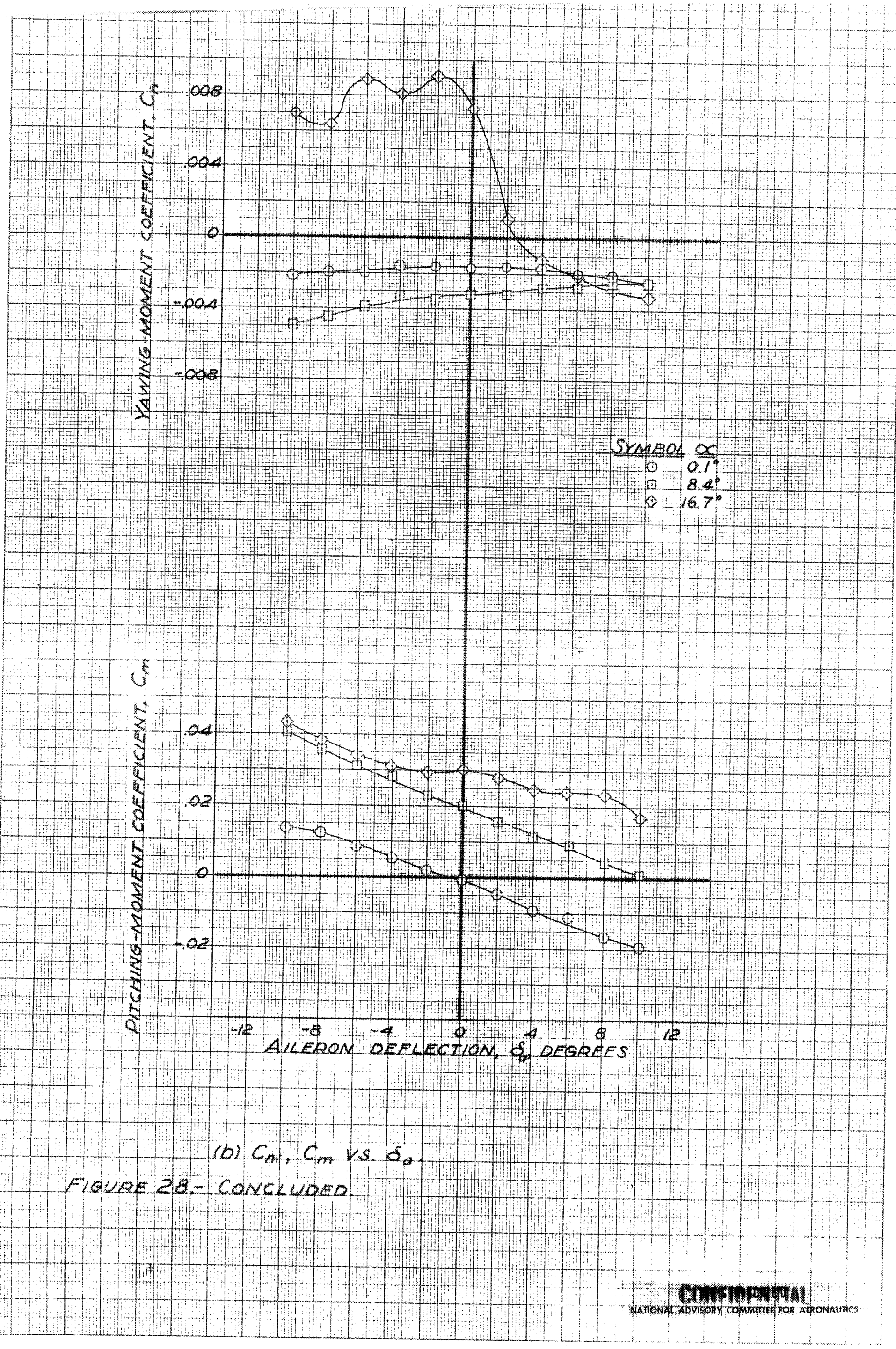

(b) C_n, C_m vs. δ_a.

FIGURE 28.- CONCLUDED.

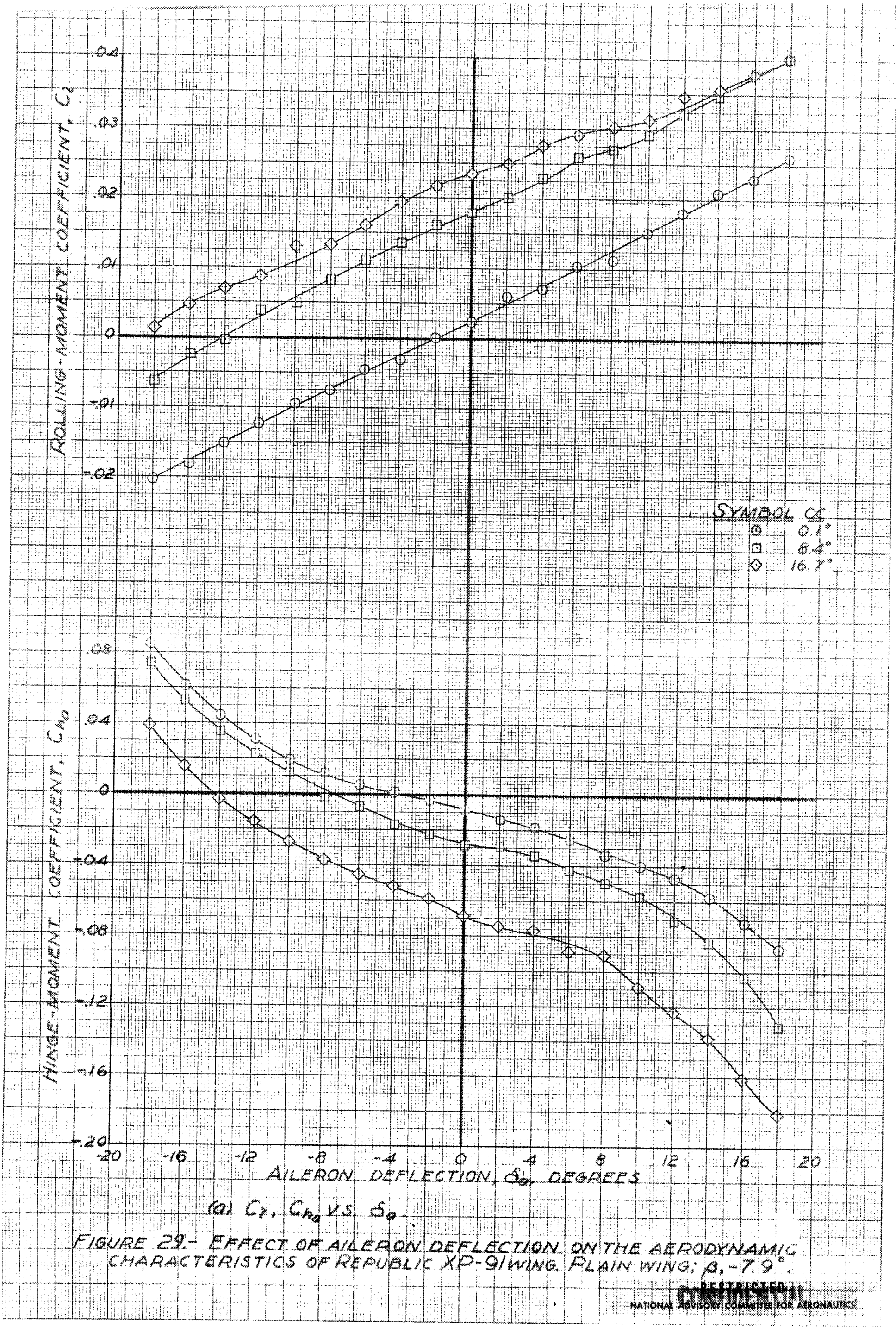

(a) C_l, C_{h_a} vs. δ_a.

FIGURE 29.- EFFECT OF AILERON DEFLECTION ON THE AERODYNAMIC CHARACTERISTICS OF REPUBLIC XP-91 WING. PLAIN WING; β, -7.9°.

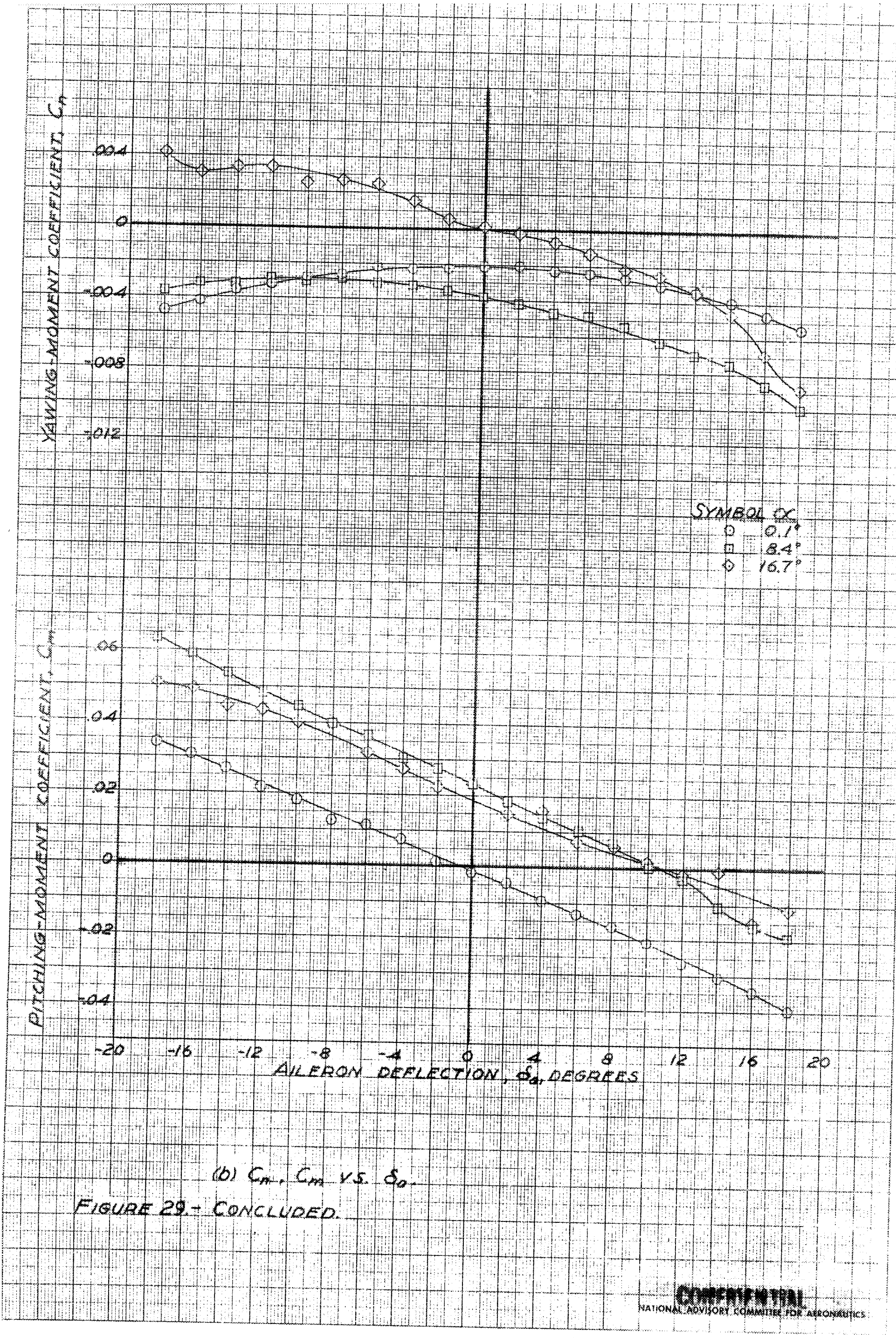

(b) C_n, C_m vs. δ_a.

FIGURE 29.- CONCLUDED.

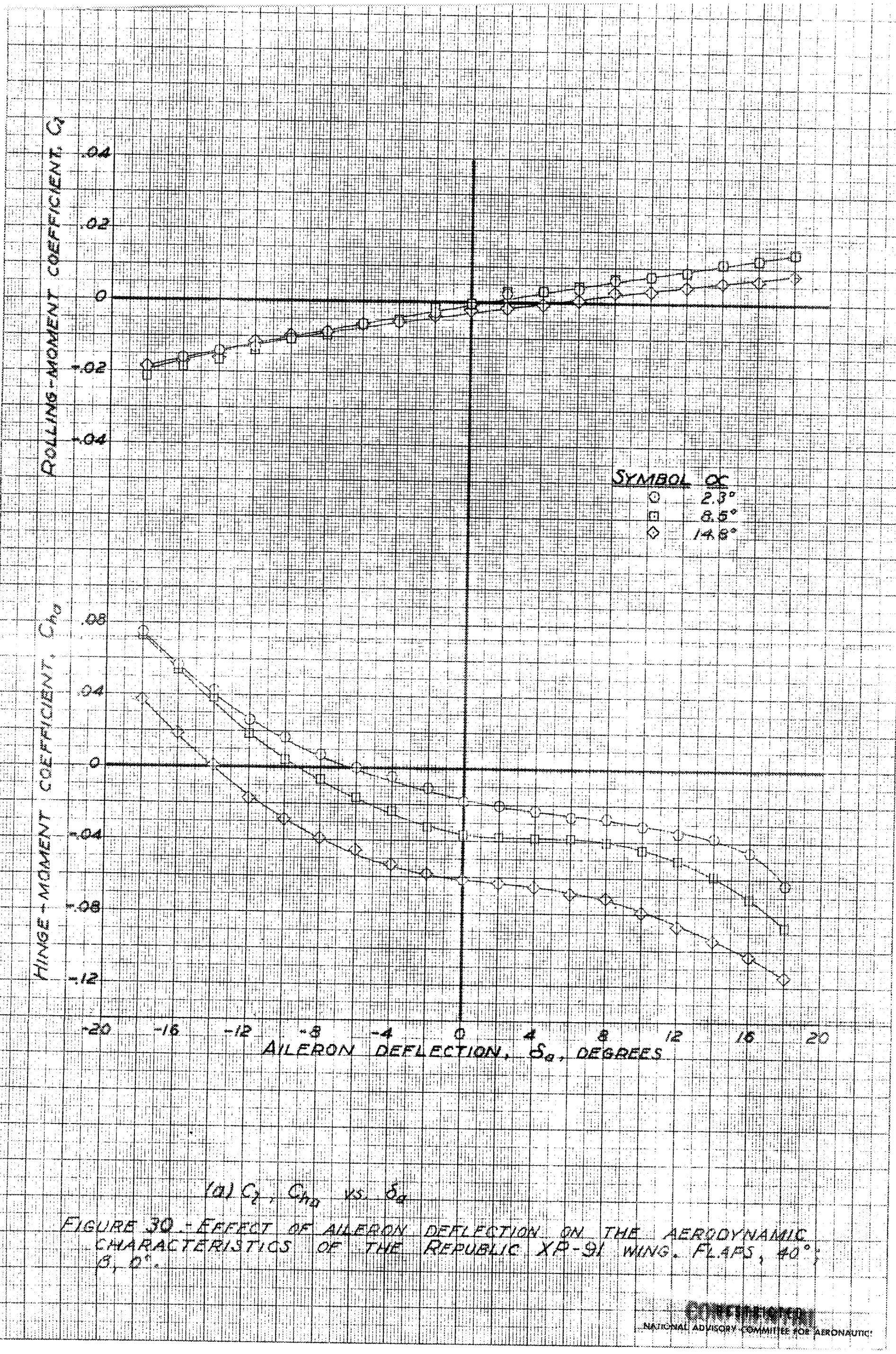

(a) C_l, C_{h_a} vs. δ_a

FIGURE 30.- EFFECT OF AILERON DEFLECTION ON THE AERODYNAMIC CHARACTERISTICS OF THE REPUBLIC XP-91 WING. FLAPS, 40°; β, 0°.

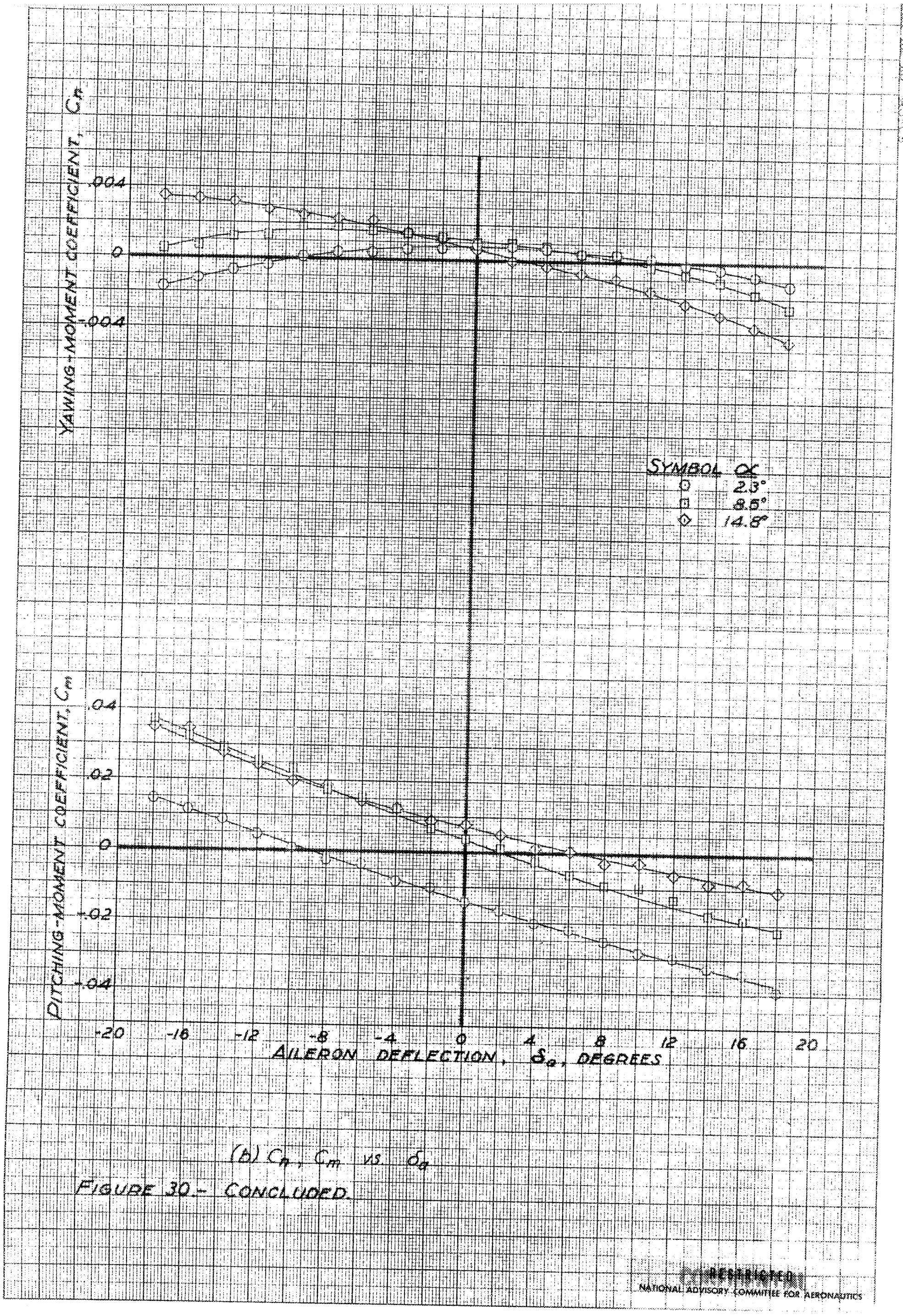

(b) C_n, C_m vs. δ_a

FIGURE 30.- CONCLUDED.

ROLLING-MOMENT COEFFICIENT, C_l

.02
.01
0
-.01
-.02

SYMBOL | α
○ | 0.1°
▽ | 8.4°
□ | 16.7°

YAWING-MOMENT COEFFICIENT, C_n

.04
0
-.04
-.08
-.12
-.16

-20 -16 -12 -8 -4 0 4 8 12 16 20

AILERON DEFLECTION, δ_a, DEGREES

(a) C_l AND C_n VS. δ_a

FIGURE 31.- EFFECT OF AILERON DEFLECTION ON THE AERODYNAMIC CHARACTERISTICS OF THE REPUBLIC XP-91 WING. OUTBOARD STRAIGHT SLATS EXTENDED 0.05 M.A.C.; β, 0.1°.

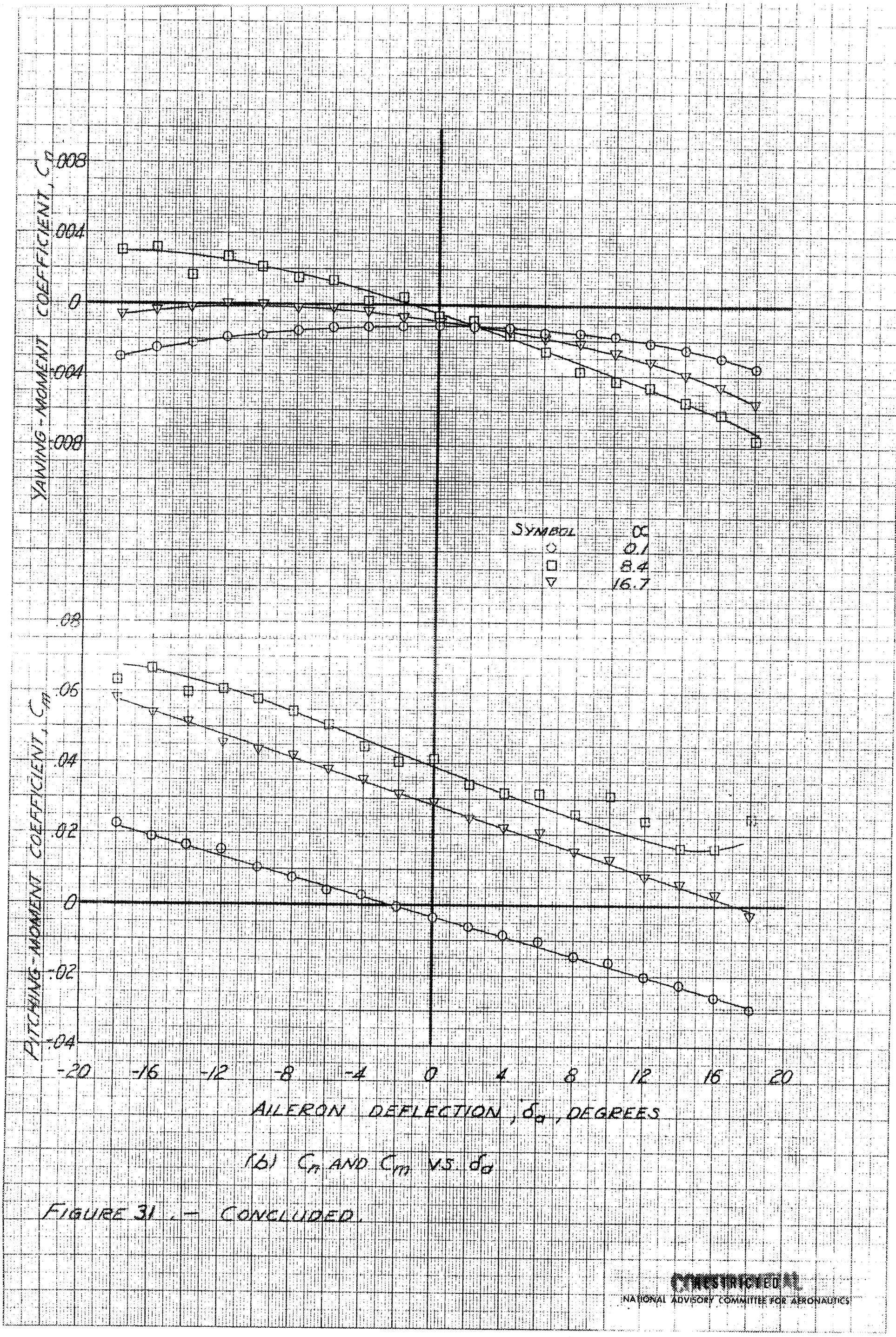

(b) C_n AND C_m VS. δ_a

FIGURE 31.- CONCLUDED.

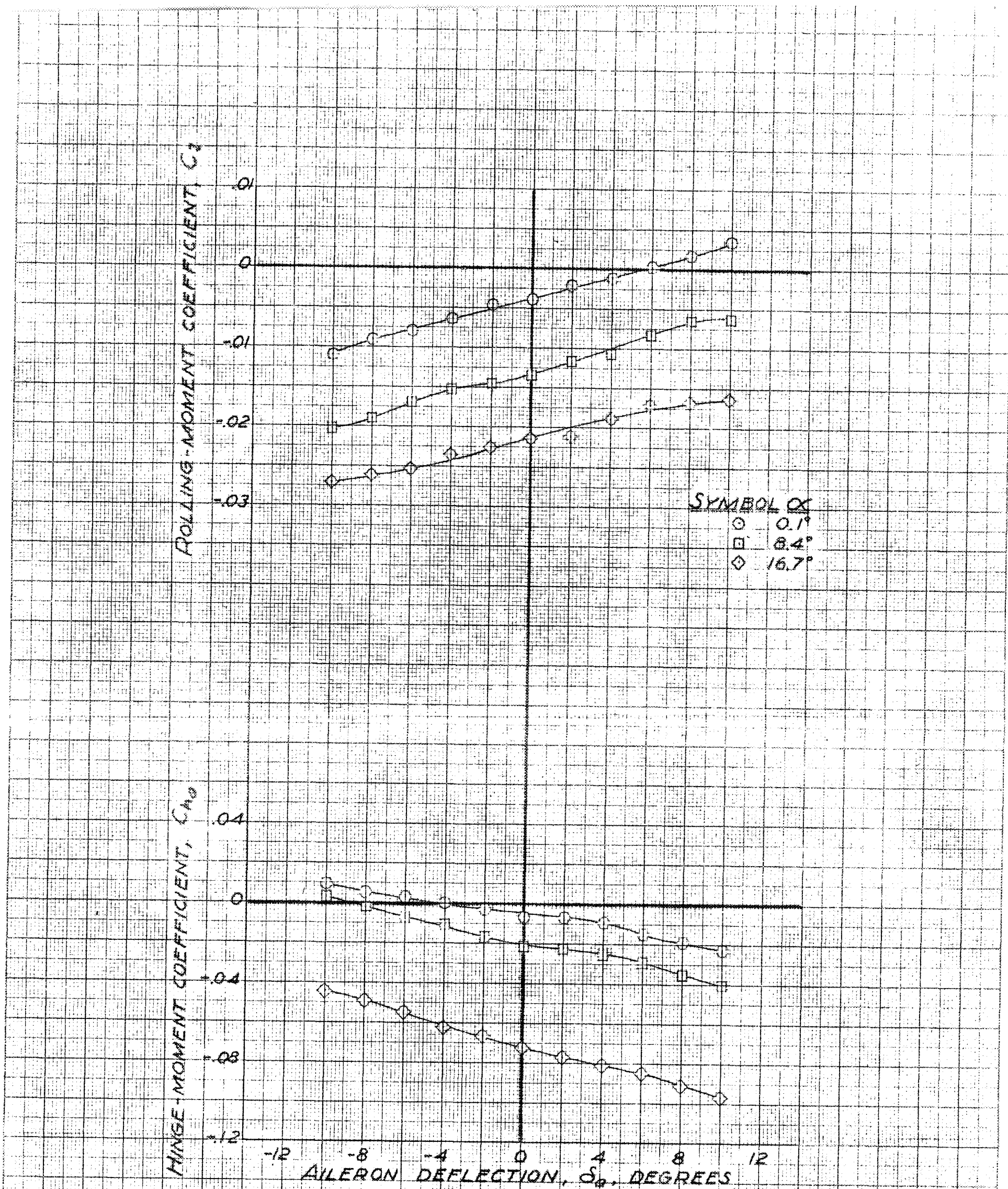

(a) C_l, C_{h_a} vs. δ_a.

FIGURE 32.- EFFECT OF AILERON DEFLECTION ON THE AERODYNAMIC CHARACTERISTICS OF THE REPUBLIC XP-91 WING. OUTBOARD STRAIGHT SLATS EXTENDED 0.05 M.A.C.; β, 5.2°.

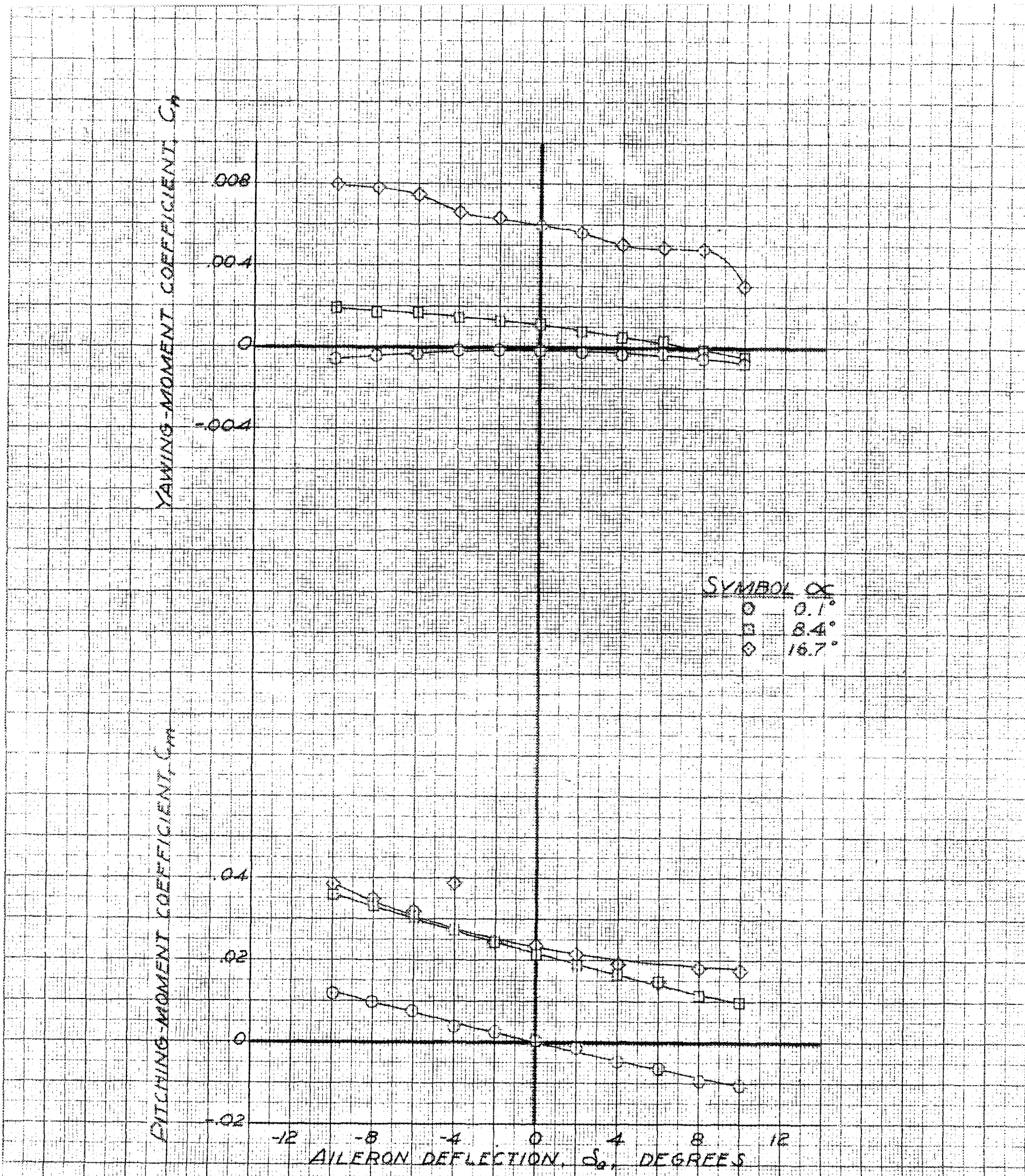

(b) C_n, C_m VS. δ_a.

FIGURE 32.- CONCLUDED.

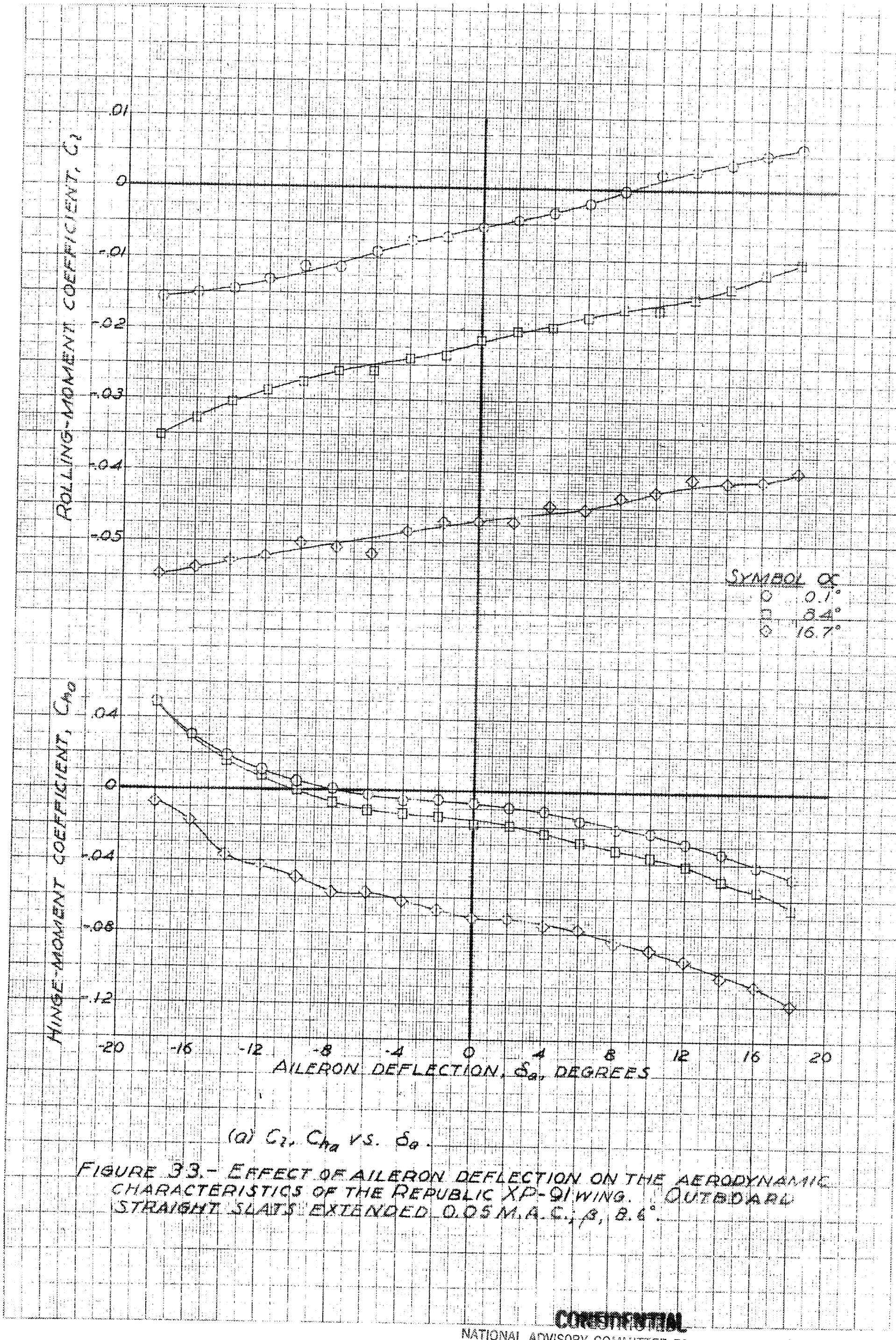

(a) C_l, C_{h_a} vs. δ_a.

FIGURE 33.- EFFECT OF AILERON DEFLECTION ON THE AERODYNAMIC CHARACTERISTICS OF THE REPUBLIC XP-91 WING. OUTBOARD STRAIGHT SLATS EXTENDED. 0.05 M.A.C.; β, 8.6°.

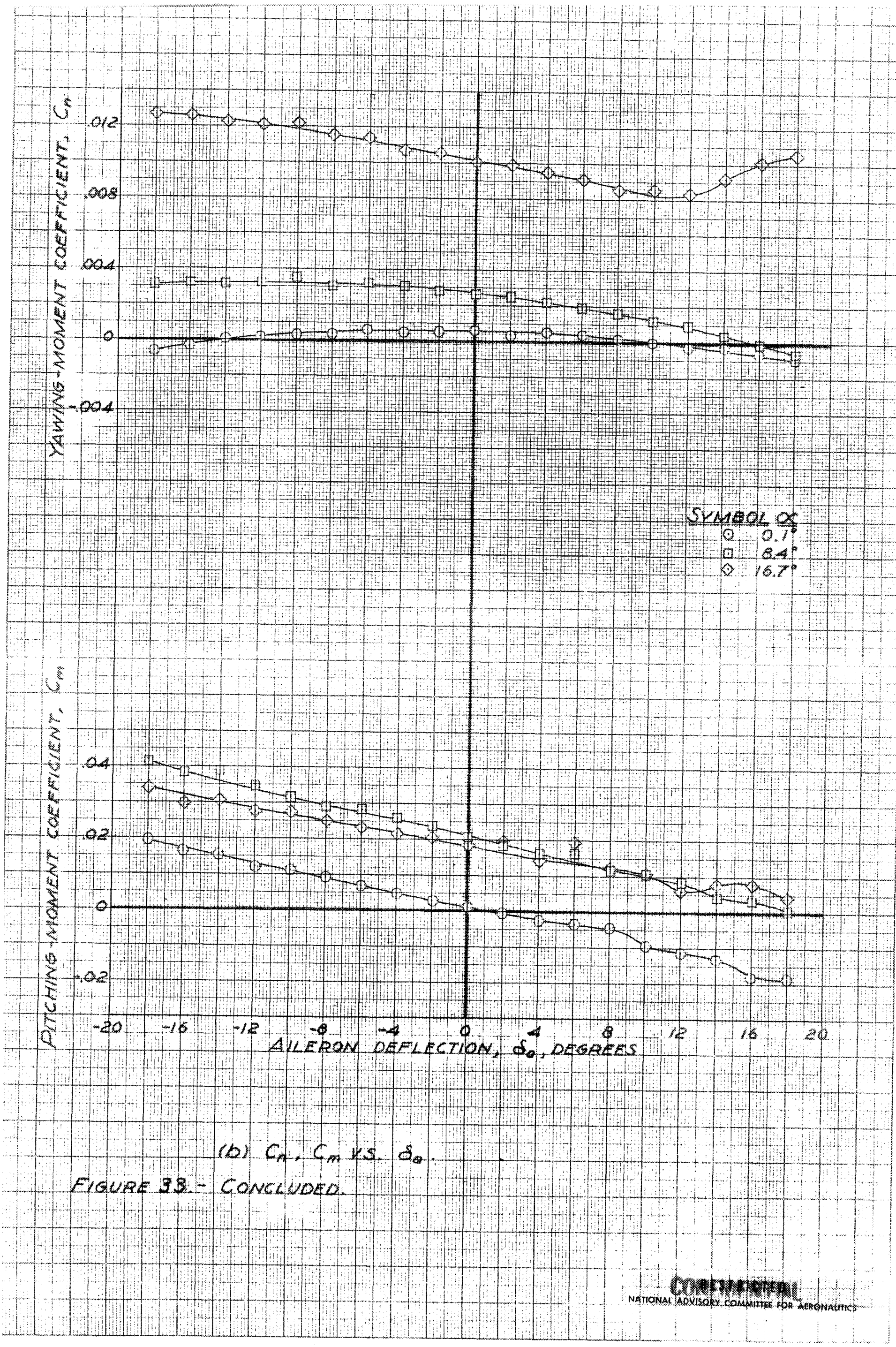

(b) C_n, C_m vs. δ_a.

FIGURE 38.- CONCLUDED.

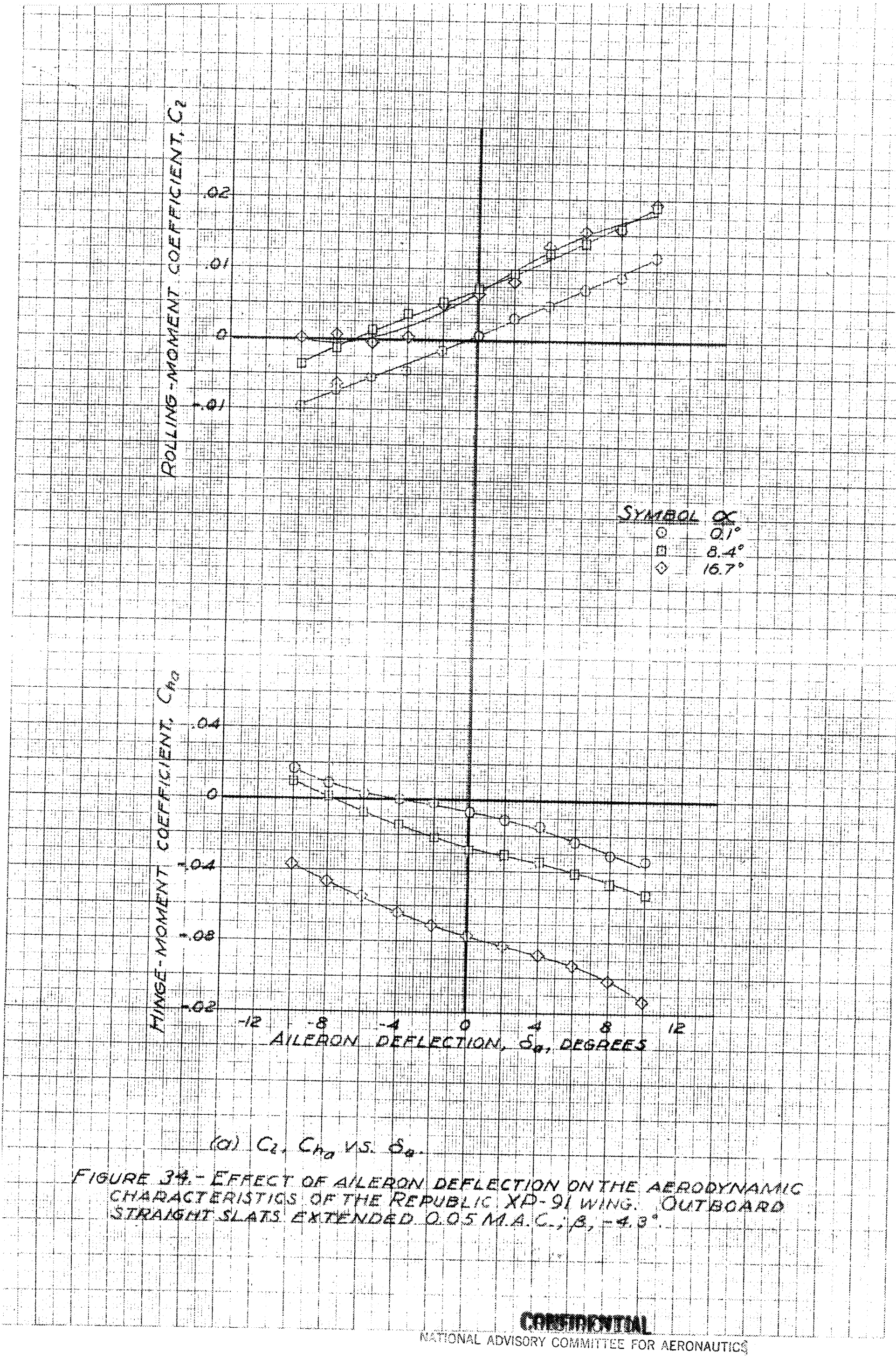

(a) C_l, C_{h_a} vs. δ_a.

FIGURE 34.- EFFECT OF AILERON DEFLECTION ON THE AERODYNAMIC CHARACTERISTICS OF THE REPUBLIC XP-91 WING. OUTBOARD STRAIGHT SLATS EXTENDED 0.05 M.A.C.; β, -4.3°.

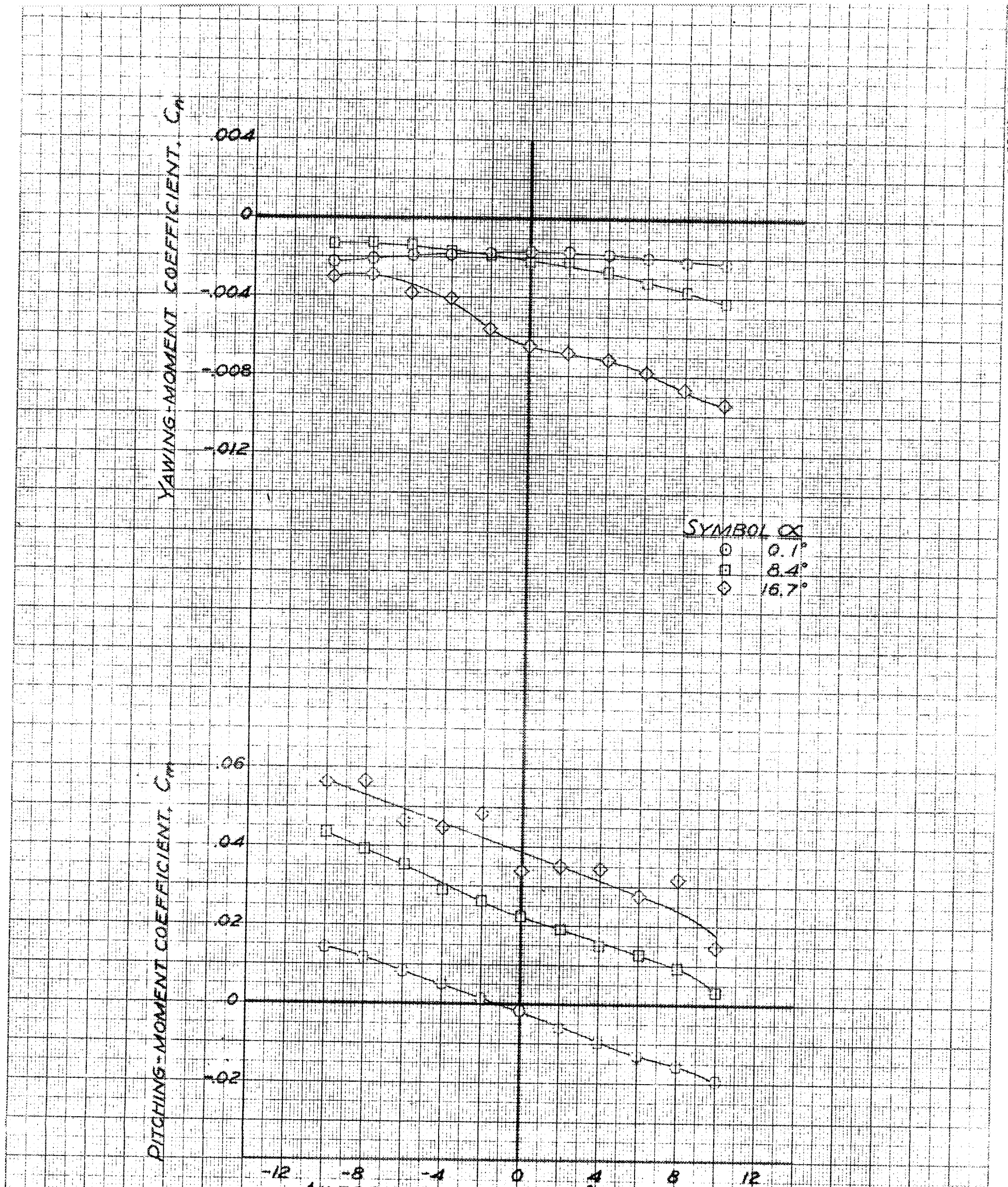

(b) C_n, C_m vs. δ_a.

FIGURE 34.- CONCLUDED.

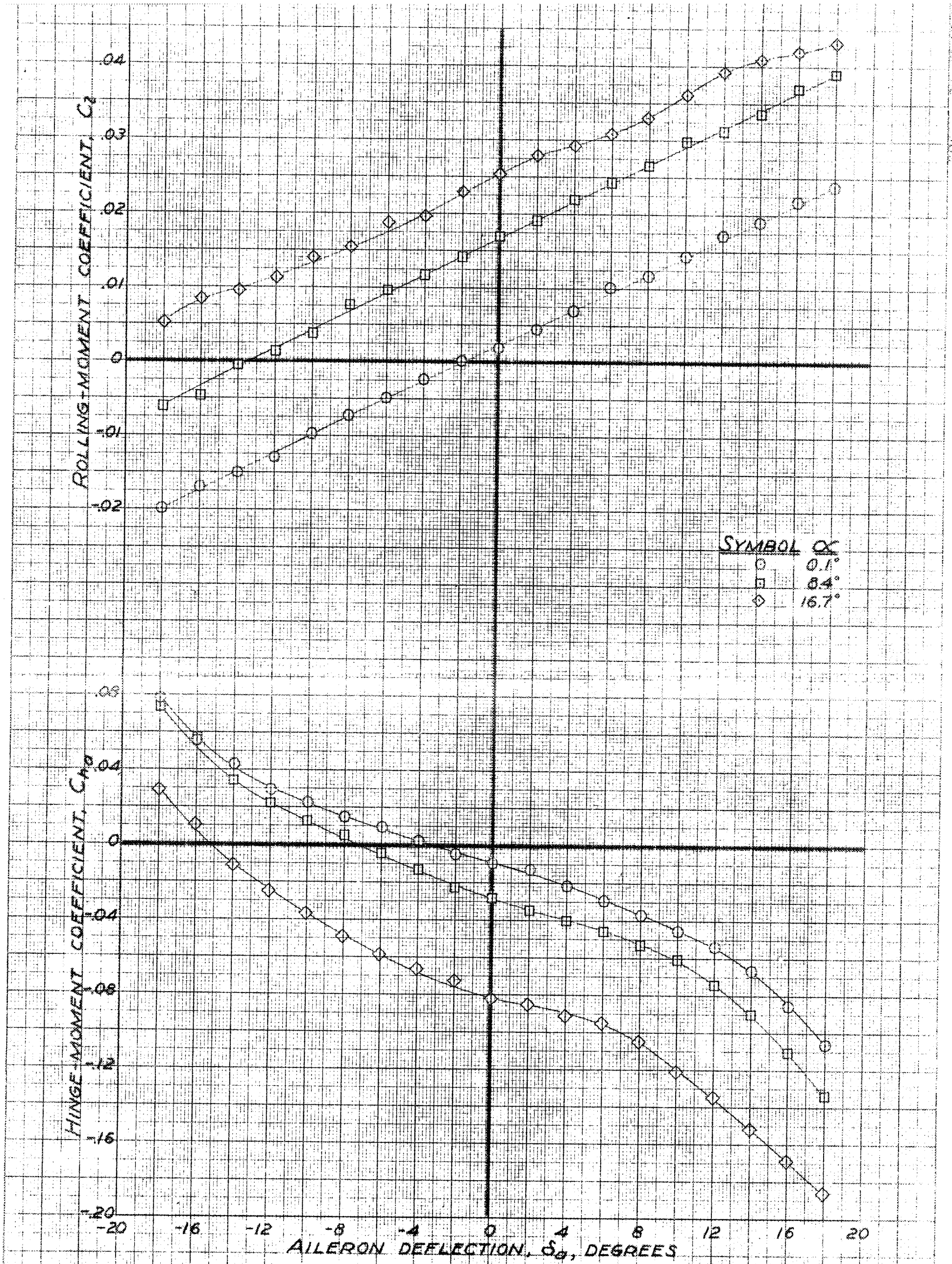

(a) C_l, C_{h_a} V.S. δ_a.

FIGURE 35.- EFFECT OF AILERON DEFLECTION ON THE AERODYNAMIC CHARACTERISTICS OF THE REPUBLIC XP-91 WING. OUTBOARD STRAIGHT SLATS EXTENDED 0.05 M.A.C.; β, -7.9°.

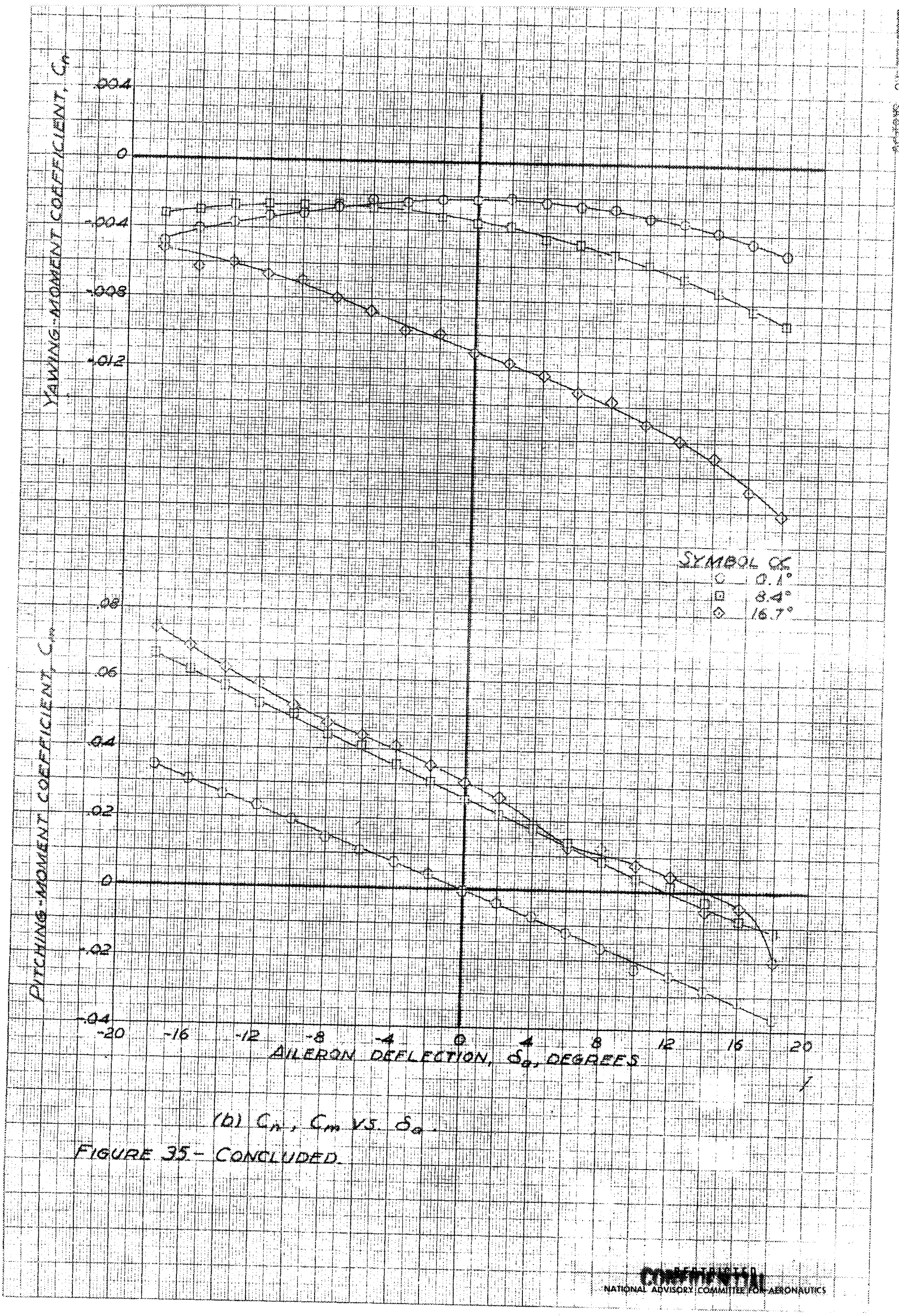

(b) C_n, C_m vs. δ_a.

FIGURE 35 - CONCLUDED.

ROLLING-MOMENT COEFFICIENT, C_l

HINGE-MOMENT COEFFICIENT, C_{h_a}

SYMBOL	α
○	2.3°
□	8.5°
◇	14.8°

.04
.02
0
-.02
-.04
.08
.04
0
-.04
-.08
-.12
-.16
-20 -16 -12 -8 -4 0 4 8 12 16 20

AILERON DEFLECTION, δ_a, DEGREES

(a) C_l, C_{h_a} vs δ_a

FIGURE 36.- EFFECT OF AILERON DEFLECTION ON THE AERODYNAMIC CHARACTERISTICS OF THE REPUBLIC XP-91 WING. FLAPS 40°, OUTBOARD STRAIGHT SLATS EXTENDED 0.05M.A.C.; δ_e, 0°

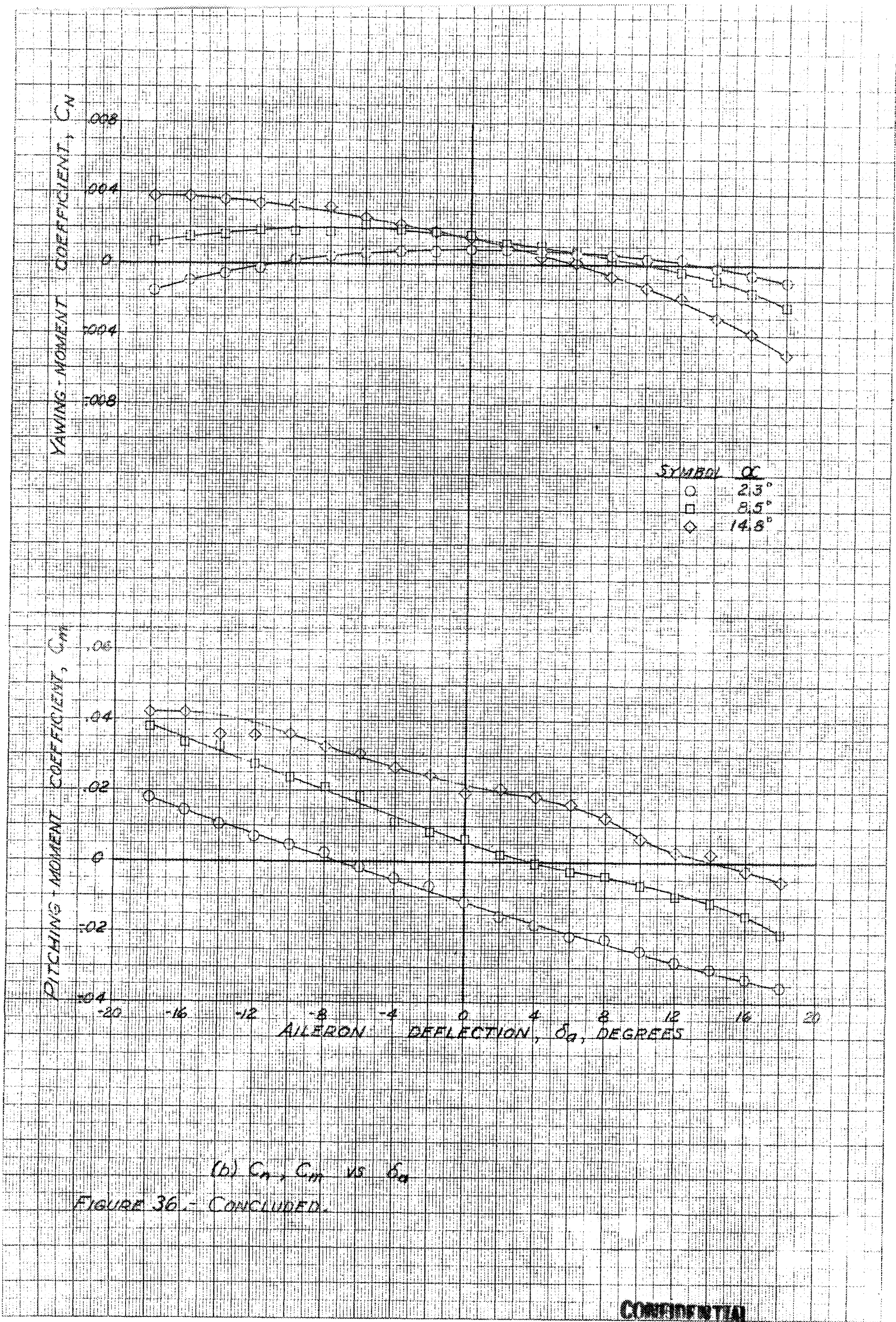

(b) C_n, C_m vs δ_a

FIGURE 36.- CONCLUDED.

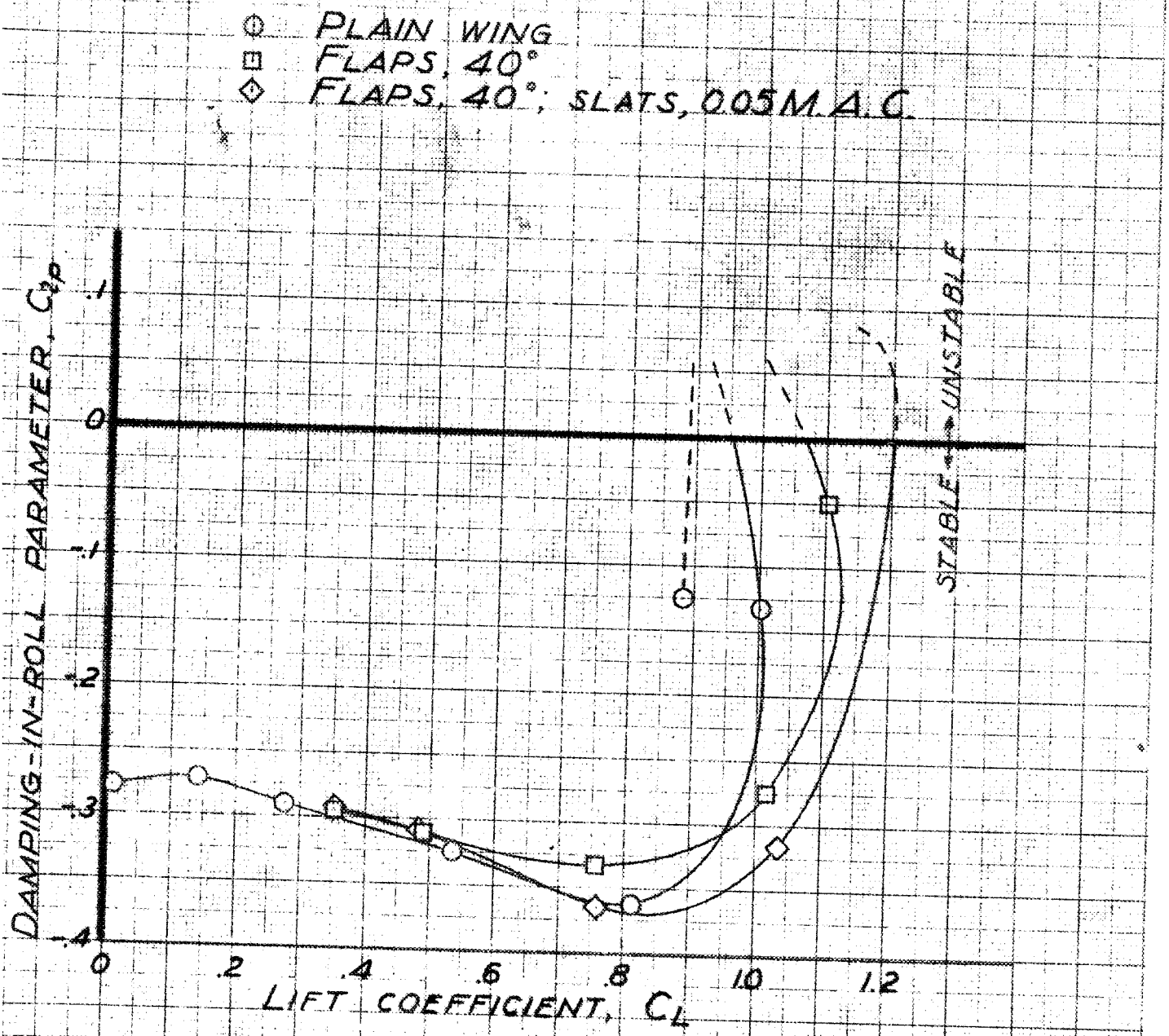

FIGURE 37.- DAMPING-IN-ROLL PARAMETER VARIATION WITH LIFT COEFFICIENT FOR THE WING PLAIN, WITH FLAPS, AND WITH FLAPS AND OUTBOARD STRAIGHT SLATS EXTENDED 0.05M.A.C.

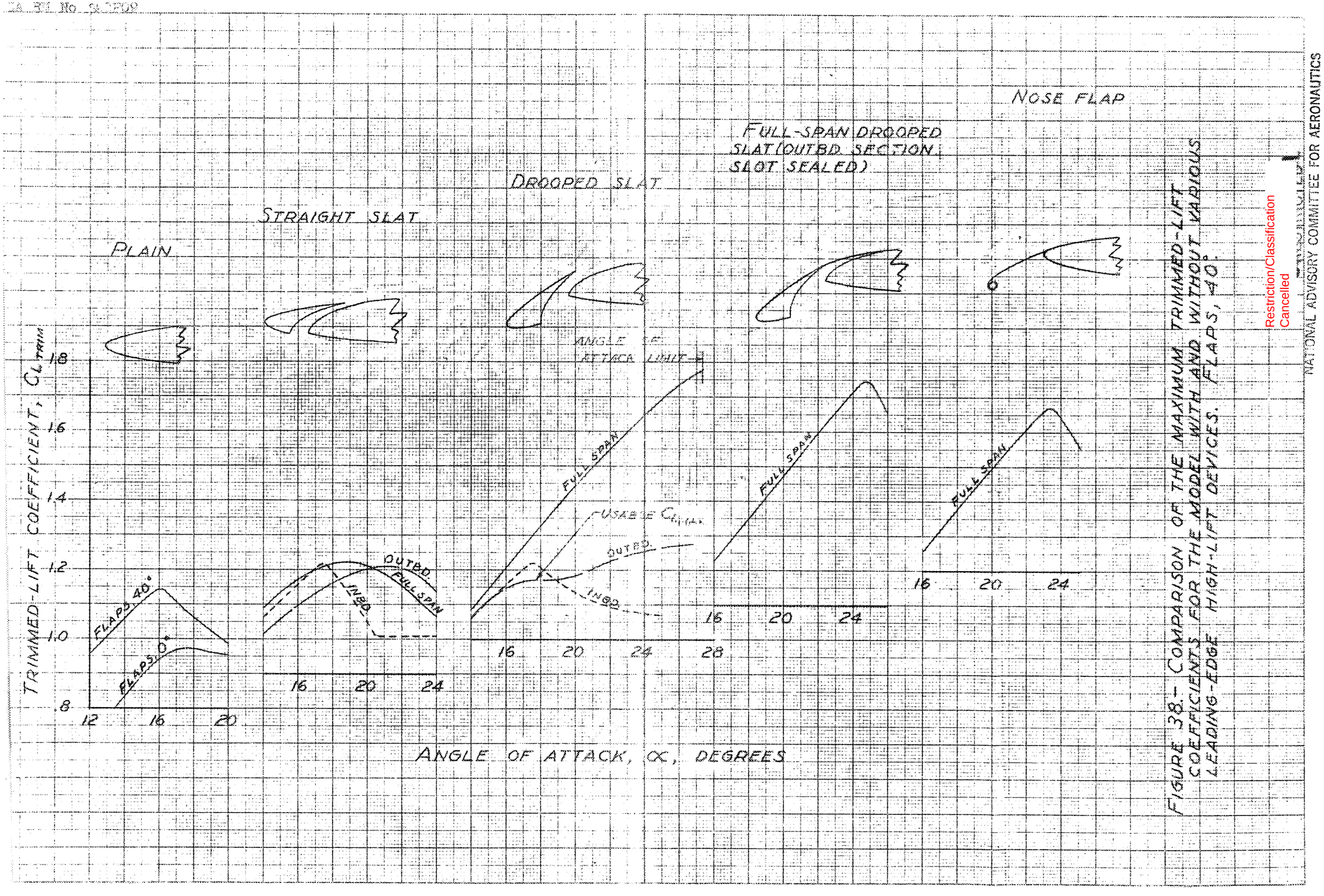

FIGURE 38.- COMPARISON OF THE MAXIMUM TRIMMED-LIFT COEFFICIENTS FOR THE MODEL WITH AND WITHOUT VARIOUS LEADING-EDGE HIGH-LIFT DEVICES. FLAPS, 40°.